Emergent behaviors in complex microbial ecosystems

by

Jiliang Hu

Submitted to the Department of Mechanical Engineering
in partial fulfillment of the requirements for the degree of

DOCTOR OF PHILOSOPHY

at the

MASSACHUSETTS INSTITUTE OF TECHNOLOGY

FEBRUARY 2024

Authored by: Jiliang Hu
Department of Mechanical Engineering
November 3, 2023

Certified by: Jeff Gore
Professor of Physics, Thesis Supervisor

Accepted by: Nicolas Hadjiconstantinou
Chairman, Committee on Graduate Students

Emergent behaviors in complex microbial ecosystems

by

Jiliang Hu

Submitted to the Department of Mechanical Engineering
on November 3, 2023, in partial fulfillment of the
requirements for the degree of
Doctor of Philosophy

Abstract

From tropical forests to gut microbiomes, ecological communities harbor diverse and abundant species. Understanding the complex emergent phenomena of diversity, stability, and invasibility in these communities within a unified framework has been a significant challenge. My PhD thesis addresses this knowledge gap by conducting the first direct test of a theory proposing that simple community-level features govern emergent behaviors. By utilizing bacterial microcosms, we demonstrate that as the number of species or the strength of interactions increases, microbial ecosystems transition through three distinct dynamical phases: from stable coexistence, to partial coexistence, to the emergence of persistent fluctuations and alternative stable states in species abundances, confirming theoretical predictions. Notably, high biodiversity and dynamic fluctuations reinforce each other under fixed conditions. By combining theoretical frameworks and microbial community experiments, we establish that community-level features determine the invasion outcome in microbial communities. We found that the communities with fluctuations in species abundance are more invasible and diverse than stable ones, leading to a positive diversity-invasibility relationship. As predicted by theory, increasing interspecies interaction strength and size of species pool leads to a decrease of invasion probability in our experiment. Although diversity-invasibility relationships are qualitatively different depending upon how the diversity is changed, we resolved the diversity-invasibility debate by showing a universal positive correspondence between invasibility and survival fraction across all conditions. Communities composed of strongly interacting species can exhibit an emergent priority effect in which invader species are less likely to colonize than species in the original pool. However, in this regime of strong interspecies interactions, if an invasion is successful it causes larger ecological effects on the resident community than when interactions are weak. Overall, this thesis uncovers predictable emergent patterns of diversity, dynamics, and invasibility in ecological communities, offering insights into a unified framework for microbial ecology.

Thesis Supervisor: Jeff Gore
Title: Professor

Acknowledgments

I would like to express my heartfelt appreciation to my thesis advisor, Prof. Jeff Gore, for his invaluable guidance during my study at MIT. His profound knowledge and genuine enthusiasm for science have not only shaped my research pursuits but also deeply influenced my personal and scientific evolution. Jeff's insightful lectures on systems biology and biophysics, complemented by our enriching weekly discussions, have been pivotal in refining my scientific taste. Throughout my graduate journey, Jeff has consistently prioritized my growth and well-being, making him a quintessential mentor. It has been both an honor and privilege to work alongside such an esteemed advisor during my time at MIT.

Throughout my academic journey, Jeff's unwavering support and genuine concern for my well-being have been evident in numerous ways. For instance, after finishing my master's at MIT, I was captivated by the innovative research in the Gore lab. I approached Jeff about the possibility of pursuing my PhD with him. During our conversation, he discussed my master's project in-depth and warmly welcomed the idea of me joining his team. Yet, with my best interests at heart, Jeff gently suggested that it might be more beneficial for me to complete my PhD in my original group and then join his lab as a postdoc, given the trajectory and timelines of graduate studies. While I was keen to directly work on my PhD with him, this advice underscored his selfless dedication to my best interests and career growth.

Jeff's unwavering support became even more evident during the pandemic. With prolonged travel restrictions keeping me away from my family, Jeff not only facilitated my return to China but also ensured I could work remotely, allowing precious moments with my family. He constantly made efforts to stay connected, even with vast time zone differences, and always emphasized the importance of family time. Outside of academic pursuits, Jeff's advice often extended to activities that would enrich my perspectives. His commitment to fostering the next generation was evident when he readily agreed to lecture and mentor students at Tsinghua. Jeff's holistic approach to mentorship, balancing both professional and personal growth, has been

truly transformative for me.

I am deeply grateful to Prof. Guy Bunin, Prof. Matthieu Barbier, Prof. Daniel Amor, Prof. Quanshui Zheng, Prof. Li Yu, Prof. Luping Xu, Prof. Alan Grodzinsky, Prof. Ming Guo, and Prof. Feng He for their generous mentorship, which has greatly influenced my development as a scientist through their remarkable intellect and knowledge. I would also like to extend my gratitude to Prof. Serguei Saavedra, Prof. Domitilla Del Vecchio, and Prof. Jean-Jacques Slotine, for their valuable advice and support as members of my thesis committee.

I would like to extend my heartfelt appreciation to the incredible members of the Gore lab, who have been a source of unwavering support, transforming our group into a warm and nurturing family. Your generous mentorship, constant encouragement, and invaluable assistance have been instrumental in my academic journey. The inspiring discussions we have shared have enriched my life in immeasurable ways. Thanks to your collective efforts, my experience at MIT has felt like being at home.

I am indebted to my parents for their unwavering dedication in raising and encouraging me to pursue my passions. My parents, Mrs. Yaohua Liang and Mr. Zonghao Hu, have showered me with boundless love and have worked tirelessly to support our family. Throughout every obstacle I've encountered in my life's journey, my pareents have consistently stood by my side as unwavering beacons of support and encouragement. Their profound love has not only fortified me to surmount challenges but has also instilled a relentless optimism in my approach to life. The depth of family bonds is immeasurable, and for their unwavering faith in me, I am eternally grateful.

I would like to seize this opportunity to express my profound gratitude to my friends for their constant support, for sharing in our experiences, and for growing together. Chao Wu, Jianyi Du, Sijie Chen, Jiaxi Zhao, Yue Wu, Li Yuan, Zhongda Wang, Yulun Wu, Luohao Wang, Yukun Hao, Shuai Zhou, Yoonho Kim, Yekuan Yang, Xiaotong Zhang, and many others, your kindness, intelligence, and patience have played an instrumental role in shaping who I am today.

Thank you all for making it happen.

Contents

List of Figures

List of Tables

Chapter 1

Introduction

1.1 Emergent phenomena, ecology, and microbes

Emergent phenomena arise when a system exhibits characteristics or behaviors not found in its individual components, highlighting the principle that the whole can be greater than the sum of its parts [9]. This concept, central to systems thinking and complexity science, underscores the idea that when individual elements interact, often in non-linear and intricate ways, they can produce unexpected and novel outcomes. Such emergent properties aren't simply additive; they cannot be predicted or deduced by examining each component in isolation [9]. Instead, they materialize as a result of the synergistic interactions between components. For instance, the flocking behavior of birds or the organized movement of ant colonies are classic examples of emergence in nature. These behaviors cannot be understood by examining a single bird or ant but emerge from the interactions among numerous individuals [29]. Emergent phenomena challenge reductionist thinking and highlight the importance of understanding systems in their entirety, especially when navigating complex domains like ecology, neuroscience, and social systems [26].

In nature, species live and engage with numerous other species in intricate communities. One of the core inquiries in ecology involves understanding how many species can coexist, the reasons some areas possess higher biodiversity than others, and the distinct dynamical behaviors exhibited by various communities. Furthermore,

these factors are pivotal in shaping how an ecosystem functions. A long-standing question in the field hinges on the question: how does the complex community dynamics emerge from species interactions? Ecological systems display a spectrum of dynamical behaviors. Consider the gut microbiota and grassland plants; their enduring patterns over time are clear indicators of global stability [44, 125, 40]. On the other hand, many natural communities present multiple stable states or "alternative stable states," broadening the scope for ecological and evolutionary research [110, 130, 11, 131, 7, 1]. Beyond these static states, certain communities are characterized by ongoing fluctuations, encompassing patterns such as limit cycles and chaos [23, 13, 47, 17, 19, 102]. These dynamical patterns provide clues about community assembly processes, their ability to sustain high diversity, and potential trajectories. For a deeper and more predictive understanding of ecology, it's crucial to delve into these dynamics.

Microbes, often deemed the invisible architects of our world, are immensely diverse and ubiquitous, encompassing a vast array of life forms such as bacteria, viruses, fungi, and protists [140]. These diminutive organisms are found in virtually every nook and cranny of our planet, from the sultry depths of hydrothermal vents in the deep-sea to the frosty expanses of Arctic tundras [52]. They not only contribute to the planet's biogeochemical cycles, making Earth habitable, but also engage in intricate interactions with plants, animals, and other microbes. The term "microbiome" refers to the collective community of these microbes inhabiting a specific environment, whether it's a patch of soil, a droplet of ocean water, or the human gut [58].

As a good example of complex ecosystems, microbial communities often hailed as the "powerhouses" of our planet, represent the intricate dynamics of complex ecosystems, having critical implications for human health, nutrient cycling, and environmental equilibrium [111]. These minute but mighty entities actively participate in processes ranging from digestion within our guts to decomposition in our soils [135]. Furthermore, their ubiquitous presence, from the deep sea to the upper atmosphere, underscores their ecological significance [66]. Additionally, these microbial assemblages offer an unparalleled platform for scientific inquiry into emergent behaviors

within ecosystems. Their small-scale nature facilitates precise experimental control, while their rapid growth rates allow for real-time observation of evolutionary and ecological dynamics. Moreover, the advancements in molecular biology techniques, such as metagenomics and transcriptomics, have made the culturing and study of these previously "unculturable" microorganisms more accessible [68]. As such, microbial communities not only hold the key to understanding larger ecological processes but also offer a convenient and comprehensive system for rigorous ecological experimentation [66, 135].

In recent years, the human microbiome, especially, has become the focal point of numerous scientific investigations [111]. Found predominantly in our digestive tracts but also colonizing our skin, respiratory system, and other body sites, these microbial residents play indispensable roles in a variety of physiological processes [66]. They aid in digestion, assist in nutrient synthesis and absorption, educate our immune system, and even produce bioactive compounds that can influence our mood and behavior. Disturbances in the balance of the human microbiome have been linked to a plethora of health conditions, from obesity and allergies to more serious ailments like inflammatory bowel disease and mental health disorders [52]. As we delve deeper into the realms of microbial research, it becomes evident that to truly understand our health and the health of our environment, we must first unravel the complexities of the microbiome and its intricate dance with its host [68]. This burgeoning field promises not only insights into fundamental biological processes but also potential therapeutic avenues harnessing the power of beneficial microbes [66, 135].

Microbial ecology is a multidisciplinary field that investigates the intricate interactions and dynamics within microbial communities, which play vital roles in shaping ecosystems [135]. These communities thrive in various environments, from oceans and soil to tropical rainforests and the human body, exerting significant influence over ecosystem functioning [66]. Understanding the complex web of interactions within microbial communities is crucial for comprehending ecosystem dynamics, addressing environmental challenges, and harnessing their potential for diverse applications [66, 135].

Microbial communities consist of diverse assemblages of microorganisms that exhibit remarkable emergent behaviors surpassing the individual characteristics of constituent species [111]. These emergent behaviors arise from intricate interactions and synergies within the community, resulting in complex and often unexpected phenomena that cannot be predicted by studying individual organisms in isolation [50]. Unraveling the mechanisms and consequences of emergent behavior is a central pursuit in microbial ecology, as it holds the key to deciphering the collective dynamics that shape ecosystem functioning and stability [56].

To understand and predict emergent behavior in microbial communities, a holistic approach that integrates ecological, genetic, and physiological factors is required [132]. Recent advancements in high-throughput sequencing, metagenomics, and computational modeling have provided unprecedented insights into the complex networks of species interactions and metabolic pathways underlying emergent phenomena [70]. By deciphering the rules governing these interactions, we can uncover the principles driving the collective dynamics of microbial communities.

1.2 Community diversity, stability, and invasibility

Ecological systems, with their myriad interactions and complexities, have always been a subject of profound curiosity and study. Among the various dimensions of ecology, the intricate relationships between diversity, stability, and invasibility stand out, forming a triad of interdependent factors that shape ecosystems and their dynamics [75, 60].

Diversity is a multifaceted concept that goes beyond just the sheer number of species in an ecosystem [75]. It encompasses species richness, evenness, and the intricate web of interactions between them. Diverse ecosystems are often likened to a well-woven tapestry, where each thread, representing a species, plays a crucial role in maintaining the overall fabric [98]. Such systems often display increased productivity, resilience, and a broader range of ecosystem services, from soil fertility to water purification [98]. The rationale is that a diverse set of species can utilize a wider

array of resources and respond more robustly to perturbations [75].

Stability in ecosystems refers to their ability to withstand disturbances, whether they be climatic changes, disease outbreaks, or human interventions [5]. A stable ecosystem doesn't just recover after a disturbance; it retains its fundamental character and continues to provide its essential functions. Diversity can be a bedrock of stability, with different species compensating for each other during times of stress, ensuring that the ecosystem remains functional [44].

Invasibility provides a measure of an ecosystem's vulnerability to colonization by non-native or alien species [32]. This introduces a paradox. Highly diverse ecosystems, because of their efficient resource use, might be thought to be less prone to invasion [75]. They leave fewer niches vacant and fewer resources unexploited, thereby offering little room for invaders [32]. However, the flip side of this argument is that diverse ecosystems, precisely because of their multiplicity of niches, might provide numerous small opportunities for a variety of invaders to gain a toehold [7].

Invasive species, once established, can dramatically transform ecosystems [45]. Their impacts range from outcompeting or predating on native species to altering nutrient cycles and physical habitat structures. Such invasions can initiate a cascade of changes that ripple through the ecosystem, potentially affecting its stability and further altering its diversity [7].

The dynamic interplay between diversity, stability, and invasibility remains a pivotal theme in ecology [125]. As human influences continue to reshape our planet, from habitat fragmentation to climate change, understanding this triad becomes even more crucial [73]. It holds keys to preserving biodiversity, restoring damaged habitats, and predicting the future trajectories of our natural systems [123]. Delving deeper into the synergies and conflicts between these three pillars will not only further our academic understanding but will also offer practical insights for a world facing unprecedented ecological challenges.

1.3 Emergent phases of diversity and stability in microbial community

Species in nature coexist and interact within intricate and diverse communities, posing challenges for ecologists in understanding the factors influencing species coexistence, biodiversity patterns, community dynamics, and their impact on ecosystem functioning [128]. The stability-diversity debate has long focused on whether community diversity enhances or weakens stability, with environmental drivers identified as potential factors influencing these community features [87, 60]. Laboratory experiments offer a valuable platform to disentangle environmental drivers from inherent community properties, such as species interactions, that shape biodiversity and dynamics. While experimental communities with few species have revealed predictable dynamics and shed light on specific interactions like predation, competition, and cross-feeding, biodiverse laboratory microcosms derived from natural habitats have shown reproducibility and predictability only at higher taxonomic levels [50, 101, 114, 46, 136]. Given the challenge of obtaining detailed information on the ecological roles of every species, the question arises: can complex community biodiversity and dynamics be predicted using simple community-level parameters?

Since Robert May's pioneering work [84], ecologists have endeavored to understand community behaviors by examining community-level parameters, such as species richness and the distribution of interaction strengths. Interaction strengths, quantifying the influence of one species on others, play a crucial role in shaping community composition and stability [101]. Previous studies have suggested that high species richness and strong interactions can lead to unstable community dynamics [84, 122, 15, 144, 91]. However, our understanding of community behavior beyond this instability threshold remains limited. Recent theoretical advancements propose that species extinctions precede complete instability, and unstable communities may exhibit fluctuations that reinforce biodiversity [57, 95, 106, 4, 115, 127, 53]. Validating these theories has been challenging due to difficulties in estimating and manipulating associated parameters.

Experimental microcosms now offer the necessary control to test these theoretical predictions based on community-level parameters [136, 101, 50]. In my thesis, I aim to uncover the relationship between stability and diversity by experimentally manipulating two key factors typically unobservable in natural settings: the strength of interspecies interactions and the size of the introduced species pool. The crucial novelty of our work is finding an experimental system in which it is possible to tune interaction strength and number of species to transition between different dynamical phases predicted by theory. Constructing an experimental phase diagram of ecological diversity and dynamics, we find remarkable agreement with theoretical predictions: a specific sequence of three qualitative phases (stable coexistence, species loss, and persistent fluctuations), and higher numbers of surviving species in fluctuating communities. Our combination of theoretical and experimental results suggests that, while we cannot access all biological mechanisms and parameters in a complex system, its diversity and dynamics may be emergent phenomena that can be predicted from just a few aggregate properties of the ecological community.

1.4 Emergent invasion outcome in microbial community

Biological invasion, delves into the study of non-native species' introduction and spread in new ecosystems, and their consequent interactions with native species and environments [78]. At its core, this field seeks to understand the dynamics driving the success of invasive species and the impacts they exert on native biodiversity, ecosystem functions, and even human societies [142]. Historically, humans have inadvertently and, at times, intentionally facilitated the dispersal of organisms across regions, leading to unintended ecological consequences [113]. The ramifications of these invasions can be multifaceted, ranging from the alteration of nutrient cycling and energy flow in ecosystems to the displacement or extinction of native species [78]. Furthermore, the economic costs associated with managing and mitigating the impacts of invasive

species can be monumental [142]. The significance of ecological invasion as a discipline has grown in recent decades, especially in the face of increasing globalization, climate change, and habitat modification [22]. Today, it is a pivotal area of study, intertwining ecology, evolution, geography, and even socio-economic considerations, as researchers and policymakers alike grapple with the challenges and implications of species moving beyond their native ranges [22].

Microbial invasions, a frequent phenomenon in diverse ecosystems, deeply influence the dynamics and functioning of microbial communities [83]. These invasions can alter nutrient cycling, disrupt established symbiotic relationships, and even impact the overall health of larger organisms within the ecosystem [133, 52]. Understanding the mechanisms driving invasion success and the ecological repercussions of these incursions is vital for forecasting and managing ecosystem adaptations to these disturbances [99]. Factors such as competition, predation, and environmental conditions can play a role in determining the outcome of these invasions [28, 69]. Moreover, the adaptability of the invasive species, as well as the resilience of the resident microbial community [111], are also critical components. While research has made strides in certain areas, many aspects of the underlying mechanisms and ecological outcomes of microbial invasions still remain complex and poorly understood.

In this thesis, I delve into the world of microbial invasions, aiming to shed light on the determinants of invasion success and the ecological impacts on resident microbial communities. By combining theoretical frameworks and empirical studies, we explore the role of community-level features, interspecies interactions, species pool size, and environmental factors in shaping invasion outcomes. Although diversity-invasibility relationships are qualitatively different depending upon how the diversity is changed, we resolved the diversity-invasibility debate by showing a universal positive correspondence between invasibility and survival fraction across all conditions. Furthermore, we found communities composed of strongly interacting species exhibit emergent priority effect, as well as large invasion effect on resident community structure under successful invasions. Our findings contribute to the growing understanding of microbial invasions, providing insights into the ecological disruptions caused by these

encroachments and offering pathways for improved management strategies.

Understanding the emergent behavior of microbial communities has broad implications across diverse fields, ranging from environmental management and biotechnology to human health [141]. By harnessing the potential of self-organization and emergent properties, we can unlock new strategies for sustainable agriculture, wastewater treatment, and the development of novel therapeutics [42]. Ultimately, the study of emergent behavior in microbial communities provides a fascinating window into the remarkable collective intelligence of microorganisms and opens avenues for harnessing their potential for the benefit of humanity [59, 31].

Chapter 2

Emergent phases of ecological diversity and dynamics mapped in microcosms

2.1 Abstract

From tropical forests to gut microbiomes, ecological communities host striking numbers of coexisting species. Beyond high biodiversity, communities exhibit a range of complex dynamics that are difficult to explain under a unified framework. Using bacterial microcosms, we perform the first direct test of theory predicting that simple community-level features dictate emergent behaviors of communities. As either the number of species or the strength of interactions increases, we show that microbial ecosystems transition between three distinct dynamical phases, from a stable equilibrium where all species coexist, to partial coexistence, to emergence of persistent fluctuations in species abundances, in the order predicted by theory. Under fixed conditions, high biodiversity and fluctuations reinforce each other. Our results demonstrate predictable emergent patterns of diversity and dynamics in ecological communities.

2.2 Introduction

In nature, species reside and interact with myriad other species in complex communities [85]. Central challenges in ecology include understanding how many species are able to coexist, why biodiversity is higher in some places than others, why communities show varying dynamical behaviors [43, 18], and how these factors shape ecosystem functioning [80]. A long-standing debate concerns whether the diversity of a community enhances or weakens its stability [87]. By studying natural communities, ecologists have identified potential environmental drivers that could impact both of these community features [60]. Laboratory experiments facilitate disentangling such environmental drivers from inherent community properties, such as species interactions, that may also shape biodiversity and dynamics. Experimental communities with few species have been shown to display predictable dynamics, such as stable equilibria and periodic oscillations [46, 136, 12, 12, 48], and allowed to understand the role of interactions ranging from predation [12, 48] to competition [46, 136] to cross-feeding [114]. In more biodiverse laboratory microcosms derived from natural habitats, however, community composition is only reproducible and predictable at family or higher levels of taxonomy [18, 20, 101, 50]. Given the relative inaccessibility of detailed information on the ecological roles of every species (capturing every interaction strength, growth rate, carrying capacity, etc.), the question arises: is it possible to predict the biodiversity and dynamics of these complex communities with simple community-level parameters?

Starting with the pioneering work by Robert May [84], ecologists have sought to predict community behaviors using community-level parameters such as the number of species and the distribution of interaction strengths between species. The interaction strengths quantify how strongly a species influences the growth and survival of other organisms in the community, and therefore determines the overall composition and stability of communities [101]. May and others have suggested that a large number of species and strong interactions lead to instability of community dynamics [84, 122, 15, 144, 91], yet we still do not understand how communities behave be-

yond the transition to instability. Recent theory suggests that a fraction of species tends to go extinct before the community loses stability [24, 93, 63], and that unstable communities can exhibit fluctuations, which could in turn reinforce biodiversity [57, 95, 106, 4, 115, 127, 53]. This body of theory has been difficult to validate because the associated parameters are hard to estimate, and manipulate [86]. Experimental microcosms have now reached the necessary controllability [136, 101, 50] to test theoretical predictions based on community-level parameters of ecological communities. We aim to uncover the relationship between stability and diversity through experimentally controlling two factors that are usually unobservable in natural settings: the strength of interspecies interactions, and the number of species introduced in the experiment (referred to as the species pool size).

2.3 Results and Discussion

2.3.1 Theory predicts that community-level features shape phases of community diversity and dynamics

We began by summarizing the predictions on community dynamics and biodiversity from the well-known generalized Lotka-Volterra (gLV) model, modified to include dispersal from a species pool:

$$\frac{dN_i}{dt} = N_i(1 - \sum_{j=1}^{S} \alpha_{ij} N_j) + D \tag{2.1}$$

where N_i is the abundance of species i (normalized to its carrying capacity), α_{ij} is the interaction strength that captures how strongly species j inhibits species i (with self-regulation $\alpha_{ii} = 1$), and D is the dispersal rate. We simulated the dynamics of communities with different species pool sizes S and interaction matrices. We sampled the interaction strength from a uniform distribution U [0, $2\alpha_{ij}$], where $<\alpha_{ij}>$ is the mean interaction strength between species (which also determines here the variance of interactions, Supp. Material). Modeling species interactions as a random interaction network captures species heterogeneity without assuming any particular community

structure [84, 122, 63]. Our simulations revealed a strong dependence of biodiversity (number of coexisting species) and dynamics on both the species pool size S (Fig. 2-1A) and interaction strength $<\alpha_{ij}>$ (Fig. 2-1B). As either of these parameters increase, communities experience a transition from I) stable full coexistence—all species survive and reach stable abundances, to II) stable partial coexistence—some species go extinct, and the surviving ones reach stability, to III) persistent fluctuations in species abundances and biomass (Fig. 2-10, 2-11, 2-12, [103]. The transition to unstable dynamics (II to III) corresponds with the loss of linear stability of the equilibrium, consistent with May's theory (Fig. 2-13). These results agree with recent theory that derived analytically the existence of a phase transition from a unique stable state (I and II) to persistent fluctuations (III) [24, 93]. To address the ecological implications of these dynamical phases, we analyzed both the fraction of species that survive at equilibrium (Fig. 2-1C, E and 2-14) and the fraction of communities that exhibit persistent fluctuations (Fig. 2-1D, F). We found that the sequence of dynamical phases is generic across the parameter space: communities generally experience species extinctions before they lose stability as either of the control parameters increase. This sequence is both predicted by analytical expressions for the phase boundaries (Fig. 2-1C-F) and robust to different choices of interaction strength distributions and modeling assumptions (Fig. 2-15, 2-16) [24]. In particular, natural ecological communities display diverse interaction types which affects the degree of symmetry in the interaction matrix (α_{ij}), (e.g., competition and mutualism may be symmetrical whereas predation is antisymmetrical). We found that varying these properties of the interaction matrix does not qualitatively affect the dynamical phases (Fig. 2-6, 2-7). Other model choices, e.g. considering pH-mediated interactions or the serial dilution of communities into fresh media (Fig. 2-7, 2-8, 2-9, 2-17) [101], further showed the robustness and generic nature of the dynamical phases. Therefore, it may be possible to predict the diversity and dynamics of ecological communities from community-level features of the interaction network.

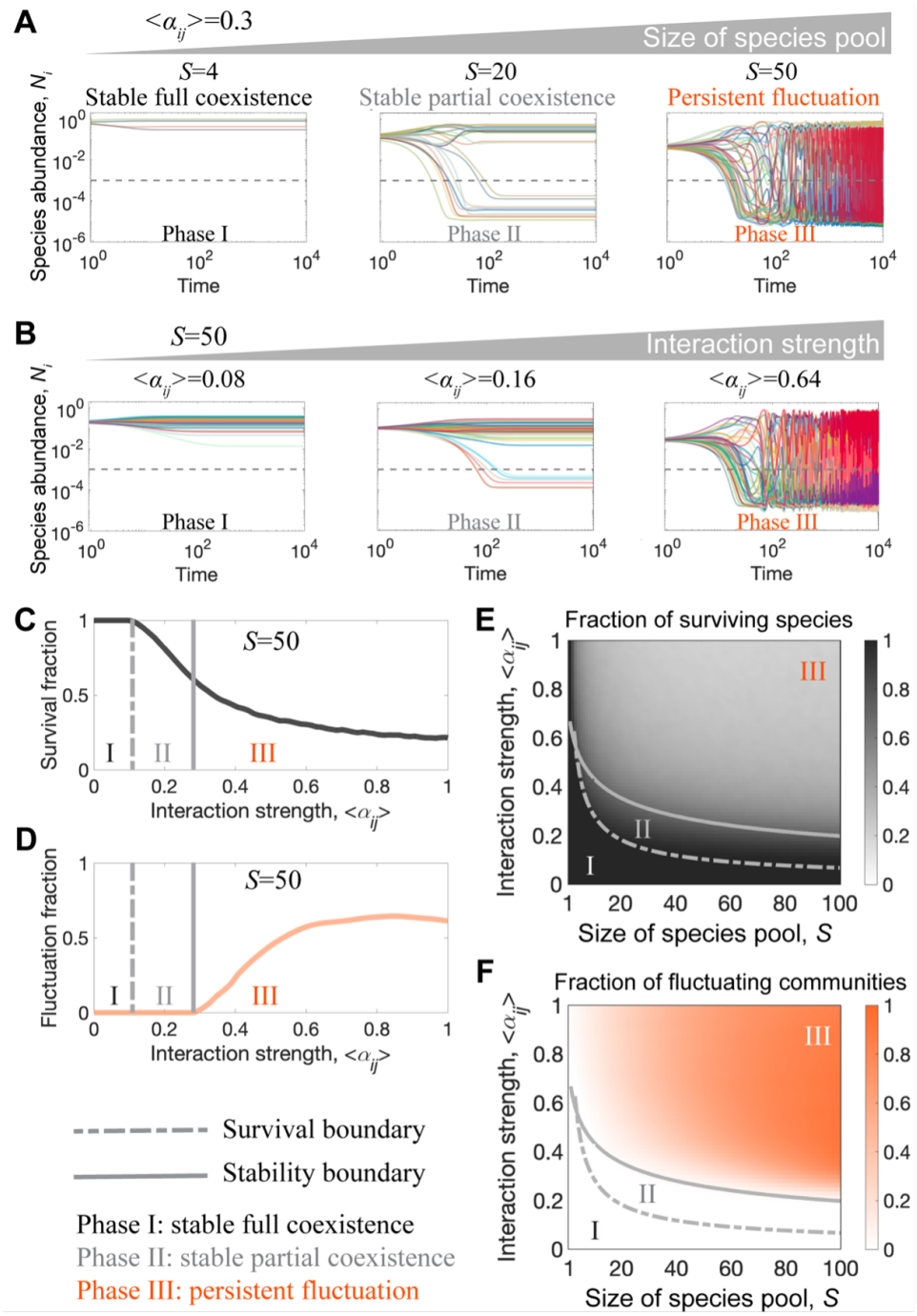
A
<α_{ij}>=0.3
Size of species pool
S=4
Stable full coexistence
S=20
Stable partial coexistence
S=50
Persistent fluctuation
Species abundance, N_i
Phase I
Phase II
Phase III
Time
B
S=50
Interaction strength
<α_{ij}>=0.08
<α_{ij}>=0.16
<α_{ij}>=0.64
C
Survival fraction
S=50
Interaction strength, <α_{ij}>
D
Fluctuation fraction
E
Fraction of surviving species
Interaction strength, <α_{ij}>
Size of species pool, S
F
Fraction of fluctuating communities
Survival boundary
Stability boundary
Phase I: stable full coexistence
Phase II: stable partial coexistence
Phase III: persistent fluctuation

Figure 2-1: Theory predicts that species pool size and interspecies interaction strength shape phases of community diversity and dynamics. (A) Representative time series of species abundance for the qualitatively different dynamics of communities with different species pool size S, under interaction strength $<\alpha_{ij}>$=0.3. Communities transition from stable full coexistence (S=4) to stable partial coexistence (S=20) to persistent fluctuations (S=80). Increasing interaction strength while fixing the species pool size (B) reveals analogous transitions. Mean fractions of (C) species that survive in the community, and (D) communities that exhibit persistent fluctuations. As interaction strength increases, communities lose species (transition from phase I to II, vertical dashed line) before losing stability (transition from phase II to III, solid vertical line). Mapping the survival fraction (E) and community fluctuation fraction (F) onto the phase space reveals that this sequence (phase I to phase II to phase III) of phase transitions is maintained as either of the control parameters increases. The gray dashed (solid) line shows the analytical solution for the survival (stability) boundary. The color maps depict the mean value over 1000 simulations [103].

2.3.2 Increasing species pool size or interaction strength leads to loss of stability in microbial communities

To experimentally test the predicted phase transitions, we built synthetic communities using a library of 48 bacterial isolates from terrestrial environments (Fig. 2-18, 2-19) [103]. Following inoculation, we exposed communities to cycles of growth, dispersal from the pool, and dilution, while monitoring community composition and biomass at the end of each daily cycle (Fig. 2-2A, [103]. Leveraging previous work [101], we tested media conditions to tune the strength of bacterial interactions. We found that the probability of coexistence in pair-wise co-culture decreased with the concentration of supplemented glucose and urea. In this media, an increase in the concentration of these nutrients therefore increases the strength of competitive interactions (Fig. 2-2B, Table A.1, A.2, A.3) As discussed in our previous work [101], high nutrient concentrations lead to extensive modification of the media (e.g. pH) and hence stronger interactions. This experimental platform allows us to control the key parameters established by theory: species pool size and interaction strength.

We experimentally mapped the phase space of community dynamics by exposing 63 species pools to three levels of interaction strength. Specifically, we tested 30 species pairs (S=2); 8 different communities for each size S=3, 6, 12, and 24; and

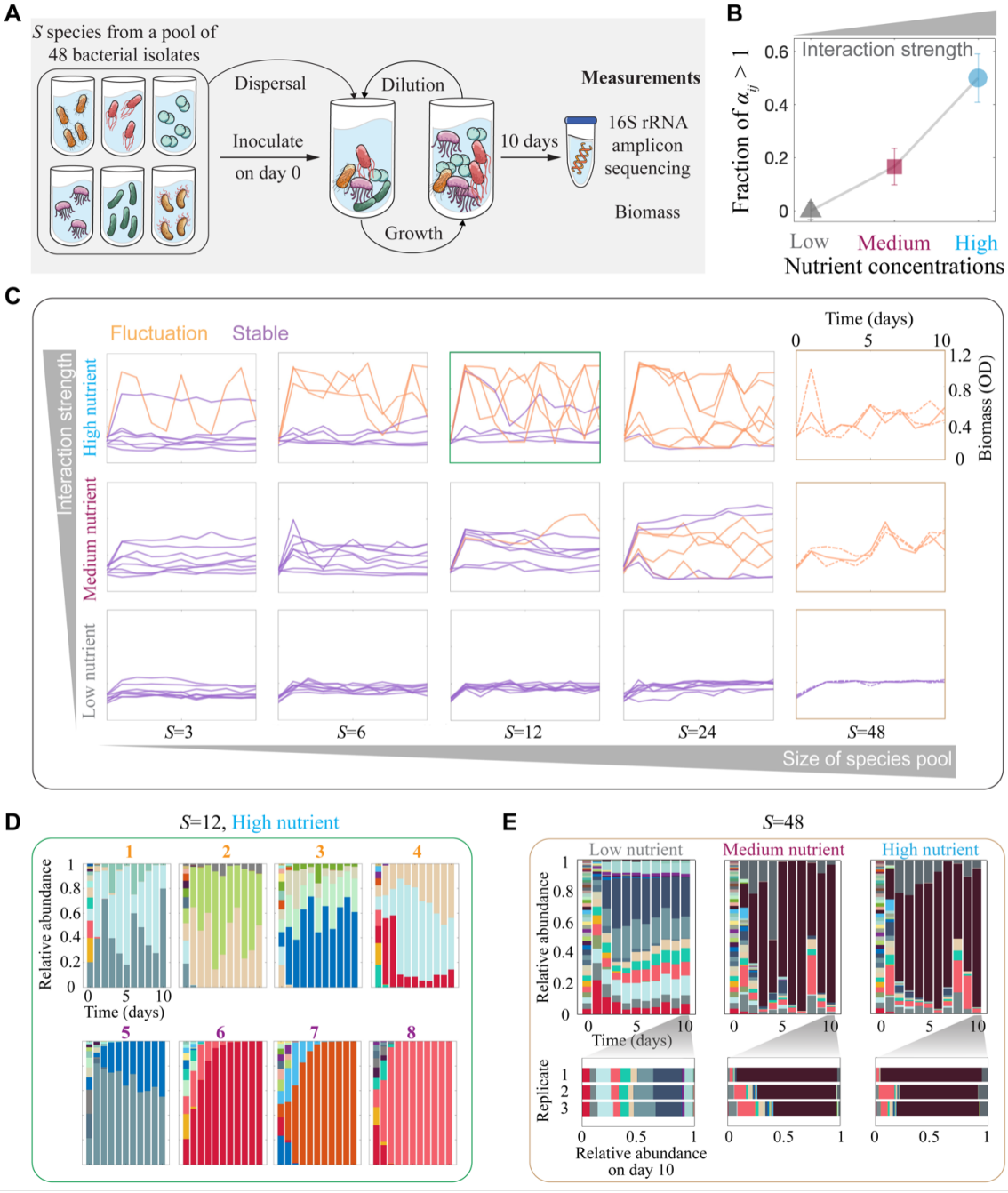
A
S species from a pool of 48 bacterial isolates
Dispersal
Dilution
Inoculate on day 0
10 days
Measurements
16S rRNA amplicon sequencing
Biomass
Growth
B
Interaction strength
Fraction of $\alpha_{ij} > 1$
0.6
0.4
0.2
0
Low
Medium
High
Nutrient concentrations
C
Fluctuation
Stable
Time (days)
0
5
10
1.2
0.8
0.4
0
Biomass (OD)
Interaction strength
High nutrient
Medium nutrient
Low nutrient
S=3
S=6
S=12
S=24
S=48
Size of species pool
D
S=12, High nutrient
1
2
3
4
5
6
7
8
Relative abundance
1
0.8
0.6
0.4
0.2
0
0
5
10
Time (days)
E
S=48
Low nutrient
Medium nutrient
High nutrient
Relative abundance
Time (days)
Replicate
1
2
3
0
0.5
1
Relative abundance on day 10

Figure 2-2: Increasing species pool size or interaction strength leads to loss of stability in microbial communities. (A) We used a library of 48 bacteria to generate species pools of different sizes and compositions. Co-cultures underwent serial dilutions with additional dispersal from the pool. Community composition and total biomass were monitored via 16S sequencing and optical density (OD). (B) In 2-species co-cultures, interaction strengths leading to the loss of coexistence ($\alpha_{ij} > 1$) increase in frequency with nutrients concentration. Error bars, s.e.m., n=30. (C) Fluctuations in community biomass increase with either species pool size or interaction strength. Solid lines stand for 8 different species pool compositions (dashed lines, replicates of the 48 species community). Purple (orange) lines highlight stable (fluctuating) dynamics. (D) Under high nutrient, half of the 12-species communities exhibit persistent fluctuations (top panels) in species abundances, and the rest reached stability (bottom). (E) Time series (top panels) for the species abundances in 48-species communities. Stability was reached only under low nutrients, and variability in end-point relative abundances increased with nutrients concentration (bottom panels, Fig. S15). Relative abundance plots show the Amplicon Sequence Variants (ASVs) data of individual replicates.

1 community of S=48 (the full species library). The resulting biomass time series were relatively stable under low interaction strength and small species pool size, while increasing these two variables progressively led to a higher fraction of communities exhibiting biomass fluctuations (Fig. 2-2C). Analyzing species abundances through 16S sequencing (Fig. 2-2D and 2-2E), we found that biomass fluctuations were highly correlated with species abundance fluctuations (Fig. 2-20, 2-21). For example, for communities with 12 species in the pool and high nutrient concentration, 4 communities reached stable equilibria, and the remaining 4 exhibited fluctuations in both biomass and species abundances until the end of the experiment (Fig. 2-2C and 2-2D). Replicates with identical species pool composition exhibited highly reproducible dynamics (Fig. 2-22, 2-23, 2-24, 2-25, 2-26, 2-27, 2-28, 2-29, 2-30), and the classification of stable and fluctuating communities was robust to different methods analyzing biomass, species composition, and variations between replicates ([103], Fig. 2-20, 2-21). We also experimentally observed this transition towards unstable dynamics under different carbon sources and dilution frequencies (Fig. 2-5). Therefore, synthetic microbial communities lose stability as either species pool size (for $S > 2$) or interaction strength increases.

2.3.3 Species pool size and interaction strength determine the diversity and dynamics of experimental communities

To understand the relationship between species extinctions and loss of community stability, we analyzed species survival across these experiments. As expected, the fraction of surviving species decreased with either species pool size or interaction strength—determined by nutrient concentration (Fig. 2-3A). For example, at medium interaction strength 83% (+/- 3%) of species were able to survive in the 30 pairwise (S=2) co-cultures, while this frequency decreased to 36% (+/- 7%) among the eight different combinations of six species communities (S=6, Fig. 2-3A). Despite the significant loss of species, none of these communities displayed persistent fluctuations (Fig. 2-3B). Such fluctuations arose with further increase of the species pool size, with half of the 24-species combinations displaying fluctuations (Fig. 2-3B). Interestingly, the species survival fraction displayed only a modest decrease entering the fluctuation regime, with 24% (+/- 2%) of species surviving in the 24-species communities as compared to 36% (+/- 7%) in the 6-species communities (Fig. 2-3A and 2-3B). Mapping these experimental results over the phase space (Fig. 2-3C and D) confirmed the theoretically-predicted (Fig. 2-1E and F) sequence of transitions: communities experience species extinctions before exhibiting persistent fluctuations, as either species pool size or interaction strength increases.

2.3.4 Fluctuating communities are more diverse than stable communities under the same conditions

Next, through analyzing species survival fraction across different species pool compositions, we addressed how fluctuations and diversity may influence each other. In simulations, the fraction of surviving species revealed a generic trend: for the same species pool size and interaction strength, fluctuating communities were more diverse than stable communities (Fig. 2-4A). This trend was also observed in experiments: the majority of fluctuating communities reached higher survival fractions than stable communities under the same conditions (Fig. 2-4B and 2-32). For example,

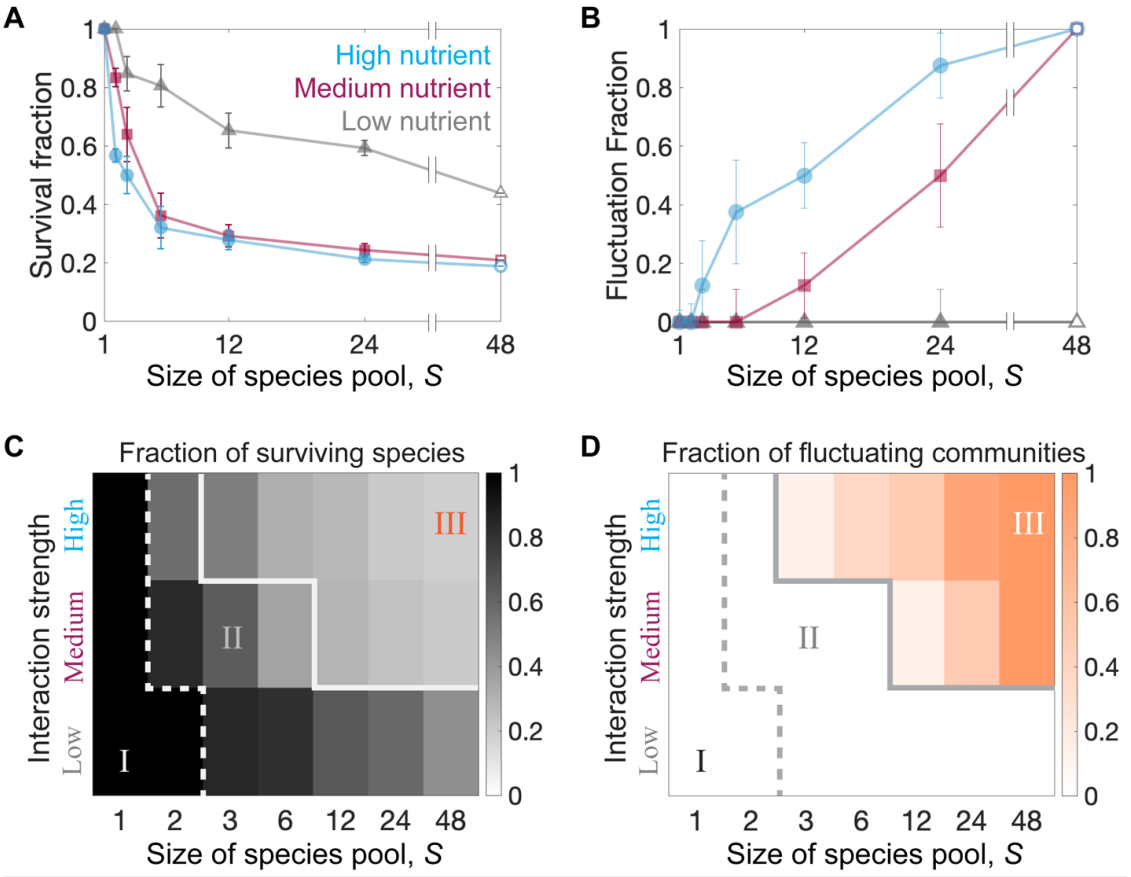

Figure 2-3: Species pool size and interaction strength determine the diversity and dynamics of experimental communities. (A) The fraction of surviving species decreases with either species pool size or interaction strength (nutrient concentration). The survival fraction decreases more slowly at high S and strong interaction strength. (B) The fraction of fluctuating communities increases with either species pool size or interaction strength. (C) Phase diagram for the fraction of species surviving in experimental communities. As communities cross the boundary of phase I (dashed line), they experience species extinctions, with a fast decay in survival fraction through phase II, and a relative maintenance of survival fraction through phase III. (D) Phase diagram for the fraction of fluctuating communities in experiments. Communities start exhibiting persistent fluctuations after crossing the boundary into phase III (solid gray line). Error bars, s.e.m., n=8.

within the 12-species communities, fluctuating communities had on average 5 +/- 1 species surviving, as compared to only 2+/- 1 species surviving in stable communities. Among the fluctuating communities, 88% (+/-5%) exhibited survival fractions above or equal to the mean, as compared to only 14% (+/- 6%) among the stable communities ($p<0.01$,(32)). Both experiments and simulations suggest that fluctuations are an emergent, diversity-dependent phenomenon, as the addition of species pools from stable communities often yielded larger, fluctuating communities (Fig. 2-33). We also found numerically that fluctuations and high diversity disappeared together as we stopped dispersal or pinned the abundance of the most abundant species (Fig. 2-10). Our results show that diversity and persistent fluctuations enhance each other, as theoretically demonstrated in previous work [95, 106].

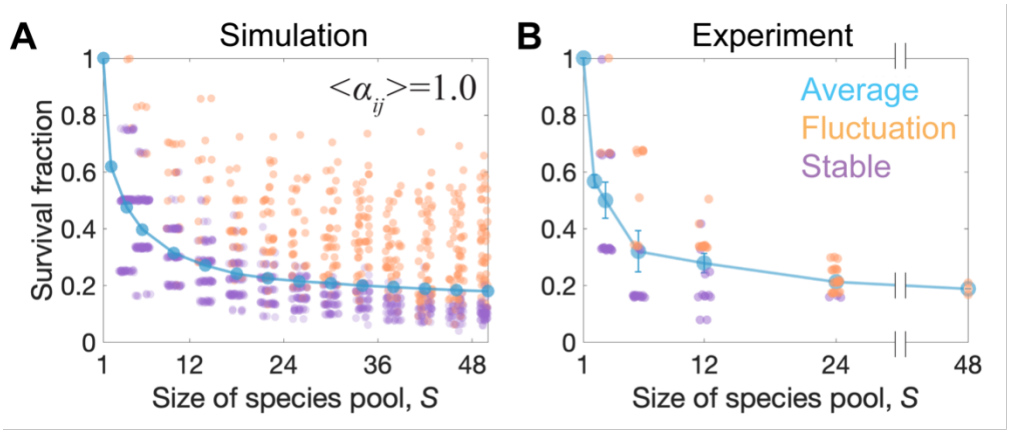

Figure 2-4: Fluctuating communities are more diverse than stable communities under the same conditions. (A) As the average survival fraction decreases with increasing species pool size S in simulations, more communities exhibit fluctuations in species abundances (orange points). While stable communities (purple) exhibit a steady decrease in species survival fraction with S, the loss of species is slower in fluctuating communities. Each point represents an individual community. (B) In experiments under high nutrient concentration (also under lower nutrients concentrations, Fig. S28), fluctuating communities exhibit a higher survival fraction than stable communities. The survival fractions of 88% (+/-5%) of the fluctuating communities are above or equal to the mean, as compared to 14% (+/- 6%) in the case of stable communities ($p<0.01$, [103]; error bars, s.e.m., n=8.

2.3.5 The phases of community dynamics are robust to changes in carbon source and dilution frequency

We found the phases of community dynamics are robust to changes in carbon source and dilution frequency. Persistent fluctuations can occur under different carbon sources. After replacing glucose by succinate in the media, high nutrients concentration still yields biomass fluctuations in some communities (Fig. 2-5). Two out of eight communities fluctuate in both glucose and succinate, four reach steady state in both glucose and succinate, and the remaining two communities fluctuate in medium with glucose, while reaching a steady state in medium with succinate. furthermore, we show community dynamics are robust to different choices of dilution frequency. 24-hours transfers and 48-hours transfers yield analogous biomass dynamics for the eight different 12-species communities under high nutrients concentration (Fig. 2-5). Communities that reach persistent fluctuations (stability) under 24-hours-transfers also reach persistent fluctuations (stability) under 48-hours-transfers. Fig. 2-5C shows the rank plot for the standard deviation of biomass between days 7 and 10 for communities under succinate. The rank of each community was based on the mean value of the standard deviation of the three replicates. A K-means clustering algorithm considering standard deviation of biomass over days 7-10 clusters communities into two fluctuating (orange points) ones and six stable (purple points) ones. Fig. 2-5D shows the rank plot for the standard deviation of biomass between days 10 and 16 for communities under 48-hours transfers. In this case, the K-means clustering algorithm considering standard deviation of biomass over day10-16 clusters communities into four fluctuating (orange points) ones and four stable (purple points) ones. The three replicates of each community are consistently classified as either fluctuating or stable ones, which are shown as three data points for each community rank.

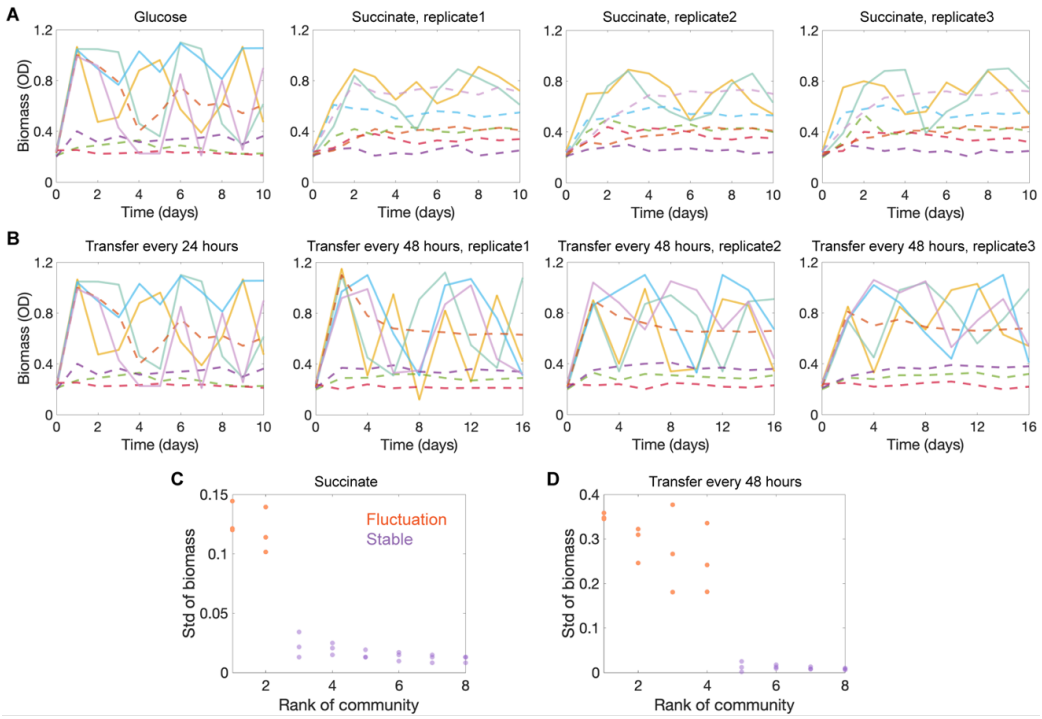

Figure 2-5: The phases of community dynamics are robust to changes in carbon source and dilution frequency. (A) Persistent fluctuations can occur under different carbon sources. After replacing glucose (leftmost panel) by succinate (right panels) in the media, high nutrients concentration still yields biomass fluctuations in some communities. Each panel shows the time series for the OD of the eight communities with different species pool composition (depicted by different colors). Solid lines (dashed lines) represent fluctuating (stable) communities. (B) Community dynamics are robust to different choices of dilution frequency. Each panel shows the time series for the OD of the eight communities with different species pool composition (depicted by different colors). Each of the three rightmost panels show the results for one of the three experimental replicates performed. (C) Rank plot for the standard deviation of biomass between days 7 and 10 for communities under succinate. (D) Rank plot for the standard deviation of biomass between days 10 and 16 for communities under 48-hours transfers.

2.3.6 The emergent phases of communities are robust to various interaction symmetries and types

To show that symmetry and anti-symmetry do not qualitatively change the phase diagram, we simulated communities in two scenarios of non-zero reciprocity, γ=0.5 and γ=-0.5 , where the reciprocity of interactions is given by γ=corr(α_{ij},α_{ji}). The qualitative patterns and order of transitions in the phase diagram (Fig. 2-6) are robust to the presence of reciprocity, although γ shifts the stability boundary (solid line in Fig. 2-6). Positive and negative reciprocity decreases and increases the values of S and $<\alpha_{ij}>$ at which communities lose stability, respectively. Moreover, positive (negative) reciprocity yields lower (higher) survival fraction and fluctuation fraction of communities. At full symmetry and anti-symmetry (γ =1, -1) there is no fluctuating phase [24], but those do not appear to be relevant from the experiment pair-competition results (Table. A.1, A.2, A.3).

To test whether the existence of positive (facilitative) interactions in the ecological network will change our conclusions, we sampled values of α_{ij} from a uniform distribution [-α_0, α_0], where α_0 varies between [0, 1.4] on the phase diagram. In this simulation, the linear interaction function in the gLV (α_{ij} N_j) is replaced with Monod function ($\alpha_{ij}N_j/(N_j+1)$) to avoid unbounded growth due to positive interactions [24, 107]. We observed similar patterns of survival fraction and fluctuation fraction between pure competitive interactions and considering positive interactions (Fig. 2-7). The first and second moment of the distribution of α_{ij} should be considered to quantify interaction strength in the stability criteria [122]]. Here we use Std (α_{ij}) to quantify the interaction strength because the first moment of α_{ij} distribution is zero. Our results demonstrate that the existence of three phases (full coexistence, partial coexistence, persistence fluctuation) and the order of transitions are robust to the interaction types in the model. These phase diagrams results demonstrate that the existence of three phases (full coexistence, partial coexistence, persistence fluctuation) and the order of transitions are robust to varying interaction types in the model (communities lose species before losing stability as the size of species pool S

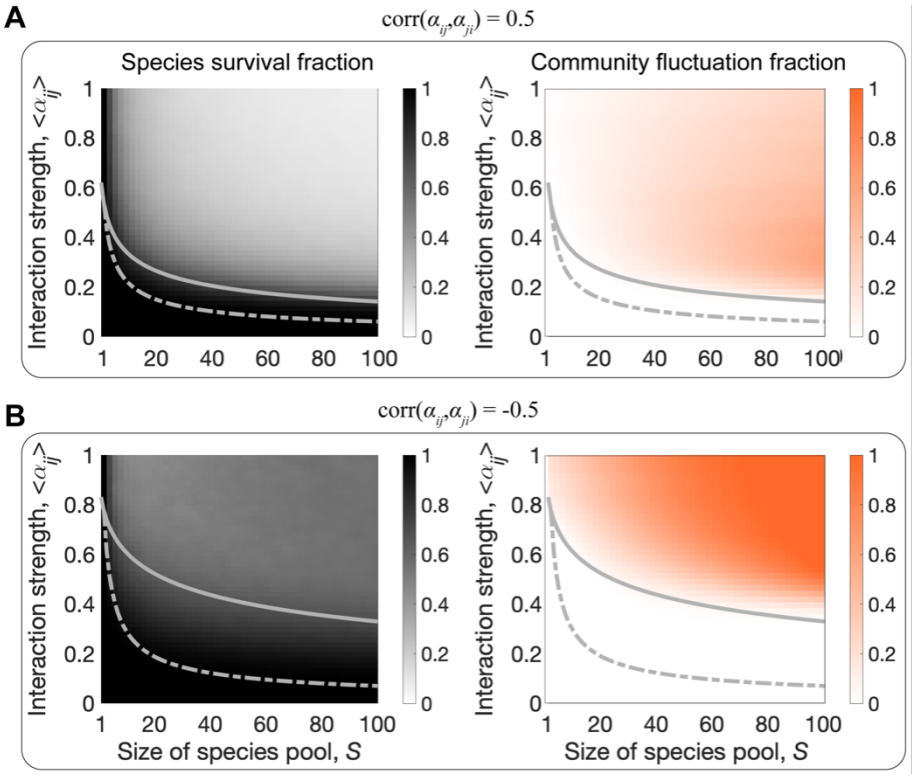

Figure 2-6: The three dynamical phases are qualitatively robust to the presence of reciprocity in interspecies interactions. The panels show the theoretical phase diagrams of species survival fraction (left) and community fluctuation fraction (right) for two cases of non-zero reciprocity, γ=corr(α_{ij},α_{ji})$\neq$0. (A) The fluctuating phase (partial coexistence phase) is larger (smaller) in the presence of positive reciprocity (corr(α_{ij},α_{ji})=0.5) than in the absence of reciprocity (corr(α_{ij},α_{ji})=0, Fig. 2-1E and F). The fluctuation fraction also increases with positive reciprocity. (B) The fluctuating phase (partial coexistence phase) is smaller (larger) in the presence of negative reciprocity (corr(α_{ij},α_{ji})=-0.5) than in the absence of reciprocity (Fig. 2-1E and F). The fluctuation fraction is higher in communities with negative reciprocity than communities with zero reciprocity. The dashed line and solid line in the figures represent survival boundary and stability boundary, respectively. Overall, the same qualitative phases and ordering are found as for communities with zero reciprocity (Fig. 2-1E and F), with non-zero reciprocity leading to quantitative differences.

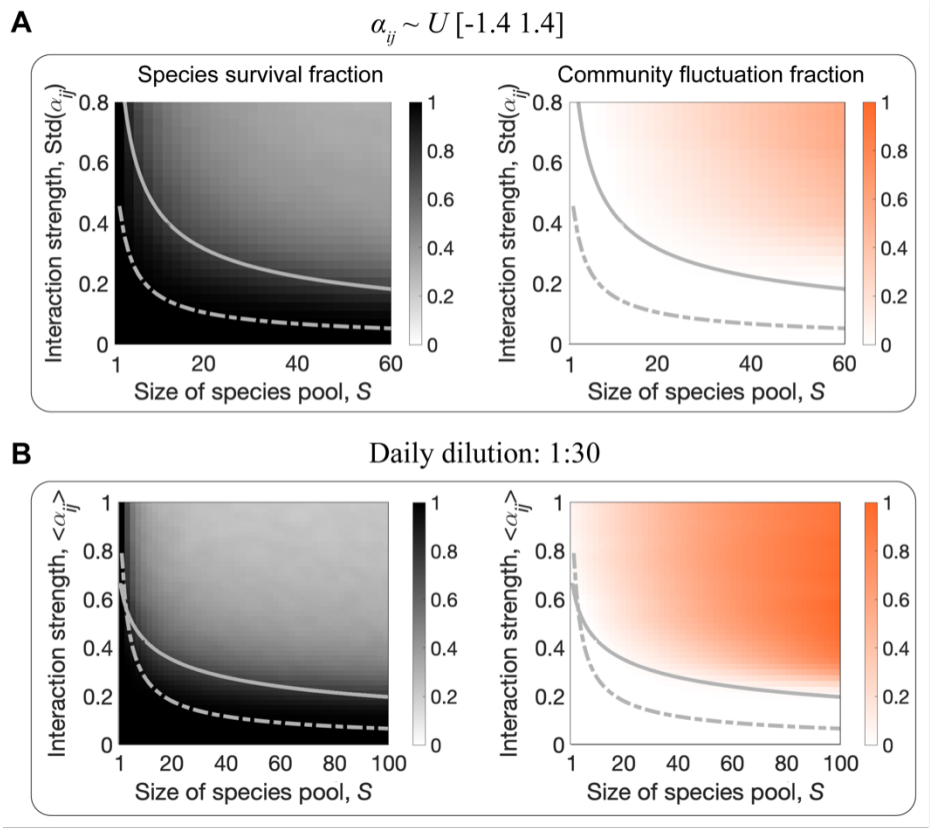

Figure 2-7: The three dynamical phases are qualitatively robust to the presence of positive interactions and serial dilutions in gLV. (A) To test whether the existence of positive (facilitative) interactions in the ecological network could change our conclusions, we sampled values of α_{ij} from a uniform distribution [-α_0, α_0], where α_0 varies between [0, 1.4] on the phase diagram. We observed patterns of species survival fraction (left panel) and fluctuation fraction (right panel) analogous to those exhibited by communities with exclusively negative interactions (Fig. 2-1). The dashed line and solid line in both panels represent survival boundary and stability boundary, respectively. Note that the strength of interactions coincides with Std (α_{ij}) in this case, since the mean of α_{ij} is zero (both moments factor into the interaction strength metric std(α_{ij})/(1-<α_{ij}>) that determines stability (17)). In these simulations, the linear interaction function in the gLV (α_{ij} N_j) was replaced with Monod function (α_{ij} $N_j/(N_j+1)$) to avoid unbounded growth due to positive interactions [24, 107].(B) In silico communities undergoing serial dilutions exhibit the same three dynamical phases (full coexistence, partial coexistence, and fluctuation) as in simulations without dilution. The two phase diagrams show that communities exposed to serial dilutions (1:30 dilution every 24 hours) lose species before losing stability as the size of species pool S or interaction strength increases, which is consistent with simulations of the continuous (no dilutions) model (Fig. 2-1E and F). The dashed line and solid line in the figures represent the survival boundary and stability boundary, respectively.

or interaction strength increases, as in Fig. 2-1E and F). The dashed line and solid line in the figures represent survival boundary and stability boundary, respectively.

2.3.7 Theoretical alternatives to the Lotka-Volterra model

The Lotka-Volterra model provides a phenomenological representation of bacterial growth and interactions, but our conclusions are not tied to this specific model. It is important to understand whether our central theoretical predictions generalize: how broadly do we expect a similar qualitative map of dynamical phases, where extinctions start to occur before the onset of fluctuations (as we increase either species pool size or interaction strength)? This empirically-observed ordering of phases is not self-evident: it is straightforward to construct few-species models that display fluctuations without extinctions, e.g. predator-prey pairs. Therefore, if our qualitative phase ordering appears across a range of many-species models and experiments, we may be seeing a broad mechanism, one that is presumably collective rather than driven by particular species.

One interesting question is whether these collective dynamics emerge from many independent pairwise species interactions (as in our random Lotka-Volterra model), or whether they are driven by one or a few system-wide factors, such as public goods impacting all species. Ratzke et al. [101] performed bacterial experiments and introduced a different model where all interactions are mediated by modifications of the environmental pH by the bacteria, whose growth is in turn modified by pH. This pH-based model, and a variant, reproduced some experimental results in [101, 103]. We slightly amend the model in [101] to represent continuous-time dilution and dispersal from the species pool (we have also simulated discrete daily dilutions and dispersal, with no impact on our conclusions).

$$\frac{dN_i}{dt} = k_{growth} N_i (1 - N_i) f(p - p_{0i}) - c_{dilution} N_i + D \tag{2.2}$$

where $f(x) = 1$, if $x \in [-p_c, p_c]$

$f(x) = -1$, otherwise

$$\frac{dp}{dt} = \sum_{i=1}^{S} c_i N_i + c_{dilution}(7 - p) \tag{2.3}$$

Equation 2.2 represents the growth of bacterial abundance N_i, which follows a logistic equation with parameter $k_{growth} = 10$ modulated by the pH value p: growth is maximal when this value is equal to species i's pH optimum p_{0i} (drawn uniformly over $[4.5, 9.5]$), with a tolerance given by $p_c = 2$. In addition, parameter $c_{dilution} = 3.4$ (continuous-time equivalent to our 1:30 daily dilution) encompasses losses due to dilution, whereas $D = 10^{-6}$ represents dispersal from the species pool. Equation 2.3 represents the change of pH induced by the bacteria and the return toward the neutral pH value of 7 due to dilution. The distribution of c_i, drawn uniformly over $[-c, c]$, thus determines the impact of bacteria on pH and indirectly the strength of interactions between bacteria.

We find that this model reproduces some of the main predictions of the Lotka-Volterra model: as seen in Fig. 2-8, the phase diagram with its three phases is qualitatively preserved in this second model, which suggests that it is highly robust to variations in modelling assumptions. Nevertheless, we believe that the LV model better reproduces our experimental results, whereas the pH-based model was more adequate in [101, 103], plausibly due to different taxa (species that exhibit ecological suicide do not appear in our species pool here) and experimental conditions (lower dilution rate) that lead to stronger impacts of pH. Indeed, there are three points that make the LV model more plausible here:

1) In our experiments, pH fluctuations are only moderately correlated (Pearson correlation coefficient: 0.54) with fluctuations in optical density or species composition (whereas the latter two are highly correlated), suggesting that pH is not the sole driving factor of stability here. (Fig 2-9A)

2) The pH-based models in [101, 103] notably aimed to allow for ecological suicide, i.e. species growing then going extinct in monoculture, which does not occur in our experiment (In our initial species pool, we only retained species that survived in all of our growth conditions for the convenience of daily dispersal, Fig. 2-31). In the

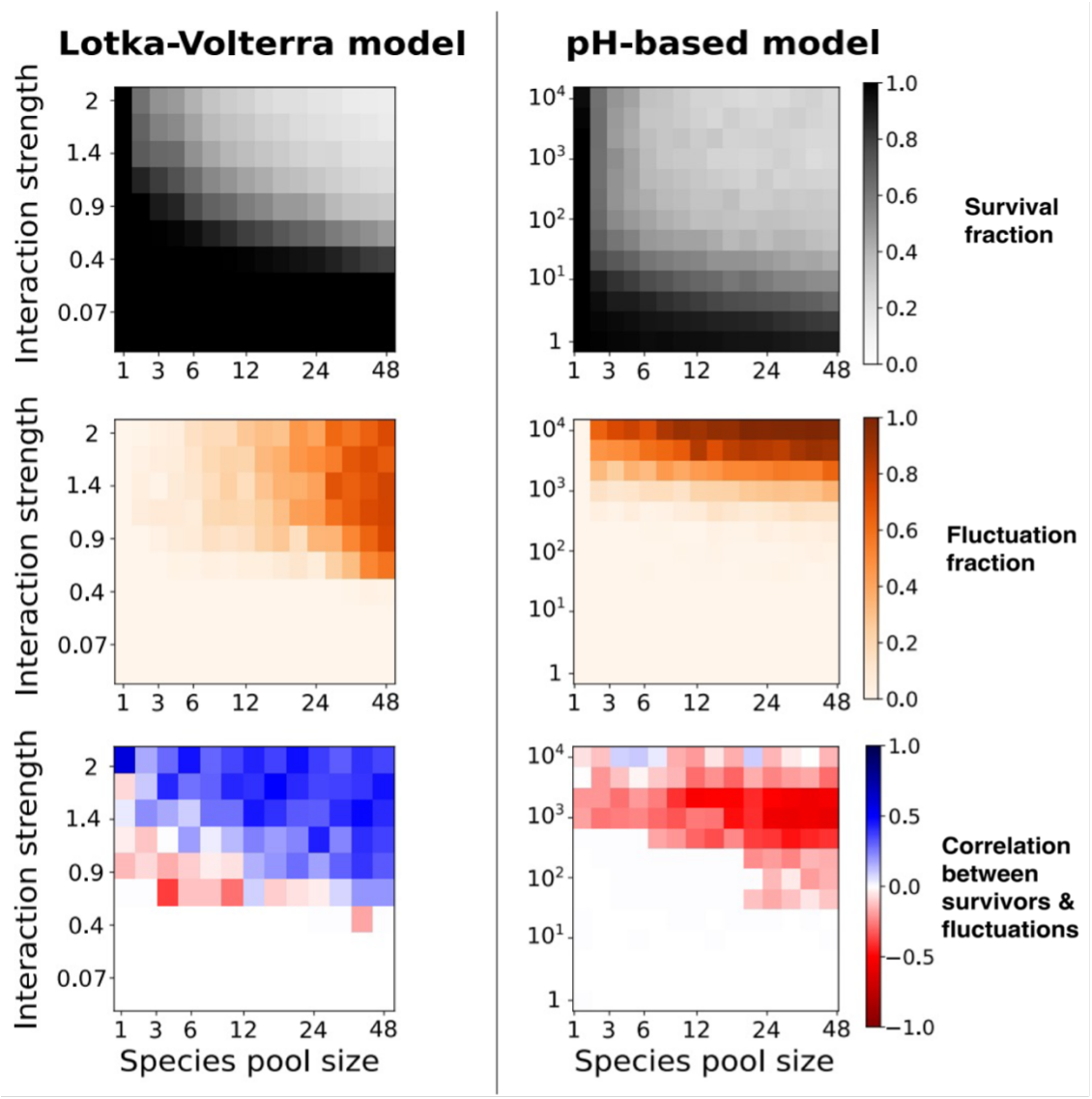

Figure 2-8: Comparison between the Lotka-Volterra and pH-based models. The topmost two rows display survival and fluctuation fraction, demonstrating that they similarly depend on the parameters of species pool size and interaction strength, in the Lotka-Volterra model (left column, equation 1, with interaction strength given by $<\alpha_{ij}>$) and a pH-based model proposed for previous experiments [101] (right column, equations 2 and 3, with interaction strength given by max (c_i)). We conclude that the three dynamical phases are qualitatively robust to different modeling choices. On the other hand, the third row shows that the two models disagree regarding correlations between the number of surviving species and the presence of fluctuations (for different communities with the same parameters) as further discussed in Fig. 2-9.

high-interaction strength regime and large initial species pool size regime, the pH-based model has two main outcomes: either many-species fluctuations, or total or near-total extinction with zero or few species surviving, and total biomass $< 5\%$ of carrying capacity (Fig 2-9B). Only the former behavior is seen in our experiments; the latter prediction of pH-based model was never observed in our experiments (Fig. 2-2C and Fig. 2-31).

3) The LV model displays positive correlation between the number of surviving species and the intensity of fluctuations, as in our experiments (Fig. 2-4 and Fig. 2-9), whereas the pH-based model displays a negative correlation (we exclude communities falling under the above extinction criterion, which were never observed in our experiment, Fig. 2-9C). The positive relation between diversity and fluctuations, validated in our experiments, is key to our theoretical argument.

These three reasons lead us to retain the Lotka-Volterra model as our prime example (see Fig. 2-17 for a best-fit illustration). This cannot rule out a different pH-based model, or a combination of pH-based and direct interactions, as a good description of the biological mechanisms at play in our experimental setting. We reach two main conclusions: i) The random Lotka-Volterra model provides a straightforward prototype of a mechanism that fits our theoretical argument. The dynamical phases are unambiguously emergent, in the sense of being driven by species diversity and local pairwise interactions. The picture is as follows: the fluctuating phase must appear after extinctions and turnover in species composition, since fluctuations are driven by a tendency to jump between alternate sets of surviving species, each of them unstable. ii) We expect this central prediction to hold broadly under different modelling choices. Indeed, we find that the pH-based model displays an analogous set of regimes and transitions (Fig. 2-8), even though its predictions do not match some of our experimental results as accurately as the LV model (Fig. 2-9). In both models, increasing the number of species and the strength of their interactions, whether direct or mediated through an abiotic factor, will typically lead to extinctions before it leads to loss of stability. This results in a phase of partial coexistence preceding a phase of instability, no matter whether species diversity and extinctions are necessary (as in the

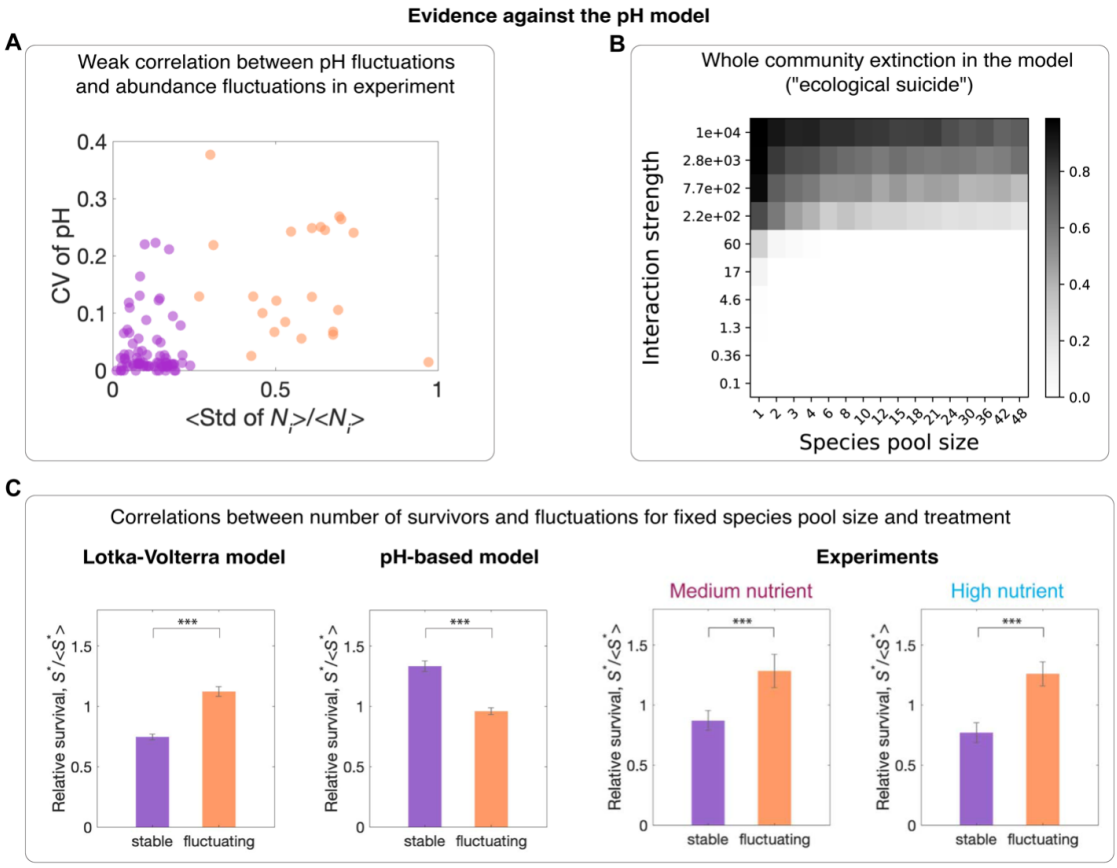

Figure 2-9: The LV model reproduces experimental observations better than the pH-based model. (A) Empirical data shows rather weak correlation (Pearson correlation coefficient: 0.54) between the intensity of fluctuations of pH and of abundances, suggesting that pH is not the sole or main driving factor in species dynamics. (B) The pH-based model proposed in [101] often displays community extinction (total abundance $< 5\%$ of carrying capacity), which we do not observe in our experiments. (C) In experiments and in the LV model, conditioning on species pool size and nutrients, various communities show positive correlations between fluctuations and diversity, measured here as $S^*/<S^*>$ the number of surviving species relative to the average number of survivors for that same pool size and nutrients. The pH-based model displays negative correlations (we exclude cases of whole community extinction which were never observed in our experiments). The relative survival fraction is statistically higher (lower) in fluctuating communities than stable communities in experiments and LV model (pH-based model, $p<0.001$). Error bars, s.e.m., n=100 for simulation data, n=51 (33) for stable communities in high (medium) nutrient, n=45 (15) for fluctuating communities in high (medium) nutrient.

random LV model) or not (as in the pH-based model) for the mechanism that drives fluctuations. We propose that this ordering, which is robust in many-species models but need not be in few-species models, can be an indicator of emergent collective behavior.

2.4 Methods and Materials

2.4.1 Bacterial isolates, media and culturing conditions

We constructed the library of 48 bacterial species using 24 bacterial isolates from soil samples taken at Middlesex Fells Reservation in Somerville, Massachusetts, and 24 isolates from the C. elegans intestine. This library is phylogenetically diverse, with isolates coming from 26 different families among 4 phylums: Proteobacteria, Firmicutes, Bacteroidota and Actinobacteriota (Fig. 2-18, 2-19).

In the case of low interaction strength (low nutrients concentration) conditions, experimental communities were cultured in Base Medium (BM): 1g/L yeast extract and 1 g/L soytone from Becton Dickinson, 10 mM sodium phosphate, 0.1 mM $CaCl_2$, 2 mM $MgCl_2$, 4mg/L $NiSO_4$ and 50 mg/L $MnCl_2$, pH adjusted to 6.5. For intermediate interaction strength (medium nutrients concentration) conditions, we used BM supplemented with 5 g/L glucose and 4 g/L urea. For the high interaction strength (high nutrients concentration) condition, we used BM supplemented with 20 g/L glucose and 16 g/L urea. All media were filter sterilized using Bottle Top Filtration Units (VWR). All of the chemicals were purchased from Sigma–Aldrich unless otherwise stated.

Both monocultures and communities of the bacterial isolates were grown in 96-deepwell plates (Deepwell plate 96/1000μL; Eppendorf) covered with AeraSeal adhesive sealing films (Excel Scientific). The incubation temperature was 30 °C for all communities. The deepwell plates were shaken at 1,200 r.p.m. on Titramax shakers (Heidolph). To minimize evaporation, the plates were incubated inside custom-built acrylic boxes.

2.4.2 Pre-cultures, daily dilutions, dispersal, and biomass measurements

Before each experiment, pre-cultures were initiated by thawing the bacteria and inoculating individual species into 600 μL of BM. The resulting monocultures were exposed to 5 daily cycles of growth and (30-fold) dilution into fresh media. At the beginning of each experiment, aliquots of these monocultures were mixed in equal volume proportions to form the synthetic communities. During the experiment, the monocultures were exposed to further dilution cycles and used to apply the daily dispersal into the synthetic communities as described below.

We created 63 different synthetic communities using randomly generated subsets of the library of isolates, each subset constituting the species pool (of size S) for each community. After mixing monocultures in equal volumes, each experimental community was initiated by inoculating 20 μL of its initial mix of isolates into 600 μL of BM, repeating the process to generate a total of 3 biological replicates per community. To form the communities with $S \leq 12$, we created random subsets of species from the soil isolates, and for $S > 12$ we randomly matched both soil and C. elegans isolates. To form synthetic communities with $3 \leq S \leq 12$, we distributed the 24 soil isolates into 8 groups (group A-H), where each group included 3 randomly chosen, different isolates. We used these groups to form 3-species communities ($S = 3$). To form eight 6-species communities ($S = 6$), we combined the eight pairs of 3-species groups (A-H) in the following way: (A+B), (C+D), (E+F), (G+H), (A+H), (B+G), (C+F), (D+E). To form eight 12-species communities ($S = 12$), we combined the eight pairs of 3-species groups (A-H) in the following way: (A+B+C+D), (E+F+G+H), (A+H+B+G), (C+F+D+E), (A+B+E+F), (C+D+G+H), (A+H+C+F), (B+G+D+E).

To form synthetic communities with $S = 24$, we randomly distributed the 24 soil isolates into 4 groups (group A-D) and the 24 C. elegans isolates into another 4 groups (group E-H), each of these groups including 6 different isolates. To form eight 24-species communities ($S = 24$), we combined the eight pairs of 6-species groups (A-H) in the following way: (A+B+C+D), (E+F+G+H), (A+H+B+G),

(C+F+D+E), (A+B+E+F), (C+D+G+H), (A+H+C+F), (B+G+D+E). We used the whole species pool (24 soil isolates and 24 C. elegans isolates) to form the single 48-species community ($S = 48$).

The resulting synthetic communities were cultured under serial dilution cycles with dispersal as follows. To apply a 10^{-6} dispersal rate, every 24hr monoculture aliquots of the species in each community pool were mixed at equal volumes, and then diluted by a 10^4 factor before inoculating 6 μL of this mix into the wells containing the corresponding experimental community matching each species pool. After this, the experimental cultures were thoroughly mixed using a 96-well pipettor (Viaflo 96, Integra Biosciences; settings: pipette/mix program, 5 mixing cycles, mixing volume 300 μL, speed 6) before applying a 30-fold dilution by transferring 20 μL of the cultures into a new plate with 600 μL of fresh media.

Experiments were extended to a total of 10 daily cycles. At the end of every daily cycle, 150 μL samples of each culture were used to measure the OD (600nm), a proxy for the total biomass in the cultures, using a Varioskan Flash (Thermo Fisher Scientific) plate reader. The remaining culture volume was stored at -80 °C for subsequent DNA extraction.

We tested the reproducibility of community dynamics under different choices of carbon sources. We replaced 2% glucose by 2% succinate in the media with high nutrients concentration, and still observed biomass fluctuations in some communities (Fig. 2-5). Among the eight different communities, two communities fluctuate in both glucose and succinate, and four communities reach steady state in both glucose and succinate. There are two communities only that fluctuate in medium with glucose while reaching a steady state in medium with succinate. The results show that emergent fluctuations in communities are reproducible with different carbon sources. Furthermore, we cultured the 12-species communities under high nutrients concentration and diluted every 48 hours. We found that both 24-hours-transfer and 48-hours-transfer regimes yield analogous biomass dynamics for the eight 12-species communities. The communities that reach fluctuating (stable) states with 24-hour-transfers also reach a similar fluctuating (stable) state with 48-hour-transfers (Fig.

2-5). These results demonstrate that the observed community dynamics are robust to different choices of dilution time regimes. To classify stable and fluctuating communities under succinate and 48-hours-transfer, we calculated the standard deviation of biomass over the last four data points (day 7-10 for communities in succinate, and day 10-16 for communities with 48h transfers). The standard deviation of biomass over time is shown in Fig. 2-5, where the classification of fluctuating (orange points) and stable (purple points) communities are based on the K-mean clustering method. The Std of biomass exhibits a sharp decrease from fluctuating to stable communities, and the classification remains the same across the three replicate communities under each condition (Fig. 2-5).

2.4.3 DNA extraction, 16S rRNA sequencing and data analysis

To monitor the dynamics of the microbial communities, we measured community composition via 16S ribosomal RNA (rRNA) amplicon sequencing. DNA extraction was performed with the QIAGEN DNeasy PowerSoil HTP 96 Kit following the protocol provided by the manufacturer. The obtained DNA was used for 16S (V4 region) amplicon sequencing. Library preparation and Illumina MiSeq sequencing were performed by the Environmental Sample Preparation and Sequencing Facility at Argonne National Laboratory. We used the R package DADA2 to obtain the amplicon sequence variants (ASVs) as described by Callahan et al.[27]. Taxonomic identities were assigned to the ASVs by using SILVA (version 132) as a reference database. For each sample. species richness was calculated as the number of ASVs with a relative abundance $\geq$0.1%, which corresponds to the 0.1% extinction threshold used in simulation (Fig. 2-10, 2-11). The phylogenetic tree (Fig. 2-19) was constructed using Simple Phylogeny [82] by the EMBL's European Bioinformatics Institute. Taxonomic identities were assigned to ASVs using Randomized Axelerated Maximum Likelihood (RAxML) using default parameters. All plot of relative ASV abundances with stack bars in this paper show the results of one replicate.

Each step in the workflow to assess community composition through amplicon sequencing presents its own biases [100]. This includes taxononomical biases in DNA extraction, PCR amplification (e.g., differences in 16S gene copy number), sequencing, and bioinformatics processing. In our study, such biases can significantly compromise the quantitative accuracy of the reported relative abundance of community members, although they are unlikely to significantly compromise our results qualitatively. In particular, these biases could lead to underestimations in community diversity if species fall below the extinction threshold as a result. Similarly, quantitative measures of abundance fluctuations could also be affected. However, these quantitative changes (e.g., under- or overestimation of specific community member) should be comparable across samples, making our qualitative results (e.g., transitions between dynamical modes in a specific order across the phase space) robust to these biases.

In our sequencing dataset, sequencing depth varied from 3579 to 67354 reads, with an average of 21609 reads. This means that we could not effectively resolve any species abundance on the order of .01% or below. Our main observables, diversity and fluctuation fraction, were calculated (Methods) only from species abundances that exceed a threshold of 0.1% (the extinction threshold). On the one hand, we were able to detect abundances for all the members of each species pool in all the data points for Day 0 (Fig. 2-2 and 2-25, 2-26, 2-27). Considering that community inoculation consisted in mixing monocultures at equal volumes at Day 0, this suggests that species-specific, sequencing-associated errors are relatively modest in our dataset. On the other hand, our communities are composed of members of a defined set of 48-species library. We did not detect any reads from any ASV that does not correspond to a member of the 48-species library, which suggests an absence of significant contamination during experimental data acquisition and processing and is an additional indicator of reliability of the sequencing data for the purposes of this study.

2.4.4 Pairwise interactions between microbial species

To measure the strength of pairwise interactions in the experiments, we randomly chose six isolates—selected from the different genera Leuconostoc, Pseudomonas, Yersinia, Pantoea, Klebsiella, and Acinetobacter—from the bacterial library. We first measured the carrying capacity K_i (i.e., the species abundance at equilibrium in the absence of any competitor species) of these isolates through exposing them to 7 cycles of daily dilutions in monoculture, followed by plating and colony counting at the end of the 7th cycle. We then co-cultured 15 pairs (all possible combinations) of these isolates over 7 dilution cycles and measured the species abundance at the end point (via sample dilution and colony counting on agar plates). Together with the measured carrying capacities, these species abundances were used to assess the strength of interactions via the relationship $\alpha_{ij} = (K_i - N_i)K_j/(N_jK_i)$, which can be easily derived from the gLV model. Table A.1 shows that all pairs of isolates coexist under low nutrient concentrations ($\alpha_{ij}<1$ for all the experimentally measured interactions). For higher nutrient concentrations, we considered 2 initial relative abundance for each pair of species (initial species ratios 95:5 and 5:95, measured via culture volume), which allows to identify cases of bistability in which either species can lead its competitor to extinction. For coexisting pairs, the value of α_{ij} was calculated as stated above. In cases of competitive exclusion (species i always drives species j to extinction), we inferred that $\alpha_{ij}<1$ and $\alpha_{ji}>1$. For bistability (the high-abundance species drives the low-abundance one to extinction), we inferred that $\alpha_{ij}>1$ and $\alpha_{ji}>1$. Tables S2 and S3 show the measured interaction matrices under medium and high nutrients concentrations. We found the interaction matrices measured in the experiment are densely connected matrices (Tables A.1, A.2, A.3), which means that $\alpha_{ij}\neq 0$ for most (or all) the species interactions. This result is consistent with previously observed microbial community interaction networks [46] and supports the assumption a dense interaction matrix in our theoretical model.

Ecological communities, including microbial communities different from the ones in our experiments, need not to be densely connected. Our model can account for

this fact through incorporating the average connectance C (the fraction of non-zero interactions in the interaction network) in the stability criteria (16). In this way, the main effect of network connectance in community dynamics is equivalent to replacing S by SC on the horizontal axis of the phase diagrams in Fig. 2-1E and 2-1F [122]. Therefore, a finite fraction of zero (or negligibly small) interaction strengths does not qualitatively change the phases of community dynamics and their relative positions on the phase diagram.

2.4.5 Numerical methods

We modeled the long-term dynamics and diversity of ecological communities using the well-known generalized Lotka-Volterra (gLV) model, modified to include dispersal from a species pool:

$$\frac{dN_i}{dt} = r_i N_i (1 - \sum_{j=1}^{S} \alpha_{ij} N_j / K_i) + D \tag{2.4}$$

where N_i is the abundance of species i (normalized to its carrying capacity), α_{ij} is the interaction strength that captures how strongly species j inhibits the growth of species i (with self-regulation $\alpha_{ii} = 1$), and D is the dispersal rate from an outside species pool to the focal community. For simplicity and without qualitatively changing our results, we considered the same growth rate $r_i = 1$ and the same carrying capacity $K_i = 1$ for all species in the main text. Fig. 2-15 shows that sampling growth rates from a uniform distribution has little effect on the phase diagram of survival fraction and fluctuation fraction. Fig. 2-15 shows that sampling carrying capacities from a normal distribution increases the partial coexistence phase while shrinking both the full coexistence phase and fluctuation phase, but does not affect the order of the phases. We further tested the theoretical predictions when considering the existence of positive (facilitative) interspecies interactions (Fig. 2-7) and varying the symmetry of the interaction matrix (Fig. 2-6). We also considered different dispersal rates (Fig. 2-16), and the effects of incorporating daily dilutions (Fig. 2-7) in these *in silico* communities. These additional results show that our qualitative phase diagrams and conclusions are robust to different choices of ecological network structure and

parameters. Although the patterns of ecological diversity and dynamics do not change as the dispersal rate varies from D=10^{-7} to D=10^{-6} (Fig. 2-16), we found that communities with zero dispersal rate exhibit lower fluctuation fraction and survival faction in the persistent fluctuation phase. Our results show that non-zero dispersal rates can sustain persistent fluctuations.

All simulations used the Runge-Kutta method on Matlab to numerically solve the LV equations (with an integration step of 0.05). A definition of 100×100 pixels was used for each phase diagram, linearly segmenting the parameter space in the ranges $<\alpha_{ij}> \in [0,\ 1.5]$ and $S \in [1,\ 100]$. In each phase diagram, each pixel shows the average result for 103 simulations. The total simulation time is 10^4 to guarantee the survival fraction and fluctuation fraction have reached steady states as shown in Fig. 2-14.

To test whether the total biomass fluctuation is consistent with species abundance fluctuation in our simulations, we simulated the time series of community biomass under various conditions (Fig. 2-12). To quantify the dynamics of biomass in the simulation, we calculated the sum of species abundance ($\sum_i N_i$ (t)). Our results demonstrate the fluctuation in species abundance is in agreement with fluctuation in total biomass. The similar fluctuations between replicates in some experiments (e.g., Fig. 2-2, medium nutrients, S=48) could be explained by the slow divergence that chaotic trajectories can exhibit during moderately long-time windows, or, alternatively, by possible limit cycle oscillations (Fig. 2-12). We focused on chaotic fluctuations when discussing the model predictions because previous theory shows that all persistent fluctuations will be chaotic as number of species in the pool S grows [24], though limit cycle oscillations only happen under finite S.

We define the steady state of simulated communities as the community state in which neither the survival fraction nor the fluctuation fraction significantly changes as time goes on. In order to consistently analyze the steady state results for all the simulated communities, we analyzed the dependence of the phase diagrams on the simulated time. Fig. 2-14 shows that neither the survival fraction nor the fluctuation fraction significantly changes after t=5×10^3. Accordingly, the phase diagrams in the

paper show the state of communities at t=10^4, unless otherwise stated.

The presence of dispersal from the species pool in Eq. (1) guarantees that all species exhibit strictly positive abundances in Fig 1B and C. Nevertheless, we consider that a species is extinct if its abundance lays below a 10^{-3} threshold. Around this threshold, the dispersal rate becomes the main factor preventing abundance decay (Fig. 2-10). The species abundance distribution in the partial coexistence phase is bimodal (Fig. 2-11); the extinction threshold 0.001 clearly separates the high-abundance surviving species from low-abundance species that will go extinct if dispersal ceases (Fig.2-10).

To differentiate between stable and fluctuating communities, we computed the average coefficient of variation of N_i between t=5×10^3 and t=10^4. We define communities with this average coefficient of variation higher (lower) than 10^{-3} as fluctuating (stable) communities (Fig. 2-10).

To compute the survival fraction, we computed the fraction of species whose abundance exceeded the extinction threshold at any time during the last 100 units of time in the simulation. Our choice of including a time window when measuring diversity is motivated by the fact that, for the case of unstable communities, species abundances fluctuate above and below the extinction threshold over time. Since we measured diversity and species compositions every 24 hours in the experiment, we consider an analogous window of 100 time units in simulations.

2.4.6 Analytical curves for boundaries between phases, and sharpness of the transitions

Starting with the pioneering work by Robert May [84], ecologists have sought to predict community behaviors using coarse-grained parameters including the number of species and the first two moments of the distribution of interaction strengths between species. The analytical boundary between the stable phase (II) and the fluctuating phase (III) was derived in Bunin 2017 [24]. For equal carrying capacities, it is shown that the boundary lies at the average standing species richness S^*=$S/2$, when

$\sigma \equiv \sqrt{S}$ std(α_{ij})/(1-$\langle\alpha_{ij}\rangle$)=$\sqrt{2}$. There and in [21] it is also shown that the loss of stability of the equilibrium coincides with real parts of some community matrix (-α_{ij}) eigenvalues becoming positive. For any distribution of interaction strengths (uniform, exponential, etc.), std(α_{ij}) and $\langle\alpha_{ij}\rangle$ can be calculated, and this criterion applied. The boundary between the fully-coexisting (I) and stable (II) phases is given by taking the prediction for the average standing species richness S^* given in [24], and setting S^*=S-1, namely the parameters when one species has gone extinct. This is not expected to be exact at large S, since the prediction in [24] is exact in conditions where S^*/S is finite at large S, while here the boundary is at S^*/S=1-1/S which approaches 1 at large S. Nonetheless, it gives good results in the range of pool diversities shown in Fig. 2-1. Other techniques for analyzing the transition are also possible [6].

Sharpness of transitions – The term "phase transition" in physics implies that the transition is sharp in systems with many degrees of freedom. The transition between phases (II) and (III) is known to be sharp [24, 93]: at high S, communities that lie above the phase boundary (e.g., $\sigma>\sqrt{2}$ with all species exhibiting equal carrying capacities) always (with probability one) exhibit persistent fluctuations, while communities below the phase boundary (e.g., when $\sigma<\sqrt{2}$ for equal carrying capacities) reach a stable equilibrium .

The transition between phases (I) and (II) is also sharp when S is large, in the following sense. Fig. S30 shows the probability of full coexistence as a function of $\langle\alpha_{ij}\rangle$, for different values of S. The x-axis is normalized by $\langle\alpha_{ij}\rangle$ where the analytical boundary is expected. This makes all curves decrease to zero in the same region, but the width of the crossover regime becomes narrower with increasing S. In other words, the width of the crossover region between the phases is small compared to the width of phase (I), for large S.

The fact that all curves decrease to zero at the same region, shows that the analytical expression indeed captures the correct dependence of the boundary in $\langle\alpha_{ij}\rangle$ on S. The fact that the crossover happens around a value of 2.1 rather than around 1, is due to the inexact theory used, as explained above.

An additional dynamical regime known as a Gardner phase has been theoretically

proposed in a model with symmetric interactions [119]. The Gardner phase is a regime where there are many deep basins of attraction, and within each one there is a further structure of many close to marginally-stable basins. Altieri et al. discussed what happens when the full symmetry of the interactions is broken, which seems to be the experimentally relevant situation (Table. A.1, A.2, A.3). In that case, the authors remark that the internal marginally-stable structure is sensitive, and easily washed out by the asymmetry. Although the deep basins might still survive when the interactions are asymmetrical, the existence of these deep basins seems to require a pool size S that is larger than we have, with multiple stable states only found for $S > 100$. Indeed, the simulations in the paper [119] were done for S=500, 2000. This is an interesting direction for future research, but likely not relevant to our present setting, where $S < 50$.

2.4.7 Analysis of experimental data

To differentiate between stable and fluctuating communities in experiments, we computed the average coefficient of variation (CV) for species abundances from day 7 to day 10. This corresponds to the average value of the standard deviation for the absolute abundance of each species N_i (over day 7, day 8, day 9 and day 10) scaled by average species abundance. Communities for which the average coefficient of variation in this time range is below (above) a 0.25 threshold are considered stable (fluctuating) communities (Fig. 2-20A). We also find that the biomass and species compositions fluctuate asynchronously across replicates of fluctuating communities starting from the same initial conditions. The significant differences in relative abundances (N_i^*= $N_i/\sum N_i$) across replicates is an additional indicator of community fluctuations. Fig. S13B shows that the two clusters identifying different community dynamics occur independently of whether differences in absolute abundance or relative abundance are used to assess the (temporal) coefficient of variation. Among the two methods, calculating the temporal variability via relative abundances yields a larger variability across samples, which leads to quantitative, but not qualitative, differences in the results. The cluster of communities' dynamics is consistent between the metric by

average coefficient of variation and by final relative composition difference across replicates, as shown in Fig. 2-20B. To further show the variability of relative abundances over time, we've calculated the variability of relative abundances over time and discussed the results in Fig. 2-20. The results show that fluctuating communities exhibit larger variability of relative abundances between replicates and over time, which is consistent with the results considering absolute species abundance (Fig. S15B). The average coefficient of variation (Fig. 2-20, 2-21) for species abundances was calculated based on only replicate for which we sequenced the whole time series, and the average difference in relative species abundances community across the three replicates for each community (Fig. 2-20, 2-21) was calculated based on relative abundances at day10.

We tested whether the classification of community dynamics as stable or fluctuating is robust to the choice of time window (day 7 to day 10) for calculating the average CV of species abundances. To do so, we calculated the average CV at different time points of the species abundance time series, with a fixed-length time window (4 days). We moved the first day of the time window from day 0 to day 7 and calculated the corresponding average CV of communities in each case. Fig. 2-21 shows that the average CV for both fluctuating and stable communities reaches steady state before the last time window (from day7 to day10). We chose the 12-species communities under high nutrients concentration for this analysis because they exhibit equal numbers of stable and fluctuating communities (n=4 for both stable and fluctuating communities). These results show that the average CV calculated in the last time window (from day7 to day10) converges rapidly to either small or large values, respectively indicating stability or long-lasting fluctuations in experimental communities.

To demonstrate that our classification of stable and fluctuating communities is robust to other classification methods, we applied a K-means clustering algorithm considering both average coefficient of variation (<Std of $N_i(t)$)>/<Mean of $N_i(t)$>), where t runs from day7 to day10 to calculate the Std and Mean of N_i(t) for the replicate with the 16S-sequenced time series; the brackets average across all species in the community) and relative differences in species abundances across replicates (Eu-

clidean distance of N_i over the 3 replicates at day 10) to classify the dynamics of our communities. Fig. 2-21 shows the results of this classification method, which are almost identical to those obtained through the stability criteria based on a CV threshold (Fig. 2-20). There is only one community which is differently classified by each method (open circle in purple in Fig. 2-21). Classifying this individual community as either stable or fluctuating does not change the three phases in the experimental phase diagram and the order of phase transitions (losing species before losing stability). Therefore, our conclusions are robust to different choices of stability criteria. Since the K-means clustering algorithm does not require set any threshold of CV, the consistence between results of K-means clustering and setting stability threshold of CV (0.25) demonstrates the classification of fluctuating and stable communities is robust to different algorithm

Although none of our conclusions on dynamical phases and transitions depends on the classification of the only community that is differently classified by each stability criteria (purple open circle in Fig. 2-21), we further analyzed both the biomass and sequencing data for the three replicates of this community. Fig. 2-30 shows that this specific community (S=12, Community 5) exhibits moderate differences in species abundances at day 10 across the three replicates. The replicate community for which we sequenced the time series also moderate fluctuations in both species' abundances (Fig. 2-27, S=12, Community 5) and biomass (Fig. 2-24, blue curves, S=12, replicate 1). This places this community at the boundary of fluctuation and stability regardless of the classification method (Fig. 2-20 and 2-21). Given that the biomass time series of the other two replicates of this community (Fig. 2-24, blue curves, S=12, replicates 2 and 3) exhibit relatively larger fluctuations in biomass than replicate 1, we classified this community as a fluctuating one (in agreement with the CV threshold criteria) in the main text.

To statistically test differences in species survival fractions between fluctuating communities and stable communities in Fig. 2-4B, we first calculated the difference of survival fraction between each community (purple or orange points in Fig. 2-4B) and the corresponding average survival fraction (blue points in Fig. 2-4B) for each

species pool size (S). We then performed an analysis of variance (ANOVA) test on the distance to the mean survival fraction for all the fluctuating communities against all the stable communities. This proved the statistical significance on the differences between the two groups, with the probability of observing these differences in a null model being very small ($p < 0.01$).

The error bars in the main text figures represent the standard error of the mean (s.e.m.). For the s.e.m. of survival fractions (Fig. 2-3A and Fig. 2-4B), we firstly calculated the mean survival fraction over each community's three replicates, and we then calculated the average and s.e.m. of these mean survival fractions across all n communities with the same pool size and nutrient conditions (n=30 when S=2; n=8 when S=3, 6, 12, 24). For the s.e.m. of fluctuation fractions (Fig. 2-3B), we could only use one replicate per community for which 16s rDNA sequencing was performed over the entire time series. Outcomes for each community were coded as Boolean values (1 for fluctuating communities, 0 for stable communities). We could then calculate the s.e.m. of this binomial distribution (n=30 when S=2; n=8 when S=3, 6, 12, 24). The definition of fluctuating and stable communities is given in Fig. 2-20.

2.5 Conclusion

The fact that two coarse-grained parameters can independently shape the phase space for community diversity and dynamics argues for caution when interpreting observed links between biodiversity and stability. On the one hand, for any given value of the interaction strength, stability negatively correlates with both size of species pool and realized diversity (number of surviving species): communities with more species are less stable (Fig 2-1F, 2-3D, 2-4A and 2-4B). On the other hand, for identical species pool sizes, stability positively correlates with diversity: weakly interacting communities exhibit relatively high stability and high realized diversity, while strongly interacting communities are relatively less stable and less diverse (Fig. 2-1E and 2-3C). We believe that the interplay between the two parameters that shape the phase diagram could underlie some of the seemingly contradictory results from field

experiments [60] addressing the diversity-stability relationship.

Our findings are consistent with two major ideas in theoretical ecology: May's suggestion that complexity leads to instability [84], and Chesson's argument that temporal fluctuations can help maintain diversity [30]. The question of whether complex dynamics are inherent to the ecological community—arising from species interactions—or driven by environmental factors has received considerable attention, yet seldom undergone a direct experimental test in many-species communities. Under laboratory conditions that minimize environmental stochasticity, and in agreement with recent theory [24, 63, 14], we found that community-level parameters representing species diversity and interactions are sufficient to predict the dynamical behaviors of complex ecological communities. These predictions are theoretically robust to varying biological assumptions (e.g., intraspecific diversity and inter-species interaction mechanisms, including resource-explicit models [35]. Therefore, the emergent phases of biodiversity and dynamics that we observed here may occur in a wide range of ecological communities. Future work should study whether these phases generalize across spatiotemporal scales, environmental conditions, and organism types to understand their prevalence and importance in shaping major ecological patterns [94, 145].

2.6 Supporting Information

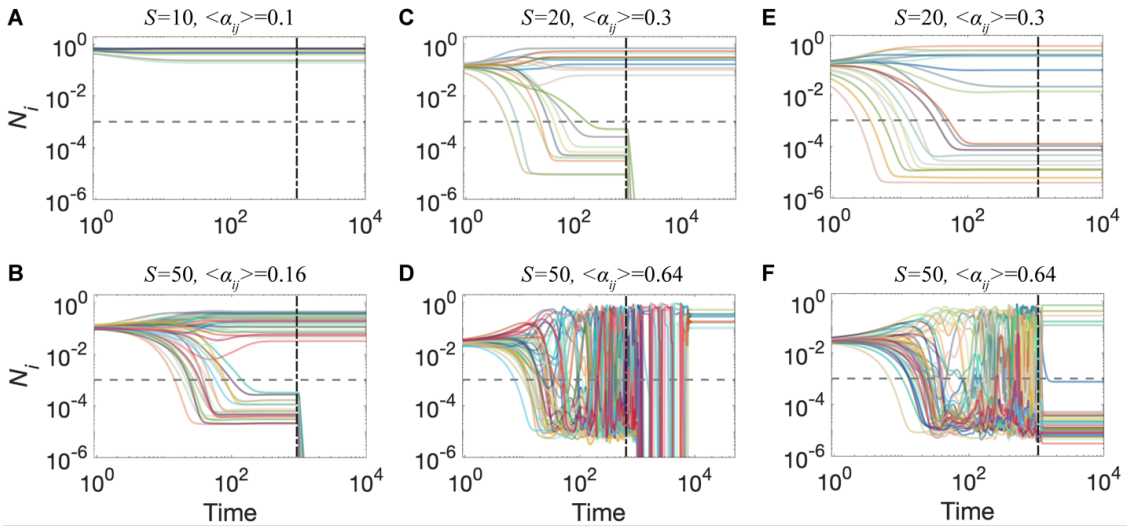

Figure 2-10: High diversity and persistent fluctuations allow and require each other, and are both sustained by dispersal. (A)-(D) Representative time series for communities in which the dispersal rate is suddenly interrupted. At t=103 (vertical dashed line), the dispersal rate changes from D=10^{-6} to D=0.0 for the rest of the simulation. (A) Before t=103, a community in phase I reaches a stable state with full coexistence. The dynamics after t=103 shows that interrupting dispersal does not significantly modify the abundances of the species. (B)-(C) Before t=103, communities in phase II reach an equilibrium in which species coexist at stable abundances, with some species laying below the extinction threshold. After stopping dispersal, only the species that are above the extinction threshold survive at stable abundances, and the rest undergo extinction. (D) A community in phase III exhibits persistent fluctuations while exposed to dispersal. After dispersal is interrupted, extinctions occur as species fall below the extinction threshold due to abundance fluctuations. After some time (approximately t=104) species extinctions have significantly reduced diversity in the community, and the surviving species reach a stable equilibrium. For the indicated parameter values, and over 103 simulations, 90% of the simulated communities reached equilibrium after interrupting dispersal. (E-F) Representative time series for communities in which the most abundant species at t=103 is pinned (its abundance is artificially kept constant) for the rest of the simulation. (E) For communities that have reached stability, in this case in phase II, pinning the most abundant species has no effect on community dynamics. (F) In phase III, after a fast transient following the species pinning at t=103 (vertical dashed line), the community reaches a stable partial coexistence where some of the species lay below the extinction threshold. Out of 103 simulations, 93% of the communities reached equilibrium after pinning the most abundant species.

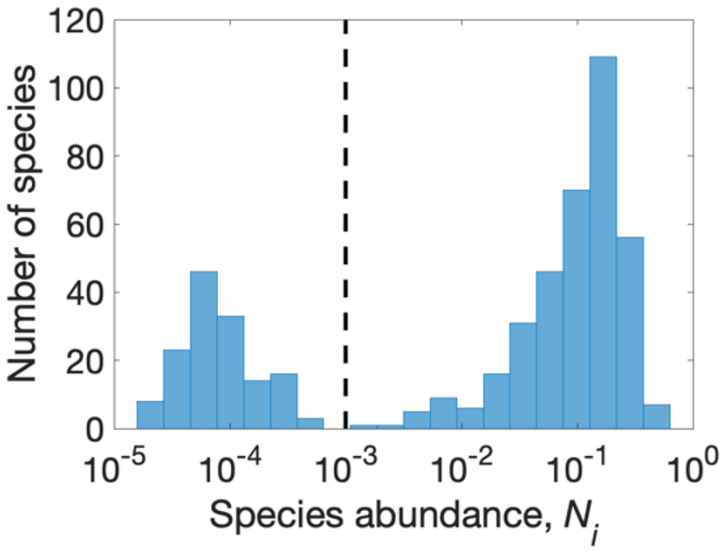

Figure 2-11: At steady state, species abundances exhibit a bimodal distribution in the partial coexistence phase. The extinction threshold 0.001 (vertical dashed line) clearly separates the high-abundance, surviving species from the low-abundant "extinct" species. Such "extinct" species would reach zero abundance if dispersal is interrupted (Fig. 2-10). The histogram shows the number of species exhibiting the indicated abundances at steady state. The corresponding dataset was generated from 10 in silico communities randomly sampled from the stable partial coexistence phase (S=50, $<\alpha_{ij}>$=0.2).

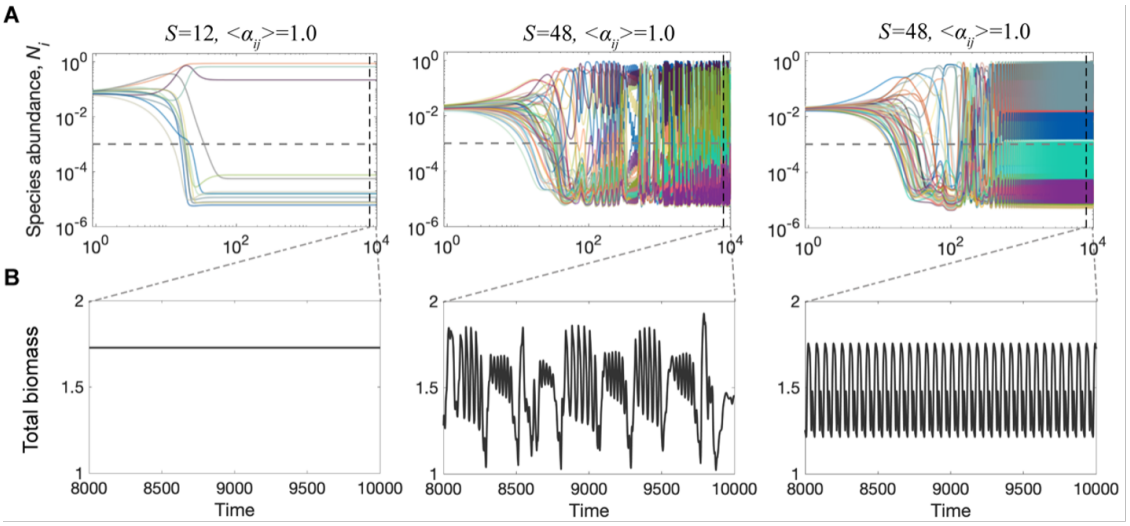

Figure 2-12: Biomass fluctuations (stability) are consistent with fluctuations (stability) of species abundances in simulations. (A)-(B) As increasing the size of species pool in communities with strong interaction strength ($<\alpha_{ij}>$=1.0), the species abundances and total biomass ($\sum_i N_i(t)$) of communities consistently lose stability and exhibit persistent fluctuations. The species abundances and biomass of communities can also exhibit limit cycle oscillations (right panels) in addition to chaotic fluctuations (middle panels), in the persistent fluctuation phase. The biomass trajectories in (B) show the last 2000 time units in (A) as indicated by the vertical dashed lines.

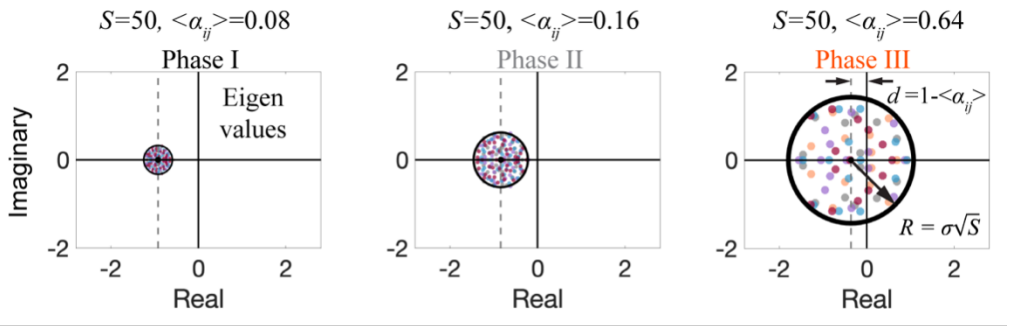

Figure 2-13: Unstable communities have (one or more) eigenvalues of the community matrix ($-\alpha_{ij}$) with positive real parts. From left to right, the panels show the eigenvalues of representative community matrices for three different values of the average interaction strength. Within each panel, different colors correspond to the eigenvalues of 4 different community matrices. All the eigenvalues lie within a circle with radius R centered at d [84, 122]. For communities in phase III, where persistent fluctuations occur, some of the community matrix eigenvalues exhibit a positive real part. It was shown that the loss of stability of the equilibrium coincides with real parts of some community matrix ($-\alpha_{ij}$) eigenvalues becoming positive, although it is not the Jacobian matrix [21]: the circular distribution of eigenvalues for interaction matrix α_{ij} is replaced by a "guitar-shaped" distribution for Jacobian matrix [119]. Although the shape of eigenvalues distributions is different between interaction matrix and Jacobian matrix, the stability criterion and the signs of eigenvalues are the same for both matrices [6, 119].

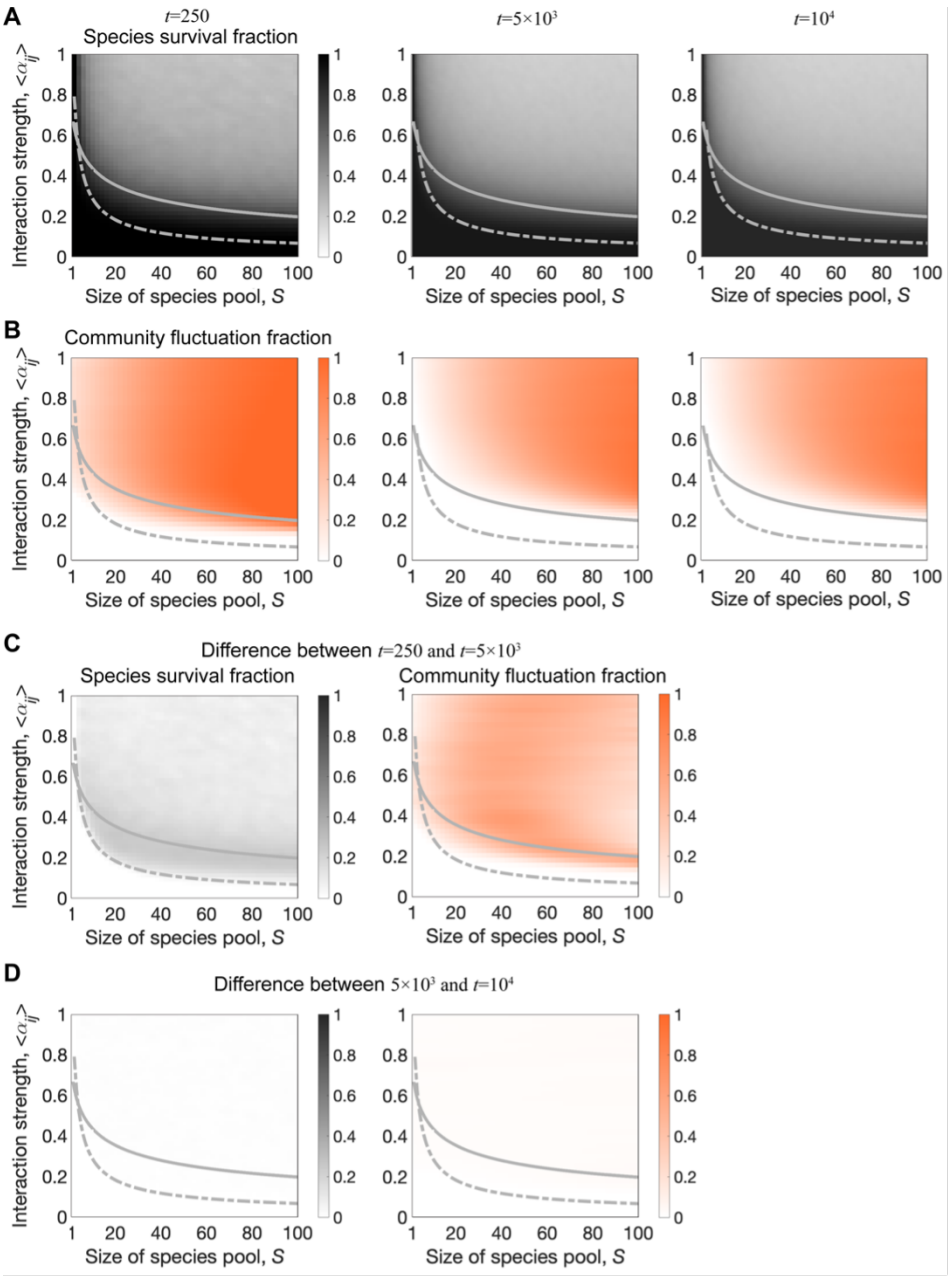
A
t=250
Species survival fraction
t=5×10³
t=10⁴
B
Community fluctuation fraction
C
Difference between t=250 and t=5×10³
Species survival fraction
Community fluctuation fraction
D
Difference between 5×10³ and t=10⁴
Interaction strength, <αij>
Size of species pool, S
0
0.2
0.4
0.6
0.8
1
1
20
40
60
80
100

Figure 2-14: After an initial transient, the survival fraction and the fluctuation fraction of simulated communities reach stable values. From left to right, the panels show phase diagrams of survival fraction (A) and fluctuation fraction (B) for communities at three different simulation times. At t=250 (left), communities have not yet reached steady state, as the phase diagrams quantitatively change as time goes on. The middle panels (t=5×10$_3$) are quantitatively different from the earlier-time phase diagrams (t=250 on the left), but do not significantly differ from phase diagrams computed at later times (t=104 on the right). This shows that these two community properties have reached a steady state before t=104. (C) Difference between the survival fractions (left) and the fluctuation fractions (right) computed at t=250 and t=5×10$_3$. (D) Difference between the survival fractions (left) and the fluctuation fractions (right) computed at t=5×10$_3$ and t=10$_4$. The dashed line and solid line in the figures represent the survival boundary and stability boundary, respectively.

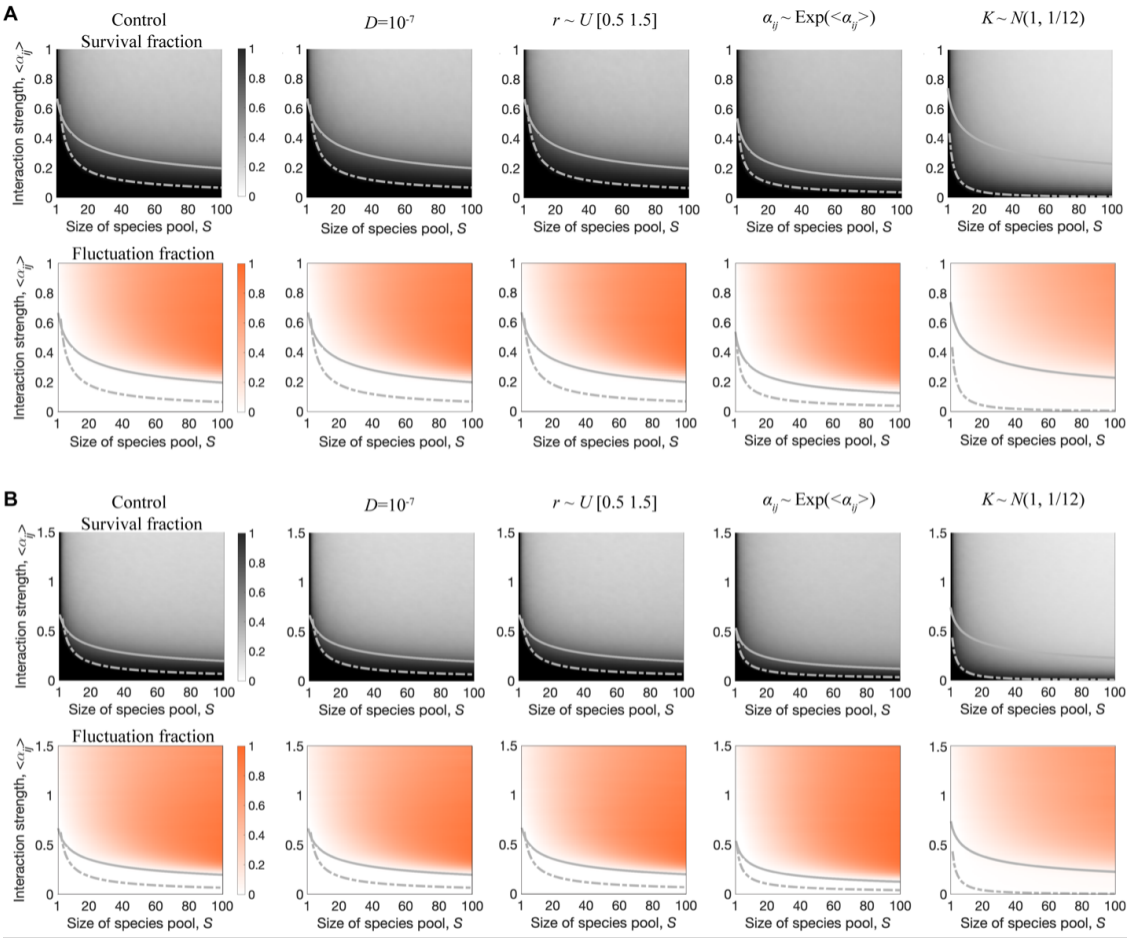

Figure 2-15: The three dynamical phases are robust to modeling choices. (A) Panels on the left (Control) show the numerical (color map) and analytical (curves) phase diagrams as in Fig. 2-1E and F. From left to right, the additional phase diagrams show the effects of lowering the dispersal rate to D=10^{-7}, sampling species growth rates from a uniform distribution, sampling interaction strengths from an exponential distribution, and sampling the carrying capacities from a Gaussian distribution. All non-specified parameter values are identical to the control case (Fig. 2-1E and F). (B) Phase diagrams analogous to those in (A), but for a higher average interaction strength $<\alpha_{ij}>$= 1.5. Overall, these phase diagrams show that the three dynamical phases are qualitatively robust to different modeling choices [24].

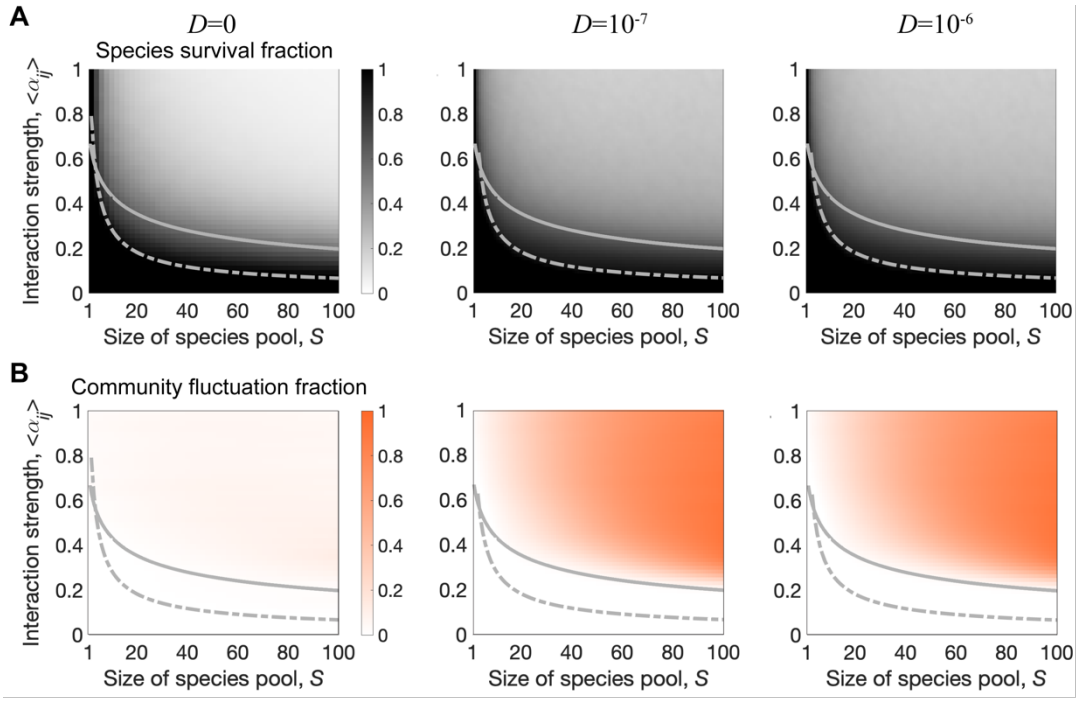

Figure 2-16: Dispersal sustains persistent fluctuations and promotes diversity. The panels show the theoretical phase diagrams of species survival fraction and community fluctuation fraction under different dispersal rates (D=0, D=10^{-7}, D=10^{-6}). Communities under no dispersal (D=0, left panels) exhibit lower survival faction (A) and lower fluctuation fraction (B) in the persistent fluctuation phase. The patterns of ecological diversity and dynamics do not significantly change as the dispersal rate varies from D=10^{-7} (middle panels) to D=10^{-6} (right panels). The dashed line and solid line in the figures represent survival boundary and stability boundary, respectively.

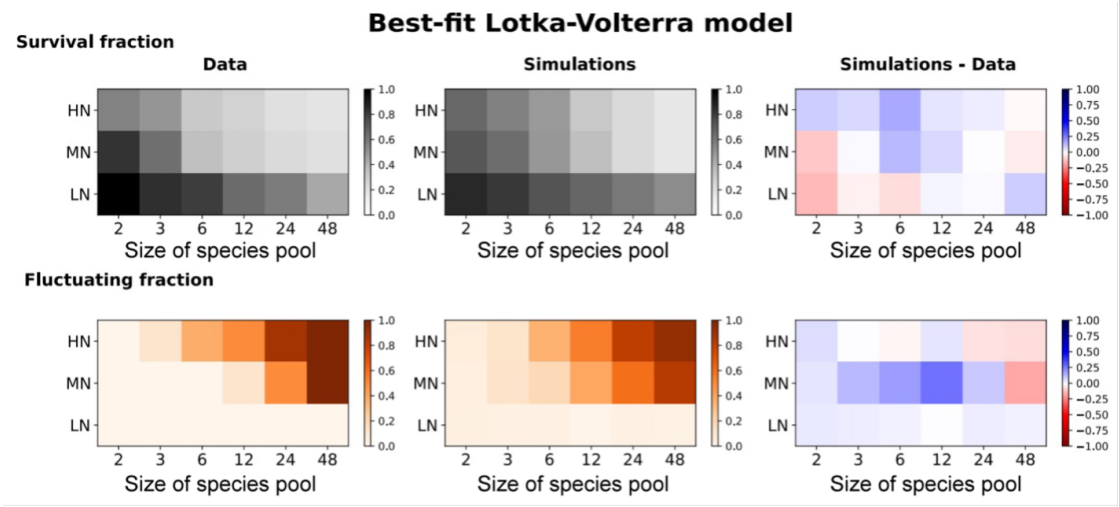

Figure 2-17: Best-fit Lotka-Volterra model. We show the heatmaps of survival fraction (top) and fraction of fluctuating communities (bottom) for data, best-fit simulations, and the difference between the two (left to right). The best-fit simulations are obtained from a Lotka-Volterra with normally-distributed interactions with the following parameters: High nutrient treatment (HN): $<\alpha_{ij}>$=0.87, std (α_{ij})=0.22. Medium nutrient treatment (MN): $<\alpha_{ij}>$=0.66, std (α_{ij})=0.41. Low nutrient treatment (LN): $<\alpha_{ij}>$=0.14, std (α_{ij})=0.17.

Figure 2-18: Taxonomic identity of the 48 bacterial isolates. The identities have been inferred from the ASV (Methods) of 16S samples taken from monocultures, which allow the classification of the 48 isolates down to the genus level. Colors are consistent with those in the main text and other supplementary figures.

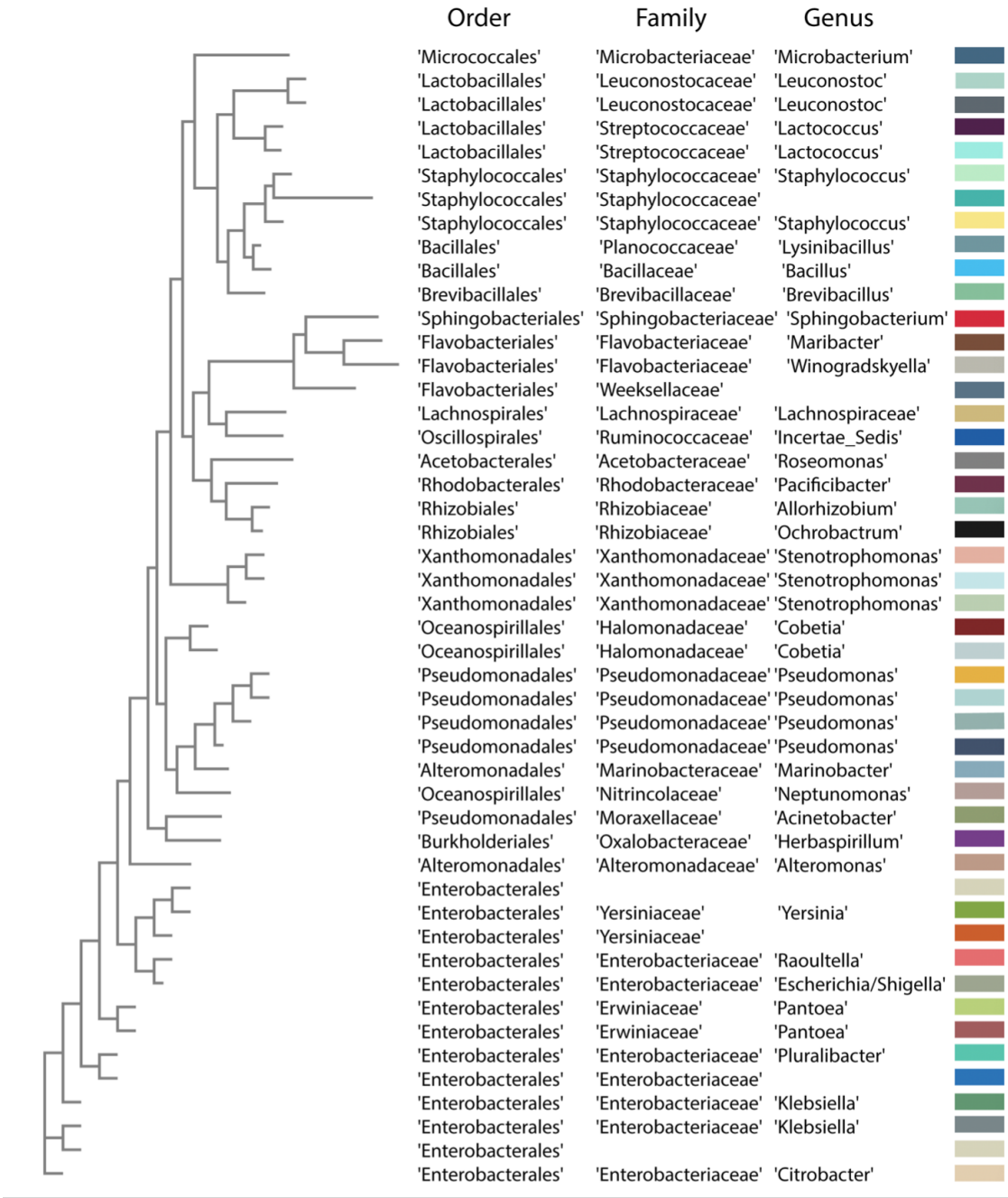

Figure 2-19: Phylogenetic tree of the 48 bacterial isolates. The tree, generated with the Distance-matrix method from EMBL-EBL [82], shows the relative phylogenetic distance between the 48 bacterial isolates. The library contains bacterial isolates from either soil or C. elegans gut samples and spans 19 different orders and 26 different families. The rectangles display the color that is used in the figures (both in the Main Text and the SI) to show the abundance of each species in the different experiments.

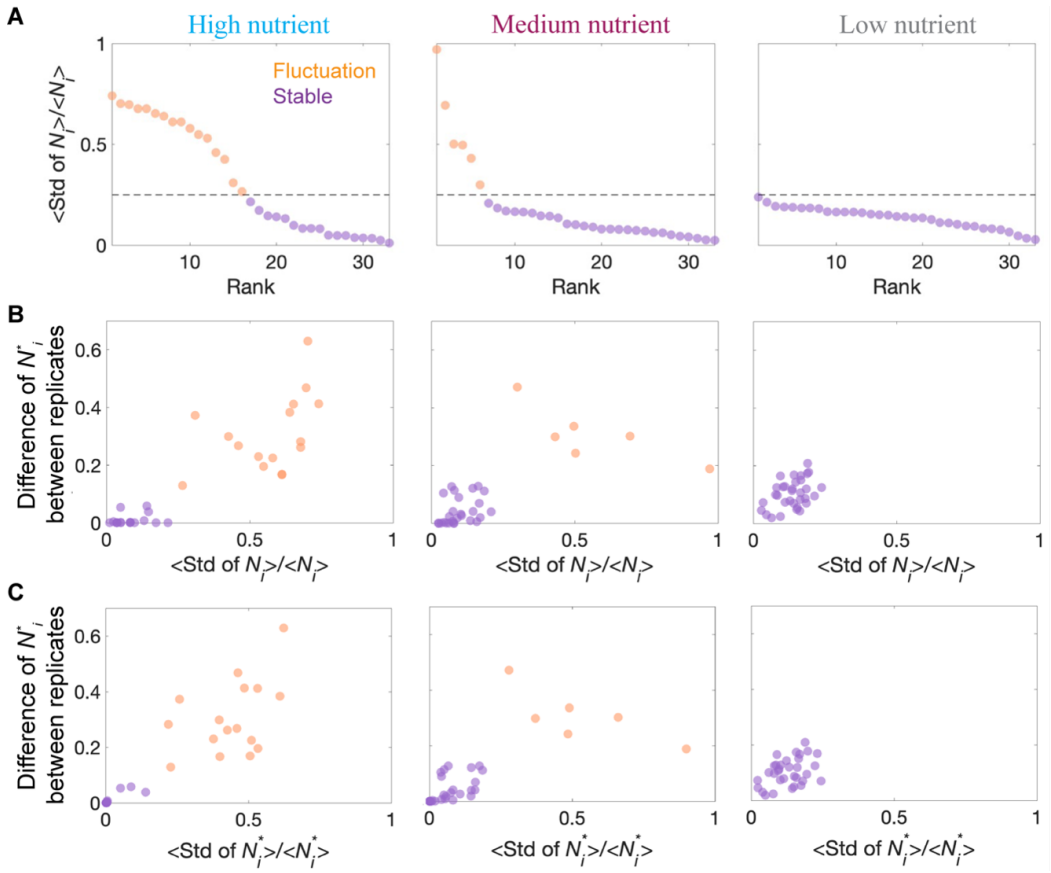

Figure 2-20: 3 different metrics consistently differentiate stable from fluctuating communities. (A) The three panels show the average coefficient of (temporal) variation (see Methods) for absolute species abundances (N_i, computed as the product of total biomass per species relative abundance) in the experimental communities in the three different nutrients concentrations. We use a stability threshold of 0.25 (dashed line) to classify communities into stable (purple) and fluctuating (orange) ones. The number of fluctuating communities increases with the average interaction strength (nutrients concentration), with all the weakly interacting (low nutrients concentration) communities exhibiting stability. (B) Average difference (Euclidean distance) in the relative abundance of each species ($N_i^* = N_i/\sum_i N_i$) across replicate communities as a function of the community's average coefficient of (temporal) variation. Stable and fluctuating communities, defined as in (A), span in different regions, with stable communities clustering near the origin. (C) Average difference (Euclidean distance) in the relative abundance of each species ($N_i^* = N_i/\sum_i N_i$) across replicate communities as a function of the community's average coefficient of (temporal) variation in relative abundance (N_i^*). Stable and fluctuating communities, defined as in (A), span in different regions, with stable communities clustering near the origin. The average coefficient of variation (Fig. 2-20, 2-21) for species abundances was calculated based on only replicate for which we sequenced the whole time series, and the average difference in relative species abundances community across the three replicates for each community (Fig. 2-20, 2-21) was calculated based on relative abundances at day10.

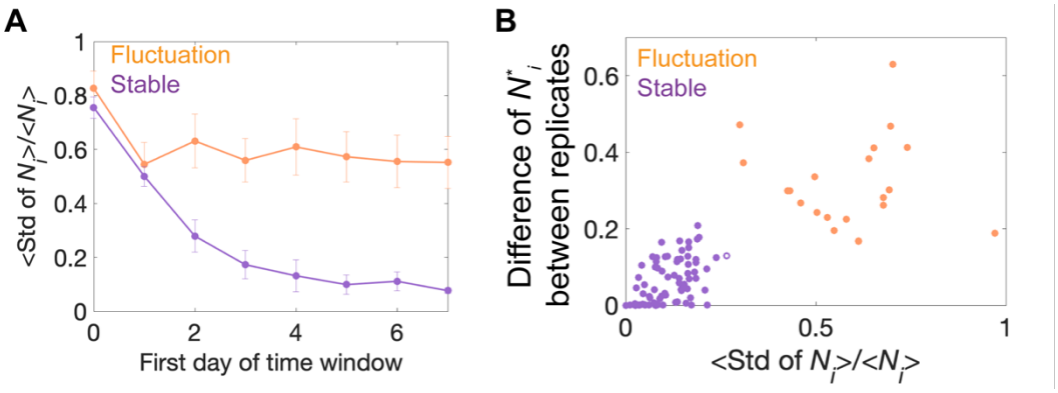

Figure 2-21: The classification of fluctuating communities and stable communities is robust to choices of classification algorithm. (A) The average coefficient of variation for species abundances reaches a steady state before day 7, enabling the classification of communities into stable and fluctuating ones. For 12-species communities under high nutrient concentrations, the average CV of both fluctuating communities (orange line, n=4) and stable communities (purple line, n=4) reaches a plateau (a constant value) before day7. The two different plateaus of average CV demonstrate that the dynamics of communities (persistent fluctuations or stability) have reached steady states before the time window (from day7 to day10) that we use to calculate the average CV in Fig. 2-20. Error bars, s.e.m. (B) using a K-means clustering algorithm considering both average CV and differences between species relative abundances across replicates confirms that the classification of fluctuating and stable communities is consistent with the CV threshold (0.25) criteria in Fig. 2-20. There is only one community (empty circle) that is differently classified by the K-means method. The classification of this single community as either stable or fluctuating changes neither the three phases in the experimental phase diagram nor the order of phase transitions (lose species before losing stability).

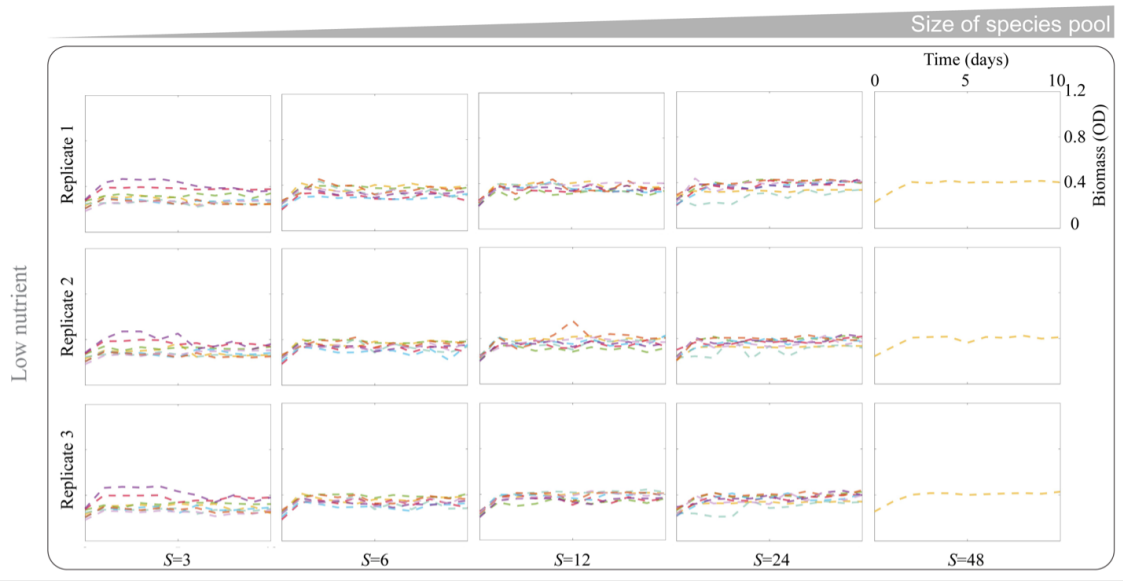

Figure 2-22: Total biomass reaches equilibrium in communities under low nutrients concentration (low interaction strength). Each panel shows the time series for the OD (600nm) of the eight communities with different species pool composition (depicted by different colors). Each column stands for a different species pool size S (for the case of S=48, there is only one community containing the full library of bacterial species). Each row shows the data for a different replicate of the experiment.

Figure 2-23: Increasing the species pool size leads to persistent fluctuations in total biomass under medium nutrients concentration (medium interaction strength). Each panel shows the time series for the OD (600nm) of the eight communities with different species pool composition (depicted by different colors). Each column stands for a different species pool size S (for the case of S=48, there is only one community containing the full library of bacterial species). Each row shows the data for a different replicate of the experiment. Solid lines (dashed lines) represent fluctuating (stable) communities, the OD fluctuations between day 7 and day 10 were considered to differentiate fluctuating and stable communities as shown in Fig. 2-20.

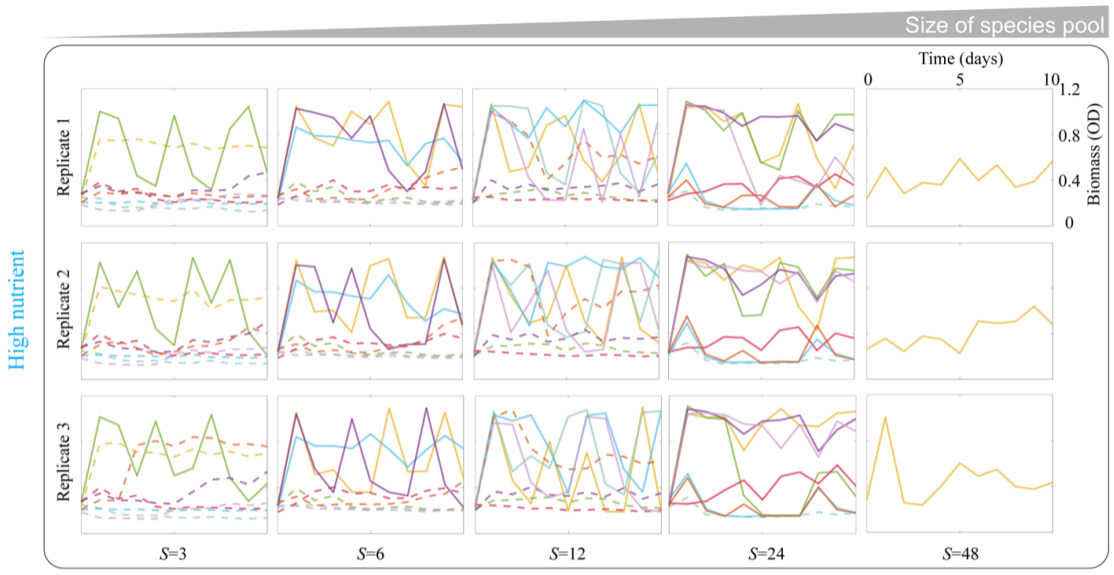

Figure 2-24: Increasing the species pool size leads to persistent fluctuations in total biomass under high nutrients concentration (high interaction strength). Each panel shows the time series for the OD (600nm) of the eight communities with different species pool composition (depicted by different colors). Each column stands for a different species pool size S (for the case of S=48, there is only one community containing the full library of bacterial species). Each row shows the data for a different replicate of the experiment. Solid lines (dashed lines) represent fluctuating (stable) communities, the OD fluctuations between day 7 and day 10 were considered to differentiate fluctuating and stable communities as shown in Fig. 2-20.

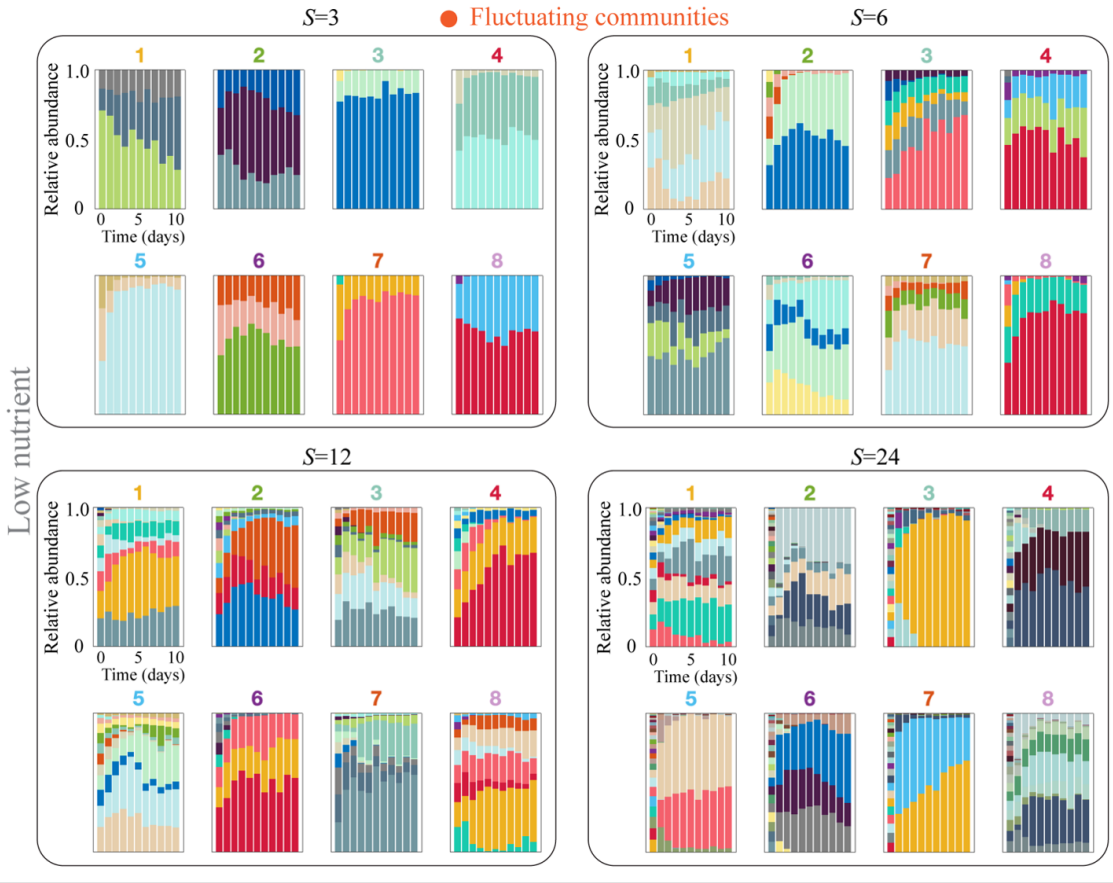

Figure 2-25: Time series for the relative species abundances of the experimental communities with low average interaction strength (low nutrients concentration). Each panel shows the full time series for each of the 8 communities with the indicated species pool size (S=3, 6, 12 and 24). Bar colors stand for species identities as in Fig. 2-18, 2-19. Under this nutrients condition, all of the communities reached a stable equilibrium (Methods). The color of the number on the top of each panel corresponds to the color assigned to the same community in Fig. 2-22.

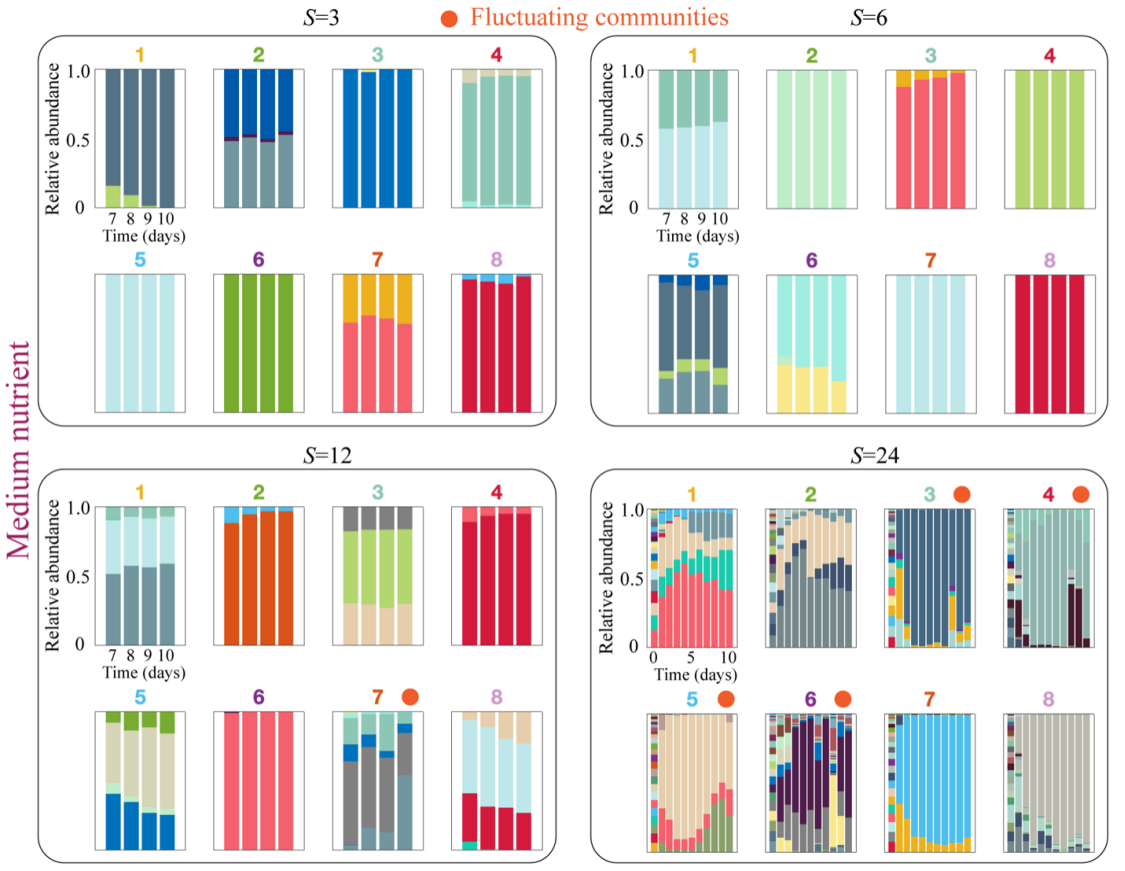

Figure 2-26: Time series for the relative species abundances of the experimental communities with medium average interaction strength (medium nutrients concentration). Each panel shows the full time series for each of the 8 communities with the indicated species pool size (S=3, 6, 12 and 24). Bar colors stand for species identities. The orange dot on top of some panels indicates that the community exhibits persistent fluctuations (Methods). The color of the number on the top of each panel corresponds to the color assigned to the same community in Fig. 2-23. For S= 3, 6, and 12, we only sequenced samples of the last 4 days (7 to 10) of the experiment.

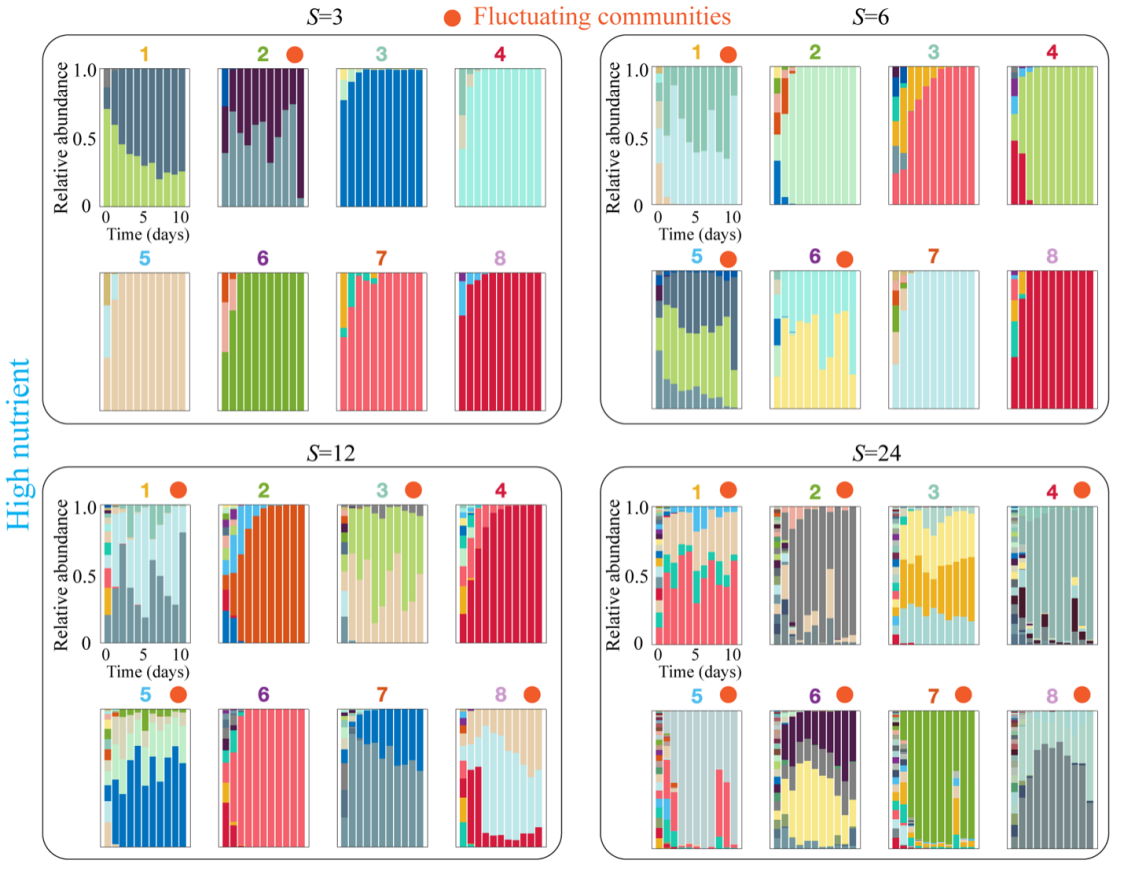

Figure 2-27: Time series for the relative species abundances of the experimental communities with high average interaction strength (high nutrients concentration). Each panel shows the full time series for each of the 8 communities with the indicated species pool size (S=3, 6, 12 and 24). Bar colors stand for species identities. The orange dot on top of some panels indicates that the community exhibits persistent fluctuations (Methods). The color of the number on the top of each panel corresponds to the color assigned to the same community in Fig. 2-24.

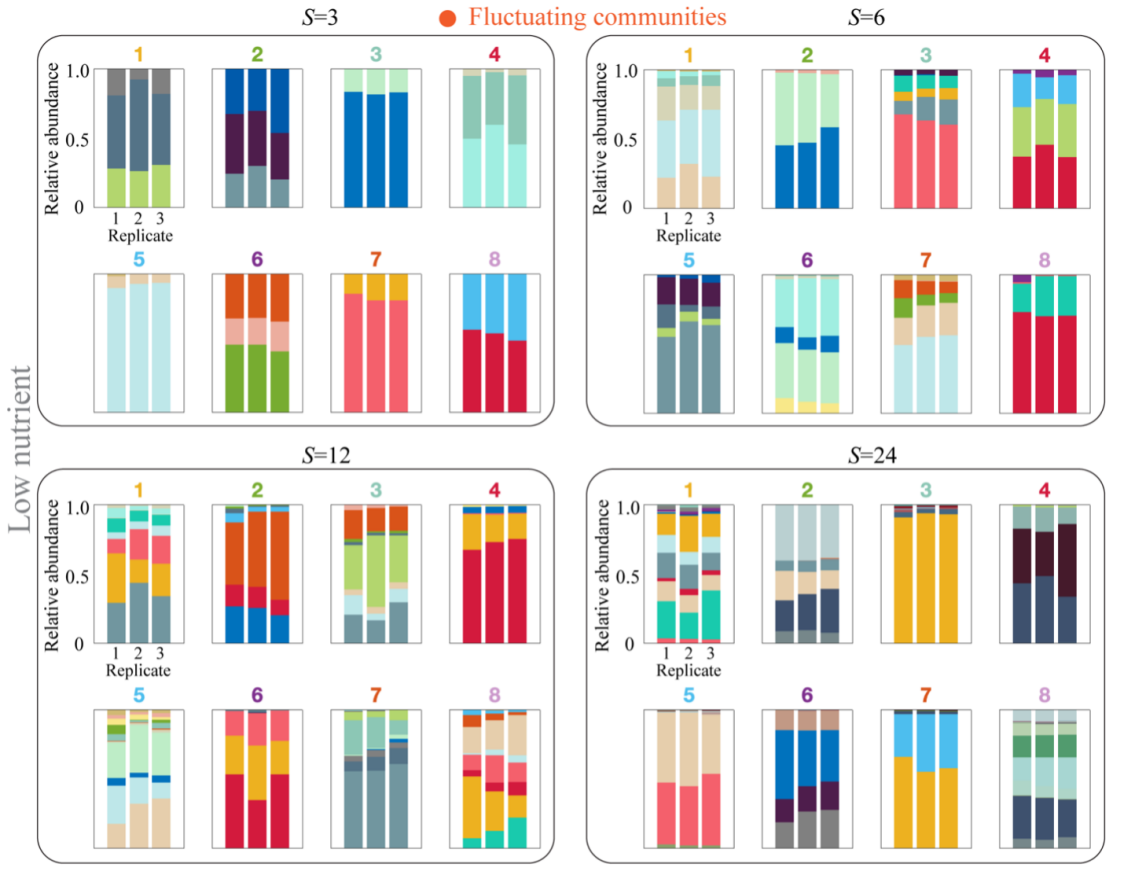

Figure 2-28: Species abundance at the end of the experiment under low nutrients concentration. Each panel shows the relative species abundances at the end experiment for each of the 3 replicate communities across 8 different compositions of the species pool for each species pool size (S=3, 6, 12 and 24). Bar colors stand for species identities. The orange dot on top of some panels indicates that the community exhibits persistent fluctuations (Methods). The color of the number on the top of each panel corresponds to the color assigned to the same community in Fig. 2-22.

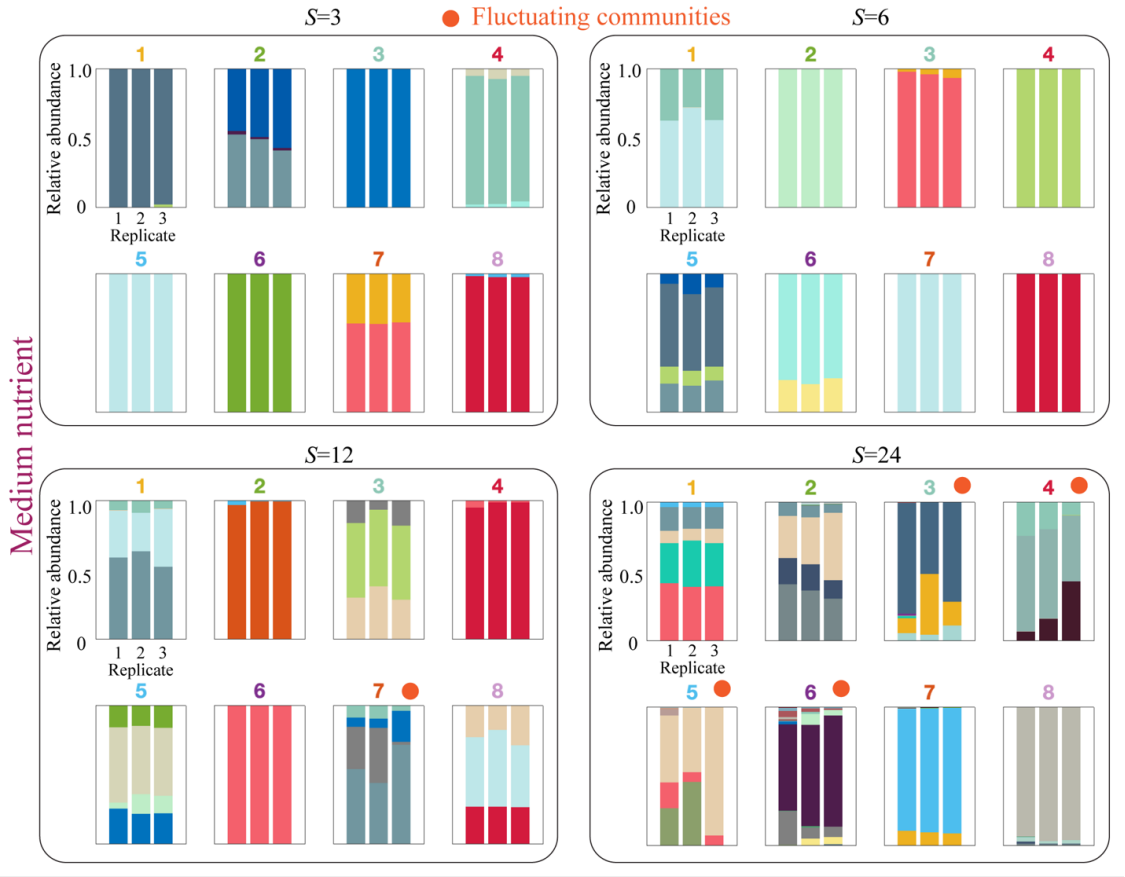

Figure 2-29: Species abundance at the end of the experiment under medium nutrients concentration. Each panel shows the species relative abundances at the end experiment for each of the 3 replicate communities across 8 different compositions of the species pool for each species pool size (S=3, 6, 12 and 24). Bar colors stand for different species identities. The orange dot on top of some panels indicates that the community exhibits persistent fluctuations (Methods). The color of the number on the top of each panel corresponds to the color assigned to the same community in Fig. 2-23.

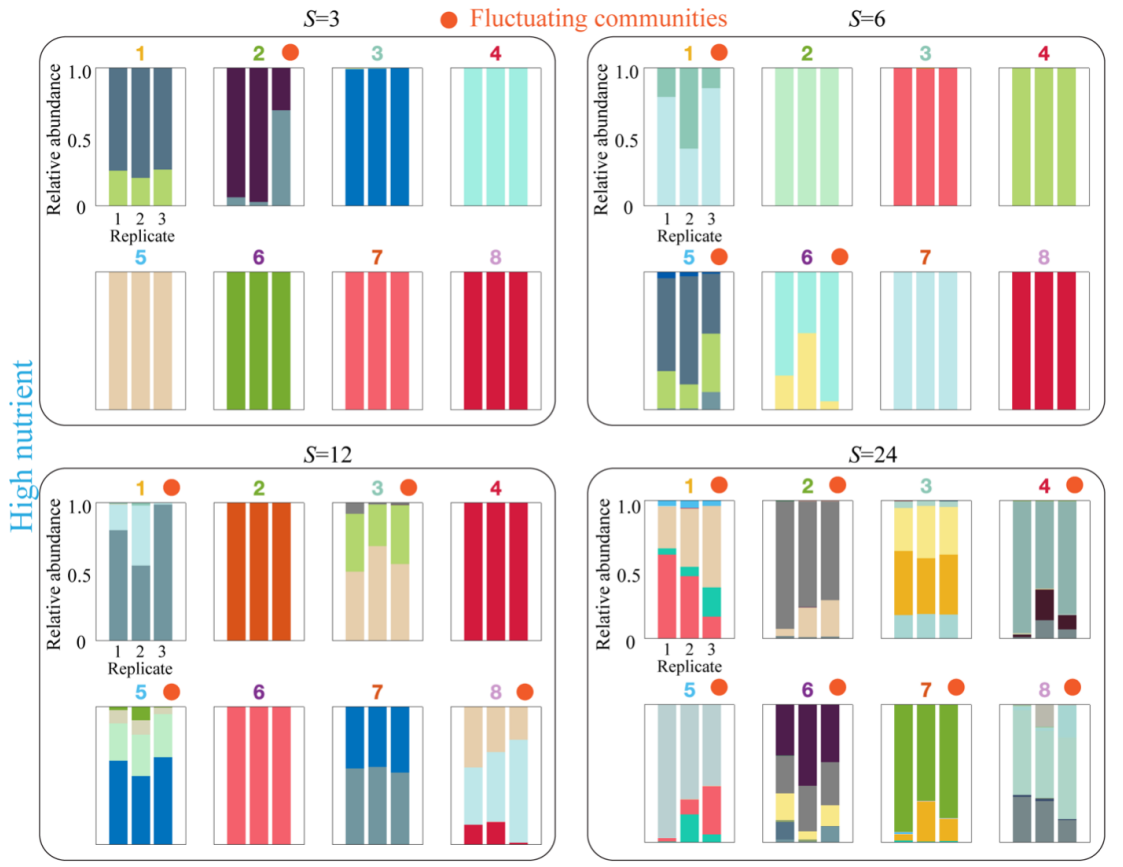

Figure 2-30: Species abundance at the end of the experiment under high nutrients concentration. Each panel shows the species relative abundances at the end experiment for each of the 3 replicate communities across 8 different compositions of the species pool for each species pool size (S=3, 6, 12 and 24). Bar colors stand for different species identities. The orange dot on top of some panels indicates that the community exhibits persistent fluctuations (Methods). The color of number on the top of each panel corresponds to the color assigned to the same community in Fig. 2-24.

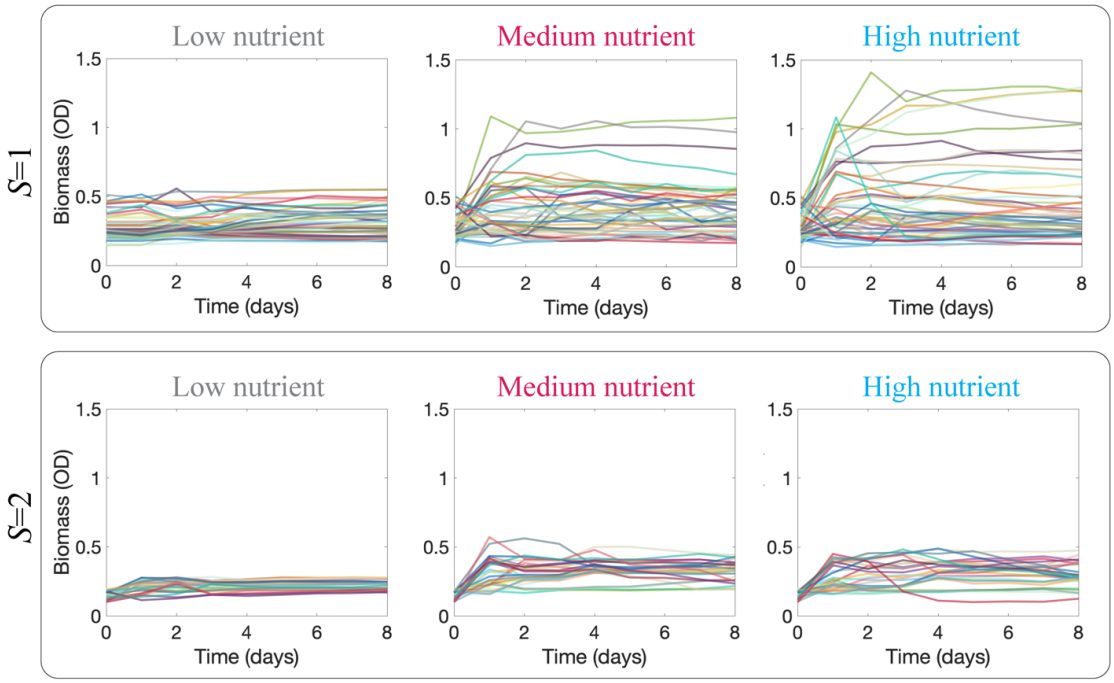

Figure 2-31: Monocultures and 2-species cocultures tend to reach stability in total biomass. On top, monocultures tend to reach a stable OD (600nm) value at the end of each daily cycle. The width of the observed range of OD values increases with nutrient concentration (low, medium, and high, from left to right). On bottom, time series for the OD (600nm) of 15 different species pair cocultures. To detect bistability, in which the outcome depends on initial species abundances, we considered two initial compositions (5:95 and 95:5 culture volume ratios between species) for each pair of species. Therefore, there are 30 pairwise cocultures tested. The variability of the OD reached in pairwise coculture also increases with nutrient concentration, but to a less extent than it does for monocultures. Different colors stand for different species identities (top) and different species pairs (bottom).

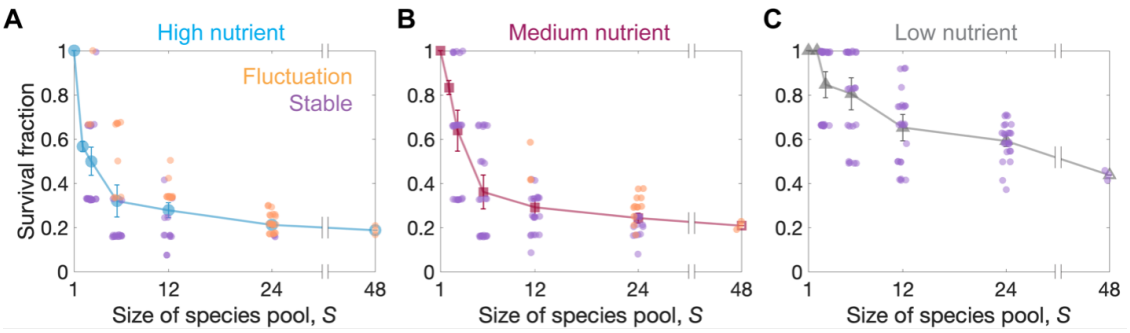

Figure 2-32: Fluctuating communities are more diverse than stable communities under the same conditions. As the average survival fraction decreases with increasing species pool size S in high (A), medium (B) and low (C) nutrient concentrations, more communities exhibit fluctuations in species abundances (orange points). For any given S and nutrients concentration, fluctuating microbial communities exhibit statistically higher survival fractions than stable communities (purple points).

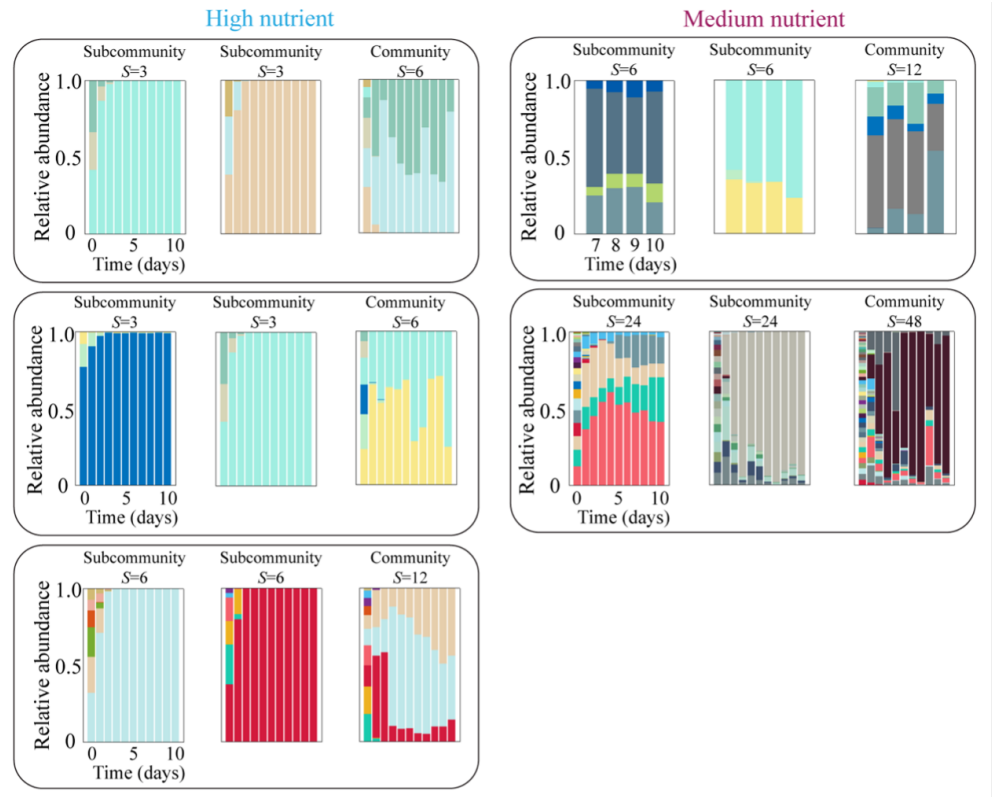

Figure 2-33: Increasing species pool size can lead to emergent fluctuations in species abundances. The panels show representative examples in which a pair of different communities reach stability, while a community with larger species pool, composed by all the species present in that pair, exhibits persistent fluctuations. Each rectangle encloses a different example involving a specific set of communities and experimental condition (nutrients concentration). The top right rectangle shows data for the last 4 days of the experiment (the only days in which these communities were sampled for sequencing), and the rest show the full time series for the 10-day experiment.

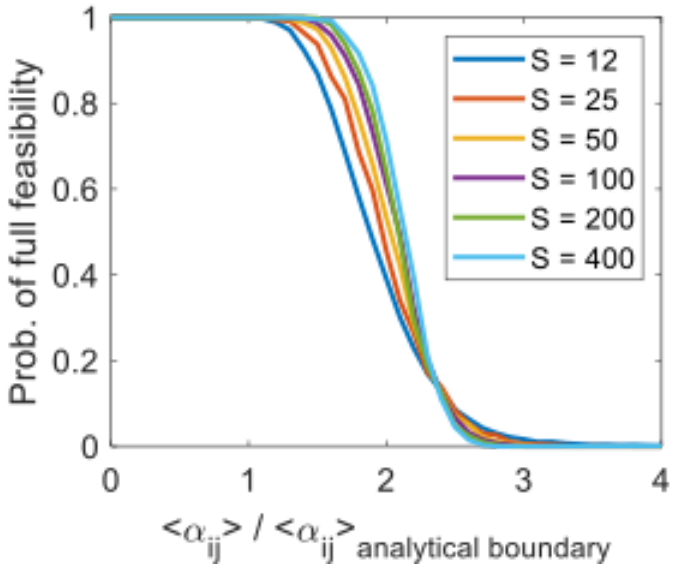

Figure 2-34: The probability of full coexistence as a function of the mean interaction strength $\langle \alpha_{ij} \rangle$ exhibits a sharp phase transition between phases (I) and (II) when S is large in simulations. The x-axis is normalized by $\langle \alpha_{ij} \rangle$ where the analytical survival boundary is expected. While all curves decrease to zero in the same region, the width of the crossover regime becomes narrower with increasing S. The fact that all curves decrease to zero at the same region, shows that the analytical expression indeed captures the correct dependence of the boundary in $\langle \alpha_{ij} \rangle$ on S.

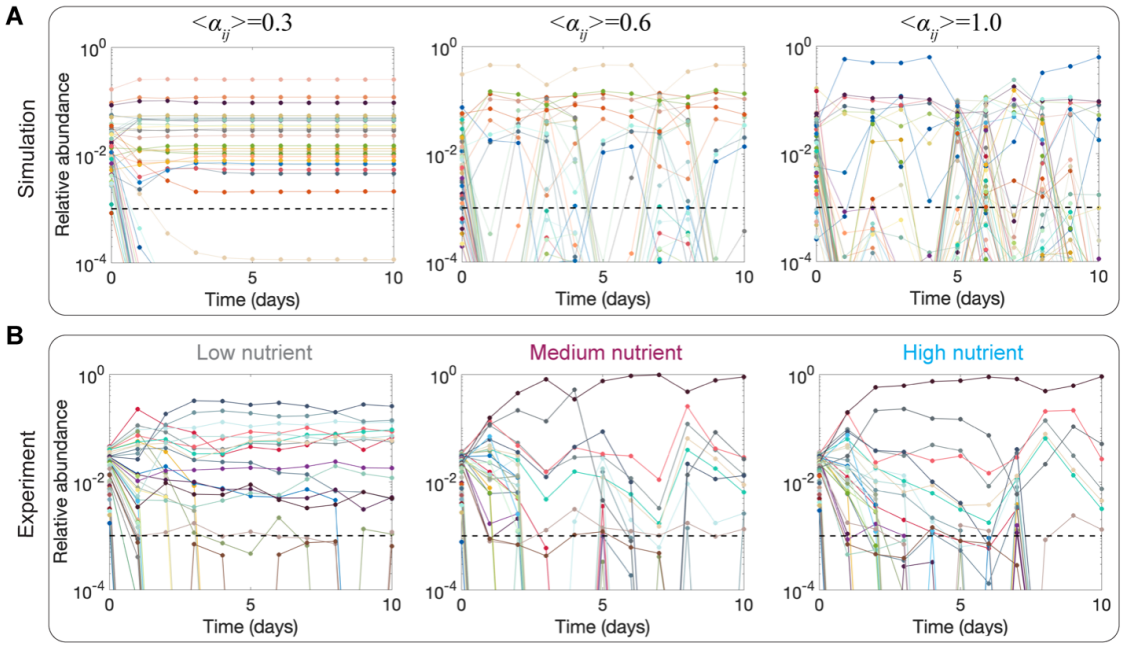

Figure 2-35: Simulated and experimental communities exhibit analogous dynamics of relative species abundances. (A) Time series of relative species abundances in a representative simulation for S=48, under low nutrients (low interaction strength, left panel), medium nutrients (medium interaction strength, middle panel), and high nutrients (high interaction strength, right panel) concentrations. We used species abundance data sampled every 24 hours of simulated time in order to match the experimental data sampling frequency. (B) Experimental time series obtained through 16S data in analogous conditions to the panels in (A). Some low abundance species (abundances below the 10^{-3} survival threshold, shown as horizontal dashed lines) exhibit fluctuation in the low nutrient concentration experiment, which can be explained by small numbers effect such as finite 16s sequencing depth.

Chapter 3

Collective dynamical regimes predict invasion success and impacts in microbial communities

3.1 Abstract

Invasions of microbial communities by species such as pathogens can have significant impacts on ecosystem services and human health. Yet, invasion outcomes are often challenging to predict: many competing explanations relate them to traits of the invading population, or to properties of the resident ecological community, such as its composition or biodiversity. By experimentally assembling microbial communities from diverse species pools, and subjecting them to invasions from species outside the pool, we first observed that a key property shaping invasion outcomes was the nature of the dynamics in the resident community. Recent findings suggest that several qualitatively distinct dynamical regimes can emerge at the community level, depending on a few parameters such as species pool size and interaction strength. Varying these parameters across experiments and in models, we were indeed able to map both resident dynamics and invasion outcomes, and analyze the influence of the former on the latter. We found that species interactions can lead to spontaneous

abundance fluctuations, associated with higher diversity and more invasions. Strong interactions can also induce alternate stable states; we observe stable communities with priority effects and low invasion probability but high impacts. These findings clarify the debated relationship between biodiversity and invasibility: the fraction of resident species surviving from the original pool, modulated by the dynamical regime, emerges here as the best predictor of further invasions. Our microcosm experiments suggest that the success and impacts of ecological invasions may be emergent properties of collective interactions and dynamics, predictable from simple community-level features.

3.2 Introduction

Ecological invasion, characterized by the spread of non-native species into novel environments, has significant consequences for biodiversity, ecosystem function, and habitat resilience [116]. Over decades, scientists have sought to unravel the myriad factors influencing why some species invade successfully while others do not. Ecologists have posited a range of determinants, from the fitness and adaptability of the invaders to the resilience and composition of native communities [104, 109, 10]. In particular, traits of the invading species have been identified as critical in shaping invasion outcomes[143]. Concepts like the Allee effects and the propagule pressure hypothesis emphasize that introducing larger initial populations of invaders can increase the likelihood of establishment and spread [41, 3]. Meanwhile, the enemy release hypothesis suggests that invasive species often succeed in new environments because they lack predators, herbivores, or pathogens[32]. Other research like biotic resistance hypothesis studied how the properties of resident communities determine the invasion outcome, which suggests that communities with high native biodiversity are more resistant to invasion than less diverse communities, due to more efficient resource use or presence of species that can compete directly with the invaders[62, 28, 112]. Beyond the characteristics of invader species and resident communities, environmental conditions have been shown to play a crucial role in shaping the invasion outcome[116].

Theories such as the storage effect and the fluctuating resource availability hypothesis posit that environmental disturbances and fluctuations might favor invader species in specific periods[76, 139, 73].

Invasions in microbial communities are also significant ecological phenomenon that occurs in various environments, ranging from soil and aquatic ecosystems to the human body[34, 121, 83, 49, 77, 33, 71]. These invasions can have profound impacts on ecosystem services and human health [34, 121, 49, 77]. Pathogenic microbes can invade host-associated microbial communities, leading to infections and diseases [49, 108, 54]. For example, the invasion of pathogenic microbes C. difficile into the gut microbiota can lead to severe diseases including diarrhea and colitis [108, 120]. Understanding the mechanisms underlying invasion success and the ecological consequences can help inform strategies for disease prevention, as well as the development of targeted therapies to control invasive pathogens[120, 37]. Similar to larger-scale ecological systems, it has been suggested that microbial communities with higher diversity are less likely to be invaded because diverse resident species may occupy all available niches and resources, leaving less room for invaders [83, 55, 134, 137]. Furthermore, it was shown that facilitative and competitive interactions between microbes can favor and prevent successful invasions, respectively [55, 69, 81, 2]. Parallel to observations in macro-organisms, external disruptions such as antibiotic interventions or nutrient level shifts can heighten the vulnerability of microbial communities to invasions by creating more available niches and resources [34, 61, 79, 64].

While research in microbial community invasions has made significant strides, it remains unclear what characteristics of resident communities determine their invasion resistance, and how entire microbial communities respond to invasion [121, 83, 65, 89]. Building upon the groundbreaking work of Robert May, ecologists have endeavored to understand community dynamics by utilizing community-level parameters [28, 5, **?**, 56, 24, 14, 95]. In this paper, we used a combination of experiments and modeling to show that simple community-level features, including stability, species pool size and interaction strength, can predict the invasibility and invasion effect of communities. Contrary to the prevalent belief that increased community diversity

results in reduced invasion probability due to fewer available niches [83, 55, 134, 137], our findings suggest that more diverse communities, given the same initial species pool size and nutrient conditions are actually more likely to be invaded due to dynamical fluctuation. Consistent with the ongoing diversity-invasibility debate [74, 118, 146], we also found that diversity-invasibility relationships are qualitatively different depending upon how the diversity is changed. To resolve the diversity-invasibility debate and unify their relationship, we normalized diversity with species pool size and get survival fraction, which displayed a universal positive correspondence with invasibility across all conditions. While existing research suggests that the sequence and timing of species introduction can influence invasion success [28, 38, 117], the underlying reasons why certain communities exhibit a pronounced priority effect, while others do not, remain underexplored [38, 117]. Our findings indicate that priority effect only emerges in communities with strong interspecies interactions and large species pool size, where the presence of alternative stable states could potentially inhibit the proliferation of invaders at low abundance [28, 56, 8]. Additionally, the ecological consequences of invasive species on resident community structure and ecosystem functioning are not yet fully understood [8, 97]. We provide evidence that invasions, when successful, have a more pronounced effect on resident community structure and biomass in contexts with strong interspecies interactions compared to weaker ones. Our results demonstrate that both invasibility and invasion effect are emergent properties shaped by the interactions of resident species, which can be predicted by simple community-level features.

3.3 Results and Discussion

3.3.1 Experiments show that the invasion probability in fluctuating communities is higher than stable ones, leading to a positive diversity-invasibility relationship

To experimentally characterize invasions in microbial communities, we built 17 different synthetic communities of size $S = 20$ using a library of 80 bacterial isolates from river and terrestrial environments (Fig. 3-1A and Fig. 3-6). We exposed each community to daily cycles of growth and dilution into fresh media, with dispersal from the species pool ($S = 20$) to mimic species dispersal in natural habitats (Fig. 3-1A). After six days of culturing, each community was exposed to an invader species (Fig. 3-1B) and we continued to culture the communities for another 6 days with dispersal of all species on each dilution cycle (Fig. 3-1A, B). For each resident community, we performed about 9 independent invasion tests with different invader species on day 6, and monitored the growth of the invader and resident species (Fig. 3-1B). Analyzing species abundances through 16S sequencing, we found that 7% +/- 2% of invasion tests were successful (relative invader abundance exceed extinction threshold 810-4 on the last day 12) (Fig. 3-1C and Fig. 3-7). Although diverse ecosystems are typically thought to be more resistant to invaders(17, 26–28), our experimental results display a significant (p=0.036) positive correlation between invasion probability and community diversity (correlation coefficient=0.51, Fig. 3-1C). Among communities of low diversity (2 – 5 surviving species) only 3% +/- 2% of invasions were successful, whereas among communities of high diversity (6 – 9 surviving species) 13% +/- 5% of invasions were successful. We therefore find that less diverse communities may resist invasions better than highly diverse ones under the same initial species pool size and nutrient conditions.

To better understand why the more diverse communities were more invasible, we next quantified the dynamics of the resident communities before invasion. We found that just under half (8 / 17) of the resident communities displayed persistent fluctu-

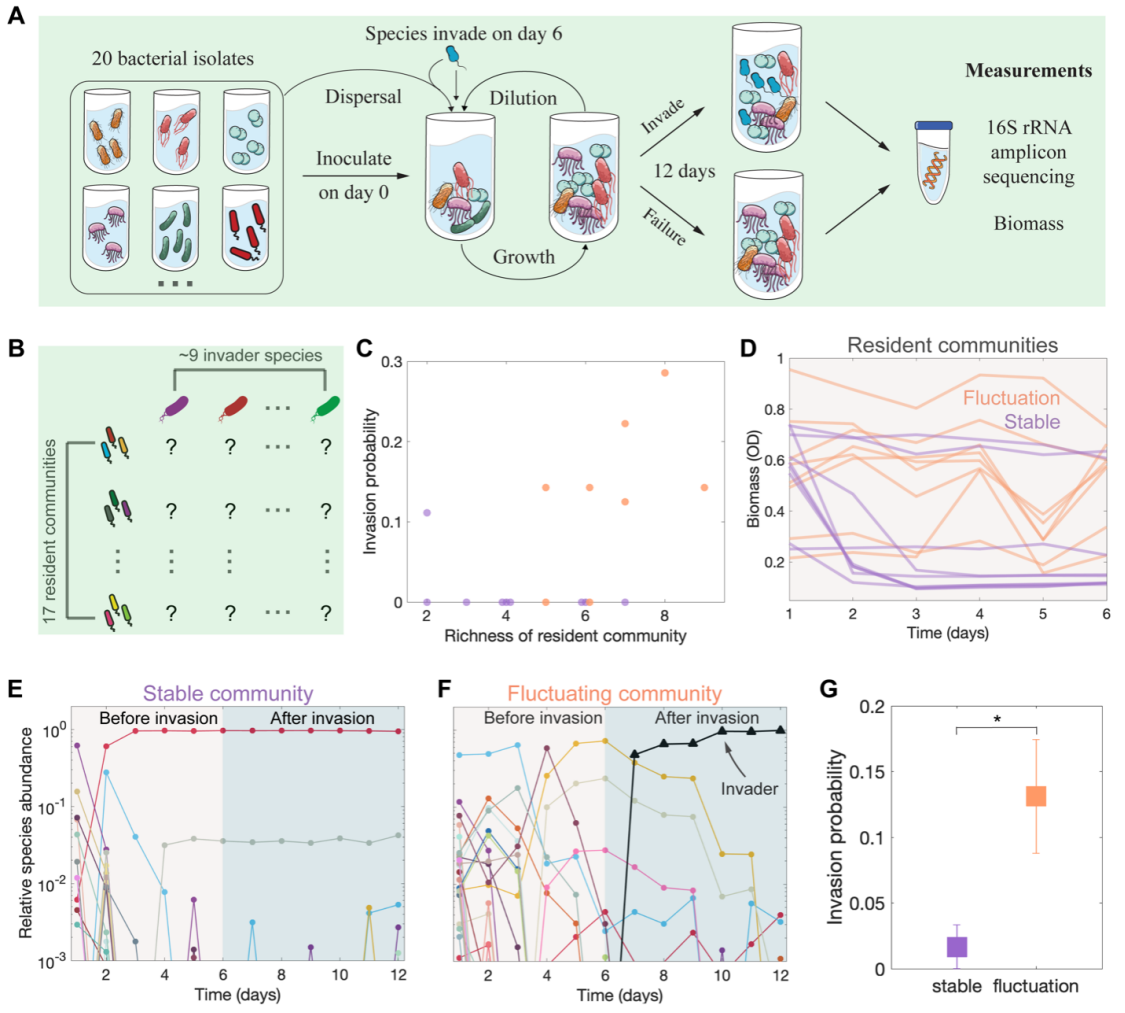

Figure 3-1: Experiments using synthetic microbial communities show that the invasion probability in fluctuating communities is higher than stable ones, leading to a positive diversity-invasibility relationship. (A) We generated different synthetic communities with S=20 species in the pool. Communities underwent serial daily dilutions with additional dispersal from the pool. We introduced invader species to the resident communities on day 6. (B) We formed 17 resident communities with different sets of species (S=20). We added invader species outside the pool into the resident communities on day 6, and then measured the community compositions and biomass on day 12 to determine the outcome and effect of the invasions. (C) The invasion probability of resident communities positively correlate with their richness (correlation coefficient=0.51). (D) 8 out of the 17 resident communities reach fluctuation in biomass (orange) and the rest 9 communities reach stable states (purple). (E) Representative time course of relative species abundance via 16S sequencing show the stable community was not invaded. (F) Representative time course of relative species abundance shows the invader successfully invade and grow in the fluctuating community. (G) The invasion probability to fluctuating resident communities is statistically higher than that to stable communities (p=0.016, the number of invasion tests is n=61 (60) for fluctuating (stable) communities. Error bars represent s.e.m..

ations in biomass and species composition, with the remainder reaching stable community states (Fig. 3-1D-F and Fig. 3-8,3-9,3-10,3-11,3-12,3-13,3-14,3-15,3-16,3-17). We found that biomass fluctuations were highly correlated with species abundance fluctuations (Fig. 3-17) and the classification of stable and fluctuating communities was robust to different methods (Fig. 3-17). Consistent with our previous results, we found that the diversity of fluctuating communities is approximately twice the diversity in stable communities (Fig. 3-1C) [56]. Given this higher diversity in fluctuating communities, we next analyzed the invasibility of communities separately for the stable and fluctuating communities to determine if this could be driving the positive diversity-invasibility relationship that we observed. Indeed, we detected 8 successful invasions out of 61 invasion tests to fluctuating communities, while there was only one single successful invasion out of 60 invasion tests to stable communities (Fig. 3-7). Our results therefore show that the probability to successfully invade fluctuating communities (13% +/- 4%) is statistically 8 fold larger than the probability of invading stable communities (1.7% +/- 1.7%) (Fig. 3-1G). Our experimental tests of invasion demonstrate that more diverse communities are more invasible because fluctuating communities are both more diverse and more susceptible to invasion.

3.3.2 Lotka-Volterra model predicts a decrease of invasion probability when stability, interaction strength and species pool size of resident communities increase

To gain insight into these surprising relationships between diversity, stability, and invasibility, we next studied invasions in the well-known generalized Lotka-Volterra (gLV) model, modified to include dispersal from a species pool:

$$\frac{dN_i}{dt} = N_i(1 - \sum_{j=1}^{S} \alpha_{ij} N_j) + D \tag{3.1}$$

where N_i is the abundance of species i (normalized to its carrying capacity), $<\alpha_{ij}>$ is the interaction strength that captures how strongly species j inhibits species i (with

self-regulation $\alpha_{ii} = 1$), and D is the dispersal rate. We simulated the dynamics of communities with different species pool sizes S and interaction matrices. We sampled the interaction strength from a uniform distribution U [0, $2<\alpha_{ij}>$], where $<\alpha_{ij}>$ is the mean interaction strength between species. Modeling species interactions as a random interaction network captures species heterogeneity without assuming any particular community structure (10, 37–39). We introduced invaders into resident communities at t=10^3 and continued to simulate the dynamics until t

Our simulations revealed rich dynamics and invasion outcomes under strong interaction strength between species (Fig. 3-2A). Some successful invasions cause dramatic effect on the structures of resident communities, whereas other invasions only yield weak change in communities (Fig. 3-2A). Consistent with our experimental results (Fig. 3-1C and G), we found a positive correlation between invasion probability and richness (Fig. 3-2B), which is because fluctuating communities exhibit larger invasion probability than stable communities under the same conditions (Fig. 3-2C). Our simulation results with the Lotka-Volterra model also predict that the invasion probability decreases when interaction strength $<\alpha_{ij}>$ and the species pool size S increase (Fig. 3-2D-F). It is important to note that although fluctuating communities exhibit smaller invasion resistance than stable communities under the same conditions, stable communities can still yield smaller invasion resistance under weaker interaction strength $<\alpha_{ij}>$ or smaller species pool size S (Fig. 3-2D-F). The Lotka-Volterra model therefore explains why our diverse and fluctuating communities are susceptible to species invasion and makes new predictions regarding how invasibility would change with the size of the species pool and the strength of interspecies interactions (Fig. 3-2D-F).

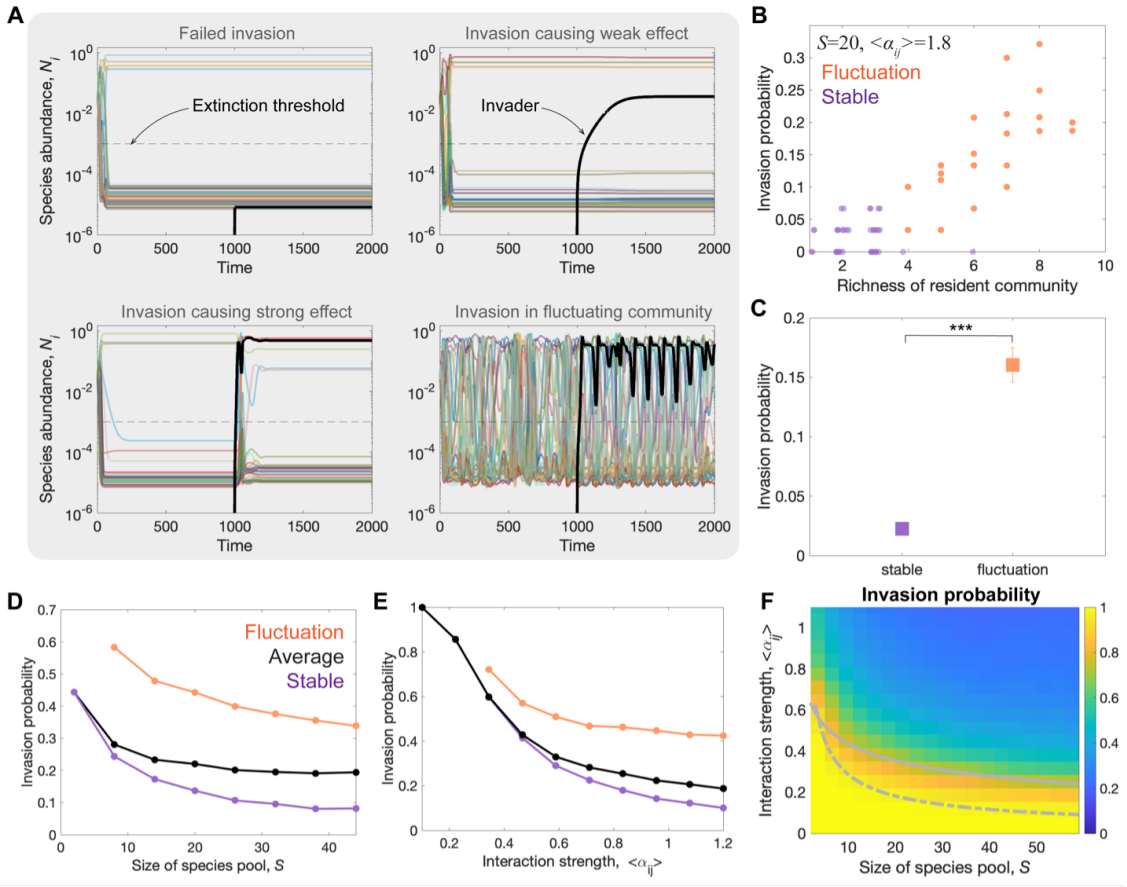

Figure 3-2: Lotka-Volterra model predicts a decrease of invasion probability when stability, interaction strength and species pool size of resident communities increase. (A) Representative time series of species abundance in simulation show diverse invasion dynamics and outcome: invader species failed to grow in the community (top left panel, the black curve represents invader); invader grow and only cause small effect on community composition (top right panel); invader successfully invade and cause large change on community composition (bottom left panel); invasion to a fluctuating resident community (bottom right panel) (<α_{ij}>=0.6, S=32). (B) Consistent with experiments (Fig 3-1C), the invasion probability of simulated resident communities positively correlate with their richness, which arises because fluctuating communities are more diverse and more invasible. (C) The invasion probability to fluctuating resident communities is statistically higher than that to stable communities ($p < 0.001$). (D) Increasing species pool size leads to a decrease in invasion probability. Fluctuating communities (orange points) exhibit higher invasion probability than stable communities (purple points). (E) Increasing interaction strength leads to a decrease in invasion probability. (F) Increasing species pool size and interaction strength leads to a decrease in invasion probability. The curves and color maps depict the mean value over 1000 simulations.

3.3.3 Increasing interaction strength and species pool size leads to higher invasion resistance of resident communities in experiment

To experimentally test the predicted dependence of invasion resistance on interaction strength and species pool size, we tuned the inter-species interaction strength by tuning the concentration of supplemented glucose and urea in the culture medium [56, 101, 103]. As discussed in our previous work [56, 101, 103], increasing the concentration of supplemented glucose and urea leads to stronger strength of competitive interactions between bacterial species due to extensive modification of the media (e.g. pH). We measured the invasion of 9 invader species to 15 synthetic resident communities under low nutrient (weak interaction) and 25 communities under high nutrient (strong interaction) conditions. Consistent with our theoretical predictions, we found that increasing interaction strength leads to an increase of invasion resistance in resident communities (Fig. 3-3A). Specifically, the invasion probability is 7% +/- 2% under high nutrient (strong interaction), which is 8 folds lower than 56% +/- 8% under low nutrient (weak interaction) (Fig. 3-3A). We also decreased the species pool size from S=20 to S=12 and found that invasion probability increased from 85% +/- 6% to 56% +/- 8% under low nutrient (Fig. 3-3B), consistent with our theoretical predictions. Our theory and experiment both indicate that increasing interaction strength or species pool size leads to a decrease in community invasibility [28, 83, 55, 134, 137].

To unify different invasibility-richness relationships in the experiments depending upon how the richness is changed (by varying interaction strength, species pool size, or stability) (Fig. 3-18), we further analyzed the dependence of invasion probability on the survival fraction of species in resident communities, defined as the fraction of species in the initial pool which survive in the end of assembly (on day 6 before invasion). The results show a strongly positive correlation of invasibility on survival fraction, where the correlation coefficient is 0.82 (Fig. 3-3C). Microbial communities cultured in low nutrient (weak interaction) media display both a larger invasion

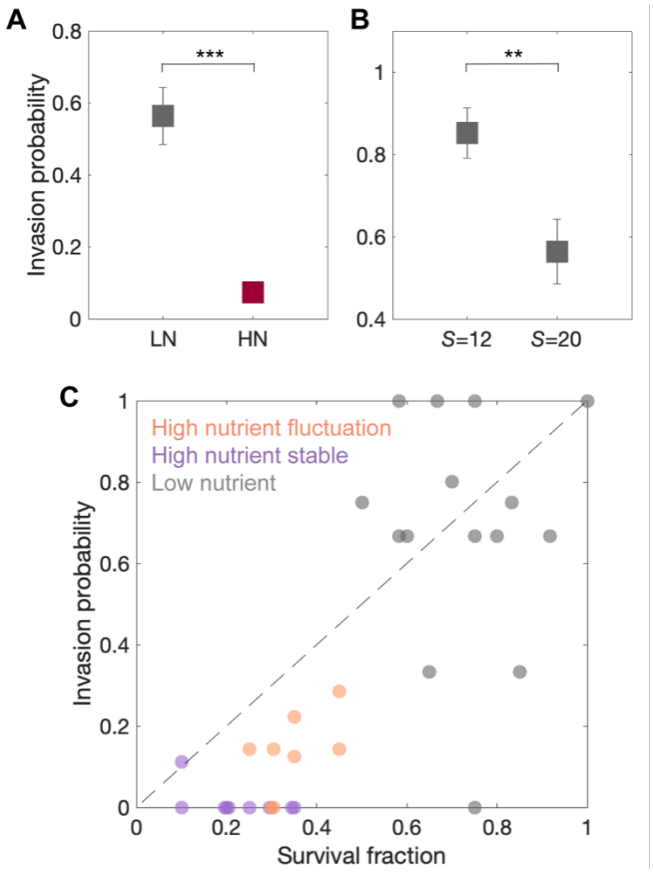

Figure 3-3: Increasing interaction strength and species pool size leads to higher invasion resistance of resident communities in experiment. (A) The invasions to resident communities under low nutrient (weak interaction) exhibit statistically higher invasion probability than communities under high nutrient (strong interaction) ($p < 0.001$, the number of invasion tests is n=120 (39) for high (low) nutrient). (B) The invasions to resident communities under smaller species pool size (S=12) exhibit statistically higher invasion probability than communities under larger species pool size (S=20) ($p = 0.007$, the number of invasion tests is n=39 (34) for S=20 (12), all communities were cultured under low nutrient). Error bars represent s.e.m.. (C) The invasion probability positively correlates with survival fraction (before invasion) across different communities and nutrient conditions (each point represents one community; correlation coefficient is 0.82). The points corresponding to communities under high nutrient are below the diagonal line, showing the invasion probability of communities under high nutrient are generally smaller than their survival fraction, which indicates the priority effect under strong interaction strength.

probability and larger survival fraction than communities under high nutrient (strong interaction) (Fig. 3-3C). Furthermore, fluctuating communities which are easier to be successfully invaded also exhibit larger survival fraction than stable communities under the same conditions (Fig. 3-3C and 3-1C). These results demonstrate that the survival fraction can serve as a unifying predictor of the invasibility of a resident community. Although it has been suggested that microbial communities with higher diversity are less likely to be invaded because they leave less available niches and resources for invaders [83, 55, 134, 137]., our results indicate that this is only true when the diversity is increased by increasing the size of the species pool (Fig. 3-3C and 3-1C). However, if diversity is modulated by a change in interaction strength or stability then more diverse communities are instead more invasible.

Despite our experimentally observed correspondence between invasion probability and survival fraction, we noted that the invasion probability for communities under high nutrient are usually lower than their survival fraction (majority of points on the bottom left (high nutrient) are below the diagonal line on Fig. 3-3C). In ecology, the priority effect refers to the phenomenon in which the community structure is influenced by the order and timing of species' arrival in a community [38, 117] mismatch between invasion probability and survival fraction under high nutrient is evidence of the priority effect in the community assembly under strong interactions in our experiment. Under weak interactions, the colonization probability of invader species is similar with the probability of a species in the initial pool surviving the process of community assembly, whereas invader species are statistically less likely to survive in the communities than the species in the initial pool under strong interactions (Fig. 3-3C)[28]. The emergent priority effect in communities composed of strongly interacting species could be explained by alternative stable states tending to inhibit the growth of invaders at low abundance[28, 56].

3.3.4 Theory predicts a universal correspondence between invasion probability and survival fraction, the emergence of priority effect and stronger invasion effect when increasing interaction strength

To understand the reason why diversity-invasibility relationship is different when varying interaction strength, species pool size or stability (Fig. 3-1C, Fig. 3-2 and Fig. 3-3), we sampled resident communities along different paths on the phase diagram, by varying species pool or interaction strength. We simulated invasions to these resident communities and found different diversity- invasibility relationship along different paths (Fig. 3-4A). The results show a positive diversity- invasibility relationship when only varying interaction strength while fixing species pool size, or randomly sampling communities under the same parameters of species pool size and interactions (Fig. 3-4A). On the contrary, a reversed negative or non-monotonic diversity-invasibility relationship was observed when varying species pool size while fixing interaction strength (Fig. 3-4A). Despite these conflicting diversity-invasibility relationships, after scaling richness with species pool size to get the dimensionless survival fraction, we analyzed the dependence of invasion probability on survival fraction, finding that all communities collapsed to a universal line in which the invasion probability is approximately equal to the survival fraction (Fig. 3-4B). The deviation from the exact collapse in small survival fraction regime (bottom left of Fig. 3-4B) indicates priority effect under strong interaction. Our results indicate that survival fraction determines invasibility, whereas diversity-invasibility relationship can be qualitatively different depending upon the origin of different diversity in different communities.

To understand the emergence of the priority effect in experiment (Fig. 3-3C), we next studied invasion outcomes in the Lotka-Volterra model under different regime of interaction strength and species pool size. We quantified the priority effect by calculating the difference between survival fraction of resident species and the invasion probability of species that invade after the resident communities have assembled,

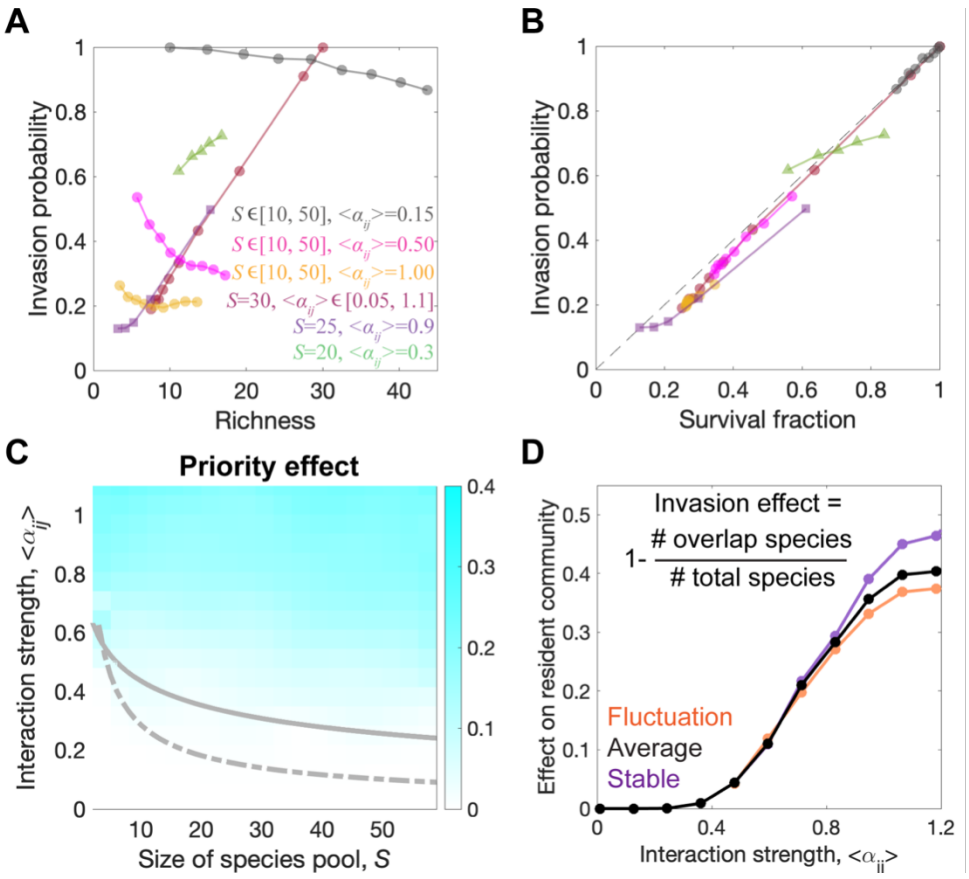

Figure 3-4: Lotka-Volterra model predicts a universal correspondence between invasion probability and survival fraction, the emergence of priority effect and stronger invasion effect when increasing interaction strength. (A) The dependence of invasion probability on final richness of resident communities is qualitatively different depending upon how the richness is changed. Invasion probability positively correlates with richness when varying interaction strength or when randomly sampling communities with a fixed species pool size and interaction strength distribution. Invasion probability can decrease with community diversity when varying species pool size. (B) Invasion probability is approximately equal to the survival fraction of species in the resident communities, no matter how we change richness, species pool or interaction strength. (C) Increasing species pool size and interaction strength leads to the emergence of priority effect, where the invasion probability of resident communities is smaller than their species survival fraction. (D) Successful invasions cause larger effect on species composition in the resident communities under stronger interaction strength. The curves depict the mean value over 1000 simulations.

where the difference was normalized by survival fraction (Fig. 3-4C). We found there is no clear priority effect in the small species pool size and weak interaction regime, where species in the initial pool and invader species display similar probability of colonizing in the communities (Fig. 3-4C). Consistent with our experimental results, increasing species pool size and interaction strength in the model leads to the emergence of priority effect in the phase where communities reach fluctuation or alternative stable states (Fig, 3-4C). We found the priority effect originated from alternative stable states or limit cycle oscillations in the strongly interacting phase, whereas chaotic fluctuations display no significant priority effect in simulation (Fig. 3-19), which can be explained by its ergodicity [24, 95]. It was suggested that successful invasions can cause strong or weak effect on resident community structure, depending on how invaders interact with resident species [28, 69, 81]. Our simulations show that invasions cause stronger change on structure of resident communities under stronger interactions, where the invasion effect is defined as the ratio of surviving species change before and after the invasion (Fig. 3-4D).

3.3.5 Increasing interaction strength leads to a stronger effect on resident communities under invasion success

To understand the effect of a successful invasion on the structure of the resident community in the experiment, we analyzed the change of biomass and species composition before and after the invasions (Fig. 3-5). The community biomass displays relatively small change after invasion under weak interaction (low nutrient, inset of Fig. 3-5A and Fig. 3-11,3-12). In the strong interaction regime (high nutrient), we found that stable communities typically transitioned from low biomass states to high biomass states under successful invasions, whereas the biomass of fluctuating communities continued to fluctuate over a similar range (Fig. 3-5A-C and Fig. 3-8,3-9,3-10). Averaging across both stable and fluctuating communities, we found that community biomass under strong interaction displayed a larger fold change (2.9 +/- 0.8) after successful invasion than those under weak interaction (1.15 +/- 0.03) (Fig. 3-5C). To

characterize the effect of invasion on species composition in the resident community, we defined the invasion effect as the fraction of surviving species that change before and after invasion. We compared the change of relative species abundance between invaded communities and control communities without adding invaders (Fig. 3-20,3-21,3-22,3-23). This analysis on species abundances through 16S sequencing further indicated that successful invasions cause stronger change in the species compositions under strong interaction (53% +/- 6%) than weak interaction (39% +/- 2%) (Fig. 3-5D), which is consistent with the simulation results with Lotka-Volterra model (Fig. 3-4D). The growth of invader species influences the community structure more dramatically when it has stronger interaction with other resident species, and the strong interplay between resident species can also cause stronger secondary effect on other resident species when their abundance change [28, 8].

Although our study was primarily focused on community-level properties that determine invasibility and invasion effect, we also analyzed properties of the invader species that correlated with invasibility and invasion effect. Perhaps surprisingly, we did not observe a significant correlation between a species' ability to invade and that species growth in monoculture (Fig. 3-24). For example, Pseudomonas (invader 4) and Enterobacterales (invader 7) were the two most successful invader species (16/35 and 6/11 invasions, respectively), yet displayed growth in monoculture that was typical of the group of nine invaders that were tested. Bacillus (invader 6) with the highest growth rate among all invaders under both high and low nutrients, only display a small fraction of invasion success (2/37). Moreover, we also observed that Pseudomonas (invader 2) and Pedobacter (invader 3) could occasionally invade communities despite being subject to a strong Allee effect that prevented the species from growing from an initially small inoculum (Fig. 3-22). Furthermore, we did not observe significant correlation between the invasion effect and invader properties either (Fig. 3-25). No matter calculating invasion probability of resident communities or different invaders, we found an absence of correlation between invasion probability and invasion effect (Fig. 3-26). Taking these together, we therefore found that monoculture growth properties were surprisingly ineffective at predicting a species success as an invader,

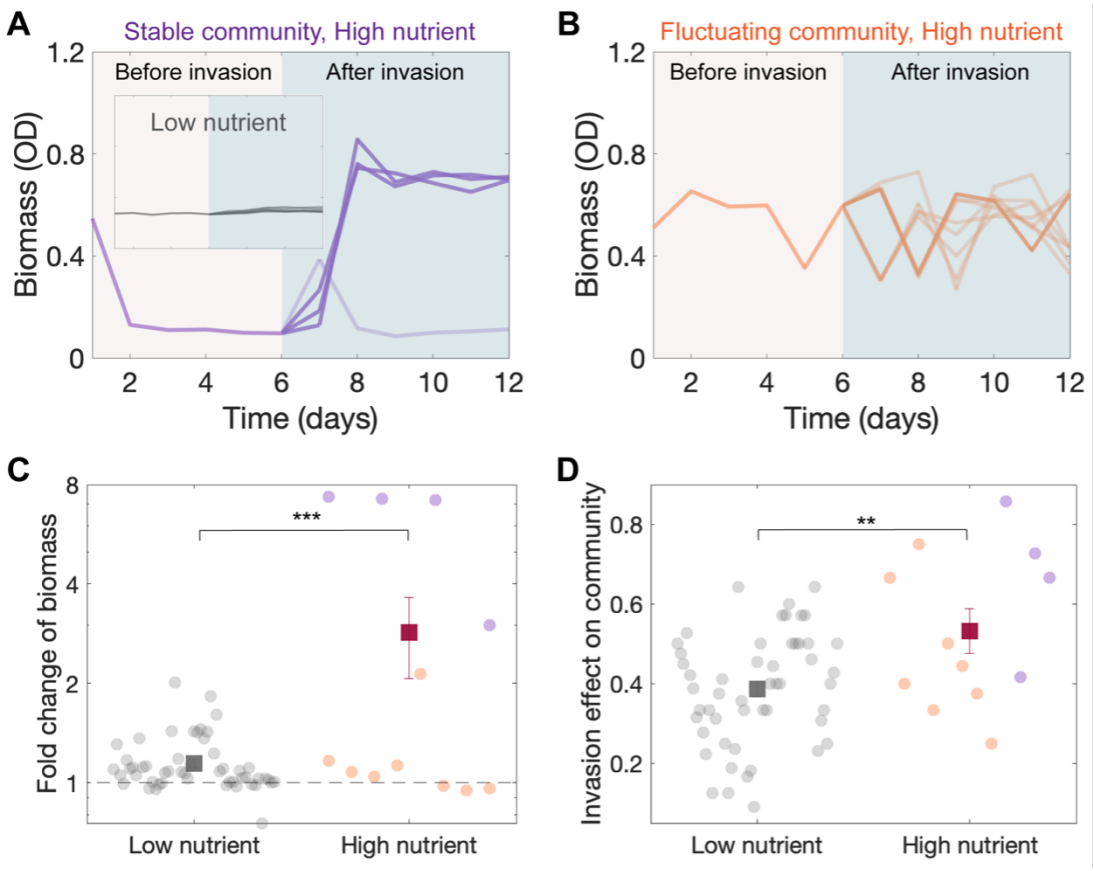

Figure 3-5: Increasing interaction strength leads to a stronger effect on resident communities under invasion success. (A) The stable communities under high nutrient experienced a large increase in biomass after successful invasions (dark purple curves). Inset shows the invasions under low nutrient only cause weak effect on community biomass as compared with high nutrient. (B) The time course of fluctuating community biomass under high nutrient before invasion and after invasion, where dark and light orange curves represent successful and failed invasions, respectively. (C) The invasions to resident communities under low nutrient (weak interaction) cause statistically lower fold change of biomass than communities under high nutrient (strong interaction) ($p < 0.001$, the number of successful invasions is n=51 (11) for low (high) nutrient). The successful invasions statistically tend to increase the biomass of resident communities under different conditions. (D) The invasions to resident communities under low nutrient (weak interaction) cause statistically lower effect on species composition change than communities under high nutrient (strong interaction) ($p = 0.0038$, the number of invasion tests is n=51 (11) for low (high) nutrient). Error bars represent s.e.m..

while resident community properties are the primary factors determining the invasion outcome.

3.4 Methods and Materials

3.4.1 Bacterial isolates, media and culturing conditions

We constructed the library of 80 bacterial species from soil, tree leaves, and Charles River water samples taken near the campus of Massachusetts Institute of Technology (Fig. 3-6).

In the case of low interaction strength (low nutrients concentration) conditions, experimental communities were cultured in Base Medium (BM): 1g/L yeast extract and 1 g/L soytone from Becton Dickinson, 10 mM sodium phosphate, 0.1 mM $CaCl_2$, 2 mM $MgCl_2$, 4mg/L $NiSO_4$ and 50 mg/L $MnCl_2$, pH adjusted to 6.5. For high interaction strength (high nutrients concentration) conditions, we used BM supplemented with 5 g/L glucose and 4 g/L urea. All media were filter sterilized using Bottle Top Filtration Units (VWR). All of the chemicals were purchased from Sigma–Aldrich unless otherwise stated.

Both monocultures and communities of the bacterial isolates were grown in 96-deepwell plates (Deepwell plate 96/500μl; Eppendorf) covered with AeraSeal adhesive sealing films (Excel Scientific). The incubation temperature was 30 °C for all communities. The deepwell plates were shaken at 1,200 r.p.m. on Titramax shakers (Heidolph). To minimize evaporation, the plates were incubated inside custom-built acrylic boxes.

3.4.2 Pre-cultures, daily dilutions, dispersal, and biomass measurements

Before each experiment, pre-cultures were initiated by thawing the bacteria and inoculating individual species into 300 μL of BM. The resulting monocultures were exposed to 5 daily cycles of growth and (30-fold) dilution into fresh media. At the

beginning of each experiment, aliquots of these monocultures were mixed in equal volume proportions to form the synthetic communities. During the experiment, the monocultures were exposed to further dilution cycles and used to apply the daily dispersal into the synthetic communities as described below.

We created 40 different synthetic communities using randomly generated subsets of the library of isolates, each subset constituting the species pool (of size S) for each community. After mixing monocultures in equal volumes, each experimental community was initiated by inoculating 10 μL of its initial mix of isolates into 300 μL of BM. The resulting synthetic communities were cultured under serial dilution cycles with dispersal as follows. To apply a $10^{-}5$ dispersal rate, every 24hr monoculture aliquots of the species in each community pool were mixed at equal volumes, and then diluted by a 10^3 factor before inoculating 6μL of this mix into the wells containing the corresponding experimental community matching each species pool. After this, the experimental cultures were thoroughly mixed using a 96-well pipettor (Viaflo 96, Integra Biosciences; settings: pipette/mix program, 5 mixing cycles, mixing volume 150 μL, speed 6) before applying a 30-fold dilution by transferring 10 μL of the cultures into a new plate with 300 μL of fresh media.

The resident communities were cultured over 6 dilution cycles before introducing the invader species. When introducing the invader species on day 6, The volume ratio between the monoculture of invader species and the resident community was 10^{-3}. After introducing the invaders on day 6, we performed another 6 daily dilution cycles with a 10^{-5} dispersal rate for all species including the invader species until the end of the experiment. At the end of every daily cycle, 150μL samples of each culture were used to measure the OD (600nm), a proxy for the total biomass in the cultures, using a Varioskan Flash (Thermo Fisher Scientific) plate reader. The remaining culture volume was stored at -80 °C for subsequent DNA extraction.

3.4.3 DNA extraction, 16S rRNA sequencing and data analysis

To monitor the dynamics of the microbial communities, we measured community composition via 16S ribosomal RNA (rRNA) amplicon sequencing. DNA extraction was performed by the Environmental Sample Preparation and Sequencing Facility at Argonne National Laboratory. The obtained DNA was used for 16S (V4 region) amplicon sequencing. Library preparation and Illumina MiSeq sequencing were performed by the Environmental Sample Preparation and Sequencing Facility at Argonne National Laboratory. We used the R package DADA2 to obtain the amplicon sequence variants (ASVs) as described by Callahan et al.[27]. Taxonomic identities were assigned to the ASVs by using SILVA (version 132) as a reference database. For each sample. species richness was calculated as the number of ASVs with a relative abundance 0.08%, which corresponds to the 0.08% extinction threshold used in simulation. Taxonomic identities were assigned to ASVs using Randomized Axelerated Maximum Likelihood (RAxML) using default parameters. In our sequencing dataset, the average sequencing depth is 17075 reads. This means that we could not effectively resolve any species abundance on the order of 0.01% or below. Our main observables, invasion success, diversity and stability, were calculated (Methods) only from species abundances that exceed a threshold of 0.08% (the extinction threshold).

3.4.4 Numerical methods

We modeled the long-term dynamics and diversity of ecological communities using the well-known generalized Lotka-Volterra (gLV) model, modified to include dispersal from a species pool:

$$\frac{dN_i}{dt} = r_i N_i (1 - \sum_{j=1}^{S} \alpha_{ij} N_j / K_i) + D \tag{3.2}$$

where N_i is the abundance of species i (normalized to its carrying capacity), α_{ij} is the interaction strength that captures how strongly species j inhibits the growth of species i (with self-regulation $\alpha_{ii} = 1$), and D is the dispersal rate from an outside

species pool to the focal community. For simplicity and without qualitatively changing our results, we considered the same growth rate $r_i = 1$ and the same carrying capacity $K_i = 1$ for all species in the main text. Our previous paper shows that sampling growth rates from a uniform distribution has little effect on the phase diagram of survival fraction and fluctuation fraction [56]. Our previous paper also shows that sampling carrying capacities from a normal distribution increases the partial coexistence phase while shrinking both the full coexistence phase and fluctuation phase but does not affect the order of the phases [56].

In our previous work, we tested the theoretical predictions when considering the existence of positive (facilitative) interspecies interactions and varying the symmetry of the interaction matrix (39). We also considered different dispersal rates, and the effects of incorporating daily dilutions in these in silico communities [56]. These additional results show that our qualitative phase diagrams and conclusions are robust to different choices of ecological network structure and parameters. Although the patterns of ecological diversity and dynamics do not change as the dispersal rate varies from 10^{-7} to 10^{-6}, we found that communities with zero dispersal rate exhibit lower fluctuation fraction and survival faction in the persistent fluctuation phase [56]. Our results showed that non-zero dispersal rates can sustain persistent fluctuations. After the resident species typically reach steady states at t=10^3, we started introducing the invader species by continuously adding dispersal of the invader to the resident community and simulated the dynamics until t=2×10^3 to determine the invasion outcome.

All simulations used the Runge-Kutta method on Matlab to numerically solve the LV equations (with an integration step of 0.05). A definition of 20×20 pixels was used for each phase diagram, linearly segmenting the parameter space in the ranges $<\alpha_{ij}> \in$ [0.02, 1.1] and $S \in$ [2, 60]. In each phase diagram, each pixel shows the average result for 10^3 simulations. The total simulation time is 2×10^3. We sampled the interaction strength from a uniform distribution U [0.5$<\alpha_{ij}>$, 1.5$<\alpha_{ij}>$] in Fig. 3-2B and 4D, where $<\alpha_{ij}>$ is the mean interaction strength between species (which also determines here the variance of interactions).

3.4.5 Reaching steady state, extinction threshold, survival fraction and stability in simulations

We define the steady state of simulated communities as the community state in which community properties (e.g., survival fraction, fluctuation fraction, and invasion probability) significantly changes as time goes on. To consistently analyze the steady state results for all the simulated communities, in our previous work, we analyzed the dependence of the phase diagrams on the simulated time [56]. Our results showed that community-level properties did not significantly changes after t=10^3. Accordingly, the phase diagrams in the paper show the state of communities at t=2×10^3, unless otherwise stated.

The presence of dispersal from the species pool in Eq. (1) guarantees that all species exhibit strictly positive abundances in Fig 3-2A. Nevertheless, we consider that a species is extinct if its abundance lays below an 8×10^-4 threshold, as consistent with the extinction in our experiment. Around this threshold, the dispersal rate becomes the main factor preventing abundance decay [56]. The species abundance distribution in the partial coexistence phase is bimodal[56]; the extinction threshold 8×10^{-4} clearly separates the high-abundance surviving species from low-abundance species that will go extinct if dispersal ceases[56].

To compute the survival fraction, we computed the fraction of species whose abundance exceeded the extinction threshold at any time during the last 100 units of time in the simulation. The survival or extinction of invader species was determined by the abundance in the last 100 units of time in the simulation. Our choice of including a time window when measuring diversity is motivated by the fact that, for the case of unstable communities, species abundances fluctuate above and below the extinction threshold over time. Since we measured diversity and species compositions every 24 hours in the experiment, we consider an analogous window of 100 time units in simulations.

To differentiate between stable and fluctuating communities, we computed the average coefficient of variation of N_i between t=10^3-100 and t=10^3. We define com-

munities with this average coefficient of variation of species abundance higher (lower) than 10^{-3} as fluctuating (stable) communities.

3.4.6 Definition of stable and fluctuating experimental communities

To differentiate between stable and fluctuating resident communities in experiments, we computed the standard deviation of biomass between day 4, day 5 and day 6. Communities for which the standard deviation of biomass over time is below (above) a 0.05 threshold are considered stable (fluctuating) communities (Fig. 3-17). We also calculated the average coefficient of variation (CV) for species abundances from day 4 to day 6. This corresponds to the average value of the standard deviation for the absolute abundance of each species N_i (over day 4, day 5, and day 6) scaled by average species abundance. The average coefficient of variation of absolute species abundance (product of biomass and relative species abundance by 16s sequencing) displays a strong positive correlation with the standard deviation of biomass over time across communities (Fig. 3-17). The average coefficient of variation of relative species abundance (by 16s sequencing) also displays a strong positive correlation with the standard deviation of biomass over time across communities (Fig. 3-17). Different metrics consistently classify the communities into two clusters: fluctuating ones on top right region and stable ones on bottom left region (Fig. 3-17). Varying the choice of time window (day 4 to day 6) to a new time window (day 5 to day 6) yield the same classification of fluctuating and stable communities. Our previous work showed that the classification of stability converges quickly to either small or large values, respectively indicating stability or long-lasting fluctuations in experimental communities [56]. We found the K-means clustering algorithm yields the same classification results of community stability. The consistence between results of K-means clustering and setting stability threshold of biomass standard deviation (0.05) demonstrates the classification of fluctuating and stable communities is robust to different algorithm.

3.5 Conclusion

Our findings show that invasibility and invasion effect can be statistically predicted by simple community-level features including community stability, species pool size, and interaction strength. As predicted by our phase diagram, increasing community diversity leads to stronger resistance to invaders only when varying species pool size and fixing community stability and environmental conditions (interaction strength), which is consistent with the biotic resistance hypothesis [62, 28, 112]. Contrary to conventional ecological beliefs, however, we demonstrated that under dynamic fluctuations or reduced interaction strength, more diverse communities might instead exhibit decreased resistance to invasion (Fig. 3-1C and 3-3C). Our results emphasize that only by concurrently considering the effects of interaction strength and stability can the diversity of native communities be used to predict invasion resistance; diversity alone is insufficient for such predictions. As a dimensionless property, it is more natural to predict invasion probability using other dimensionless variables in principle, rather than using dimensional richness. By normalizing richness with species pool size, we obtained the survival fraction, a dimensionless predictor that closely approximates invasion probability across different conditions (Fig. 3-3C and Fig. 3-4B). This survival fraction is influenced by factors such as species pool size, interaction strength, and stability (Fig. 3-2B, C and 3-3C).

Applying the insights developed here to natural communities requires that we draw a parallel between the three recognized types of diversity in ecology—alpha, beta, and gamma diversity—and the three species number variables we've investigated in our study: richness, survival fraction, and species pool size [62, 74, 105]. Specifically, richness and species pool size can be seen as analogs for alpha (local diversity) and gamma (regional diversity) diversities, respectively. Beta diversity, which defined as the ratio between regional and local diversity, is the reciprocal of the survival fraction. Consequently, our discovery of a universal positive relationship between invasibility and survival fraction suggests an overarching negative correlation between invasibility and beta diversity. While directly measuring the survival fraction in

natural communities can be challenging, the ratio of local richness to regional richness in natural habitats may serve as a reliable approximation of survival fraction [62, 74, 105], acting as a singular predictor for invasion probability. Building upon our earlier discoveries regarding emergent phases in communities [56], our current data suggests the priority effect is most pronounced in the phase of alternative stable states, under conditions of strong interactions and a large species pool (Fig. 3-2E and 3-3C). Conversely, the sequence and timing of species introduction have minimal impact on the final community structure in the global equilibrium phase when both interaction strength and species pool size are limited (Fig. 3-2E and 3-3C). Future work is necessary to determine whether these community-level features can predict invasion outcomes across spatiotemporal scales, environmental conditions, and organism types.

3.6 Supporting Information

Figure 3-6: Taxonomic identity of the bacterial isolates. The identities have been inferred from the ASV (Methods) of 16S sequencing, which allow the classification of the 80 isolates down to the genus level. Colors are consistent with those in the main text and other supplementary figures.

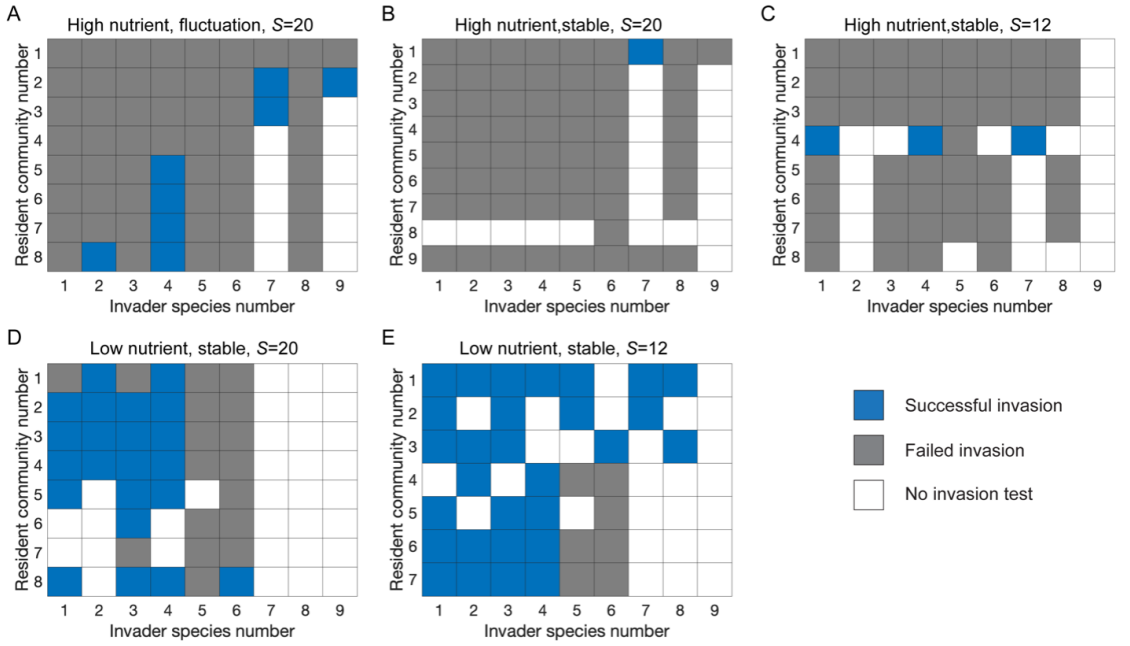

Figure 3-7: Introducing different invaders into different resident communities and measuring the invasion outcome through 16s sequencing. The invasion outcome matrices show that increasing nutrient and species pool size lead to a decrease in invasion probability.

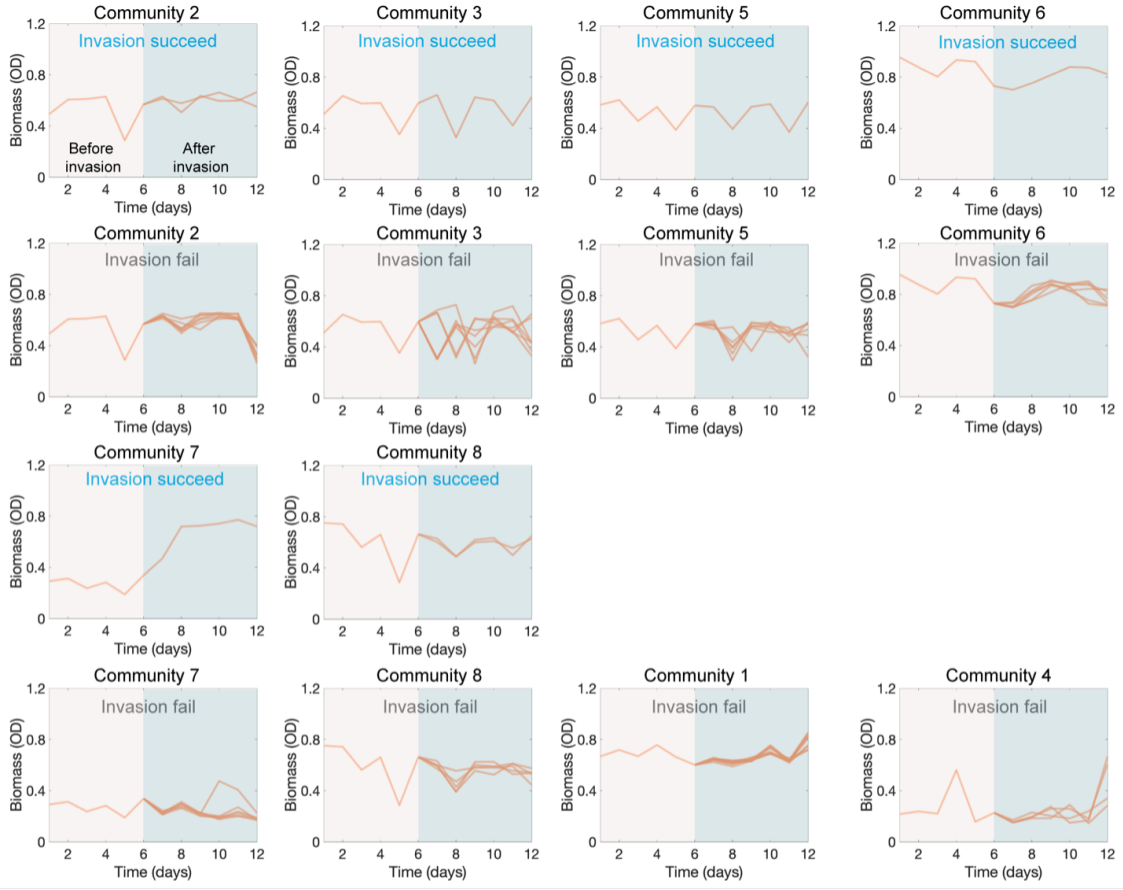

Figure 3-8: Time series for the biomass of the fluctuating communities with species pool size S=20 under strong average interaction strength (high nutrients concentration). Each panel shows the time series for the OD (600nm) of one fluctuating community with species pool size S=20 under high nutrient. The invaders were introduced on day 6, and the time series of successful invasions and failed invasions for the same communities were displayed in different panels.

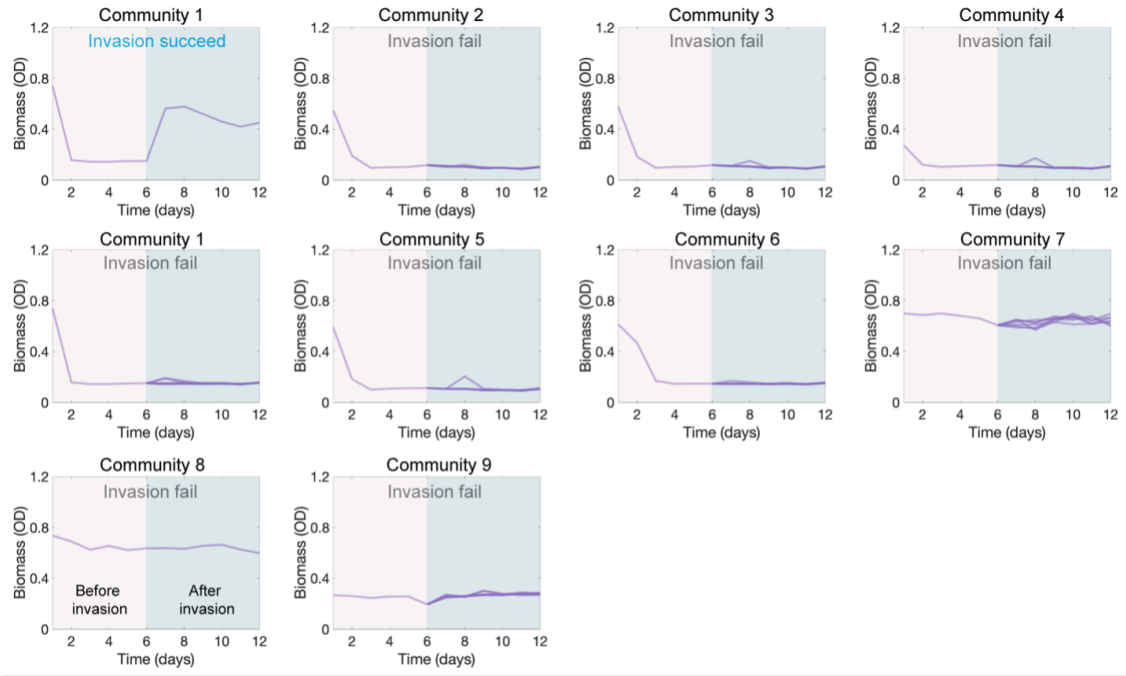

Figure 3-9: Time series for the biomass of the stable communities with species pool size S=20 under strong average interaction strength (high nutrients concentration). Each panel shows the time series for the OD (600nm) of one stable community with species pool size S=20 under high nutrient. The invaders were introduced on day 6, and the time series of successful invasions and failed invasions for the same communities were displayed in different panels.

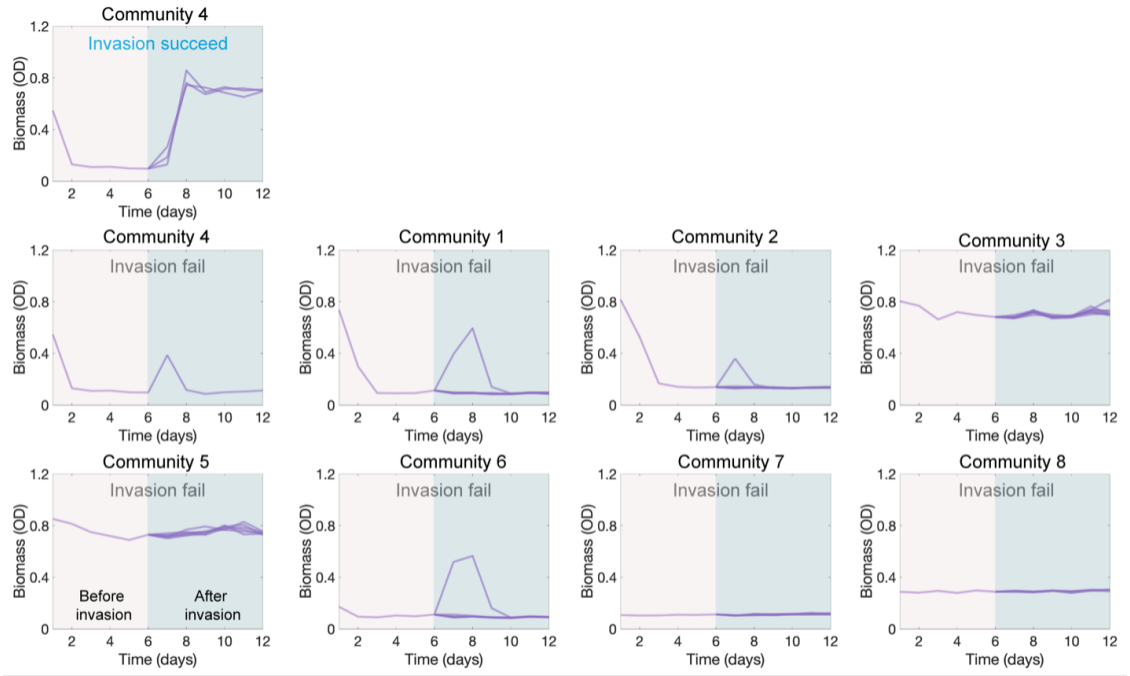

Figure 3-10: Time series for the biomass of the stable communities with species pool size S=12 under strong average interaction strength (high nutrients concentration). Each panel shows the time series for the OD (600nm) of one stable community with species pool size S=12 under high nutrient. The invaders were introduced on day 6, and the time series of successful invasions and failed invasions for the same communities were displayed in different panels.

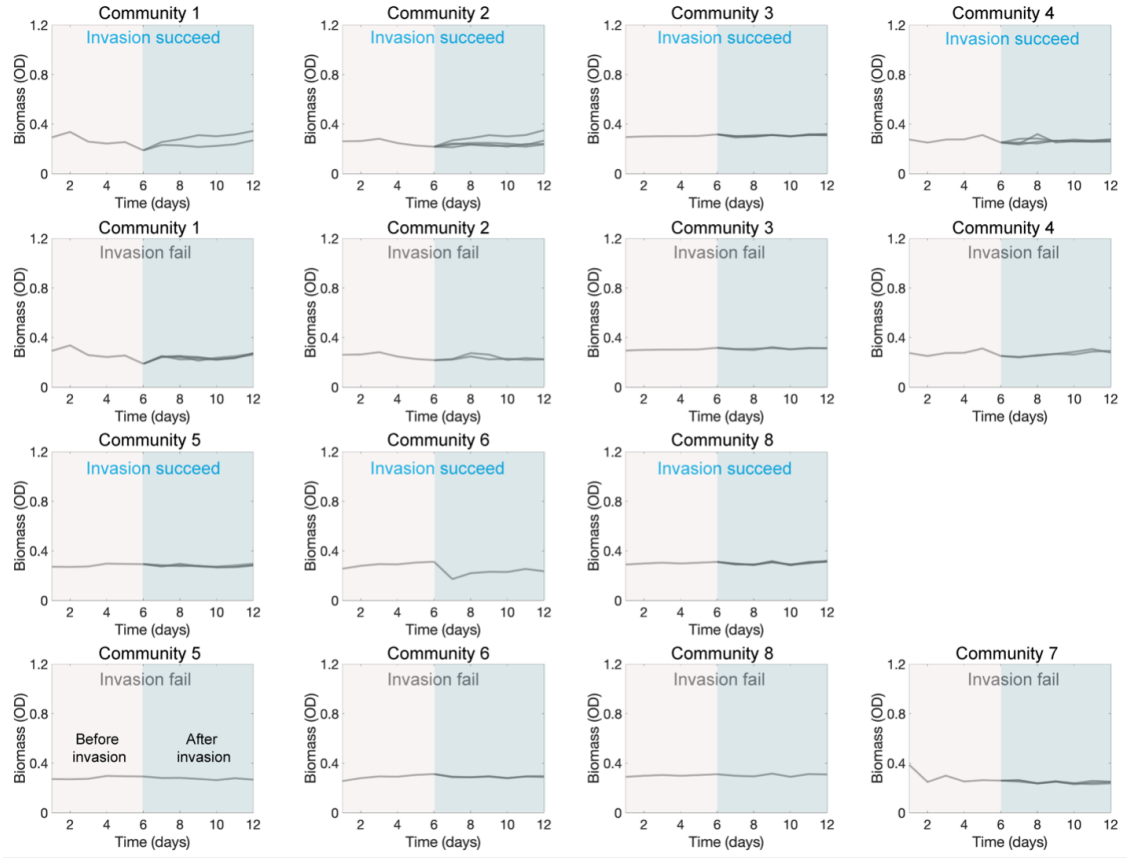

Figure 3-11: Time series for the biomass of the stable communities with species pool size S=20 under weak average interaction strength (low nutrients concentration). Each panel shows the time series for the OD (600nm) of one stable community with species pool size S=20 under low nutrient. The invaders were introduced on day 6, and the time series of successful invasions and failed invasions for the same communities were displayed in different panels.

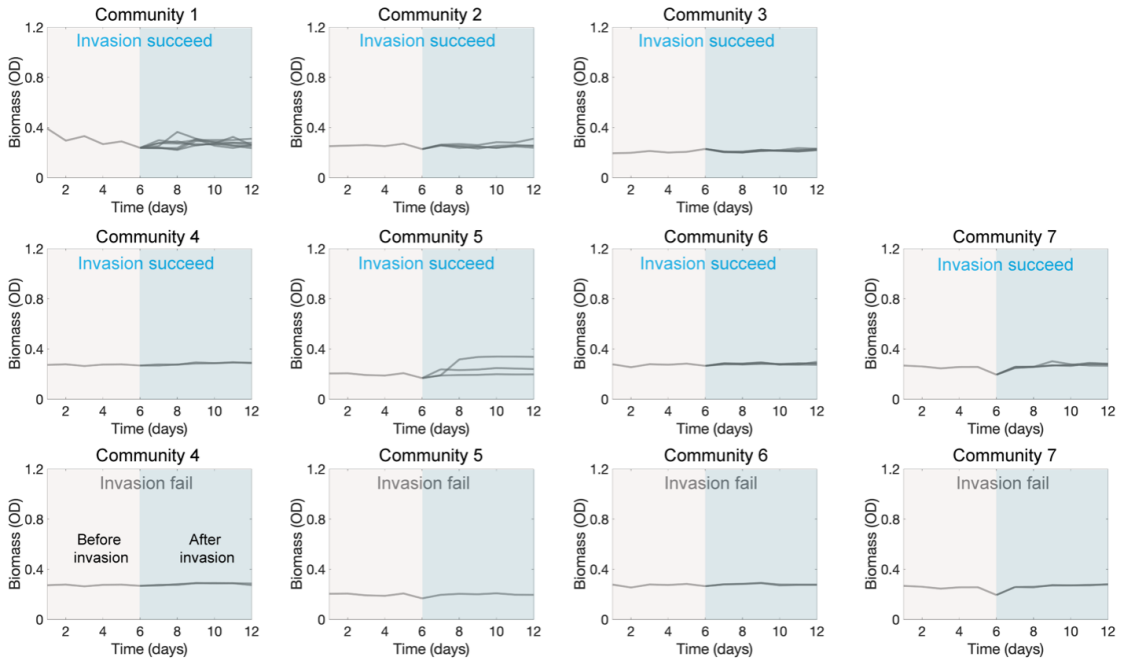

Figure 3-12: Time series for the biomass of the stable communities with species pool size S=12 under weak average interaction strength (low nutrients concentration). Each panel shows the time series for the OD (600nm) of one stable community with species pool size S=12 under low nutrient. The invaders were introduced on day 6, and the time series of successful invasions and failed invasions for the same communities were displayed in different panels.

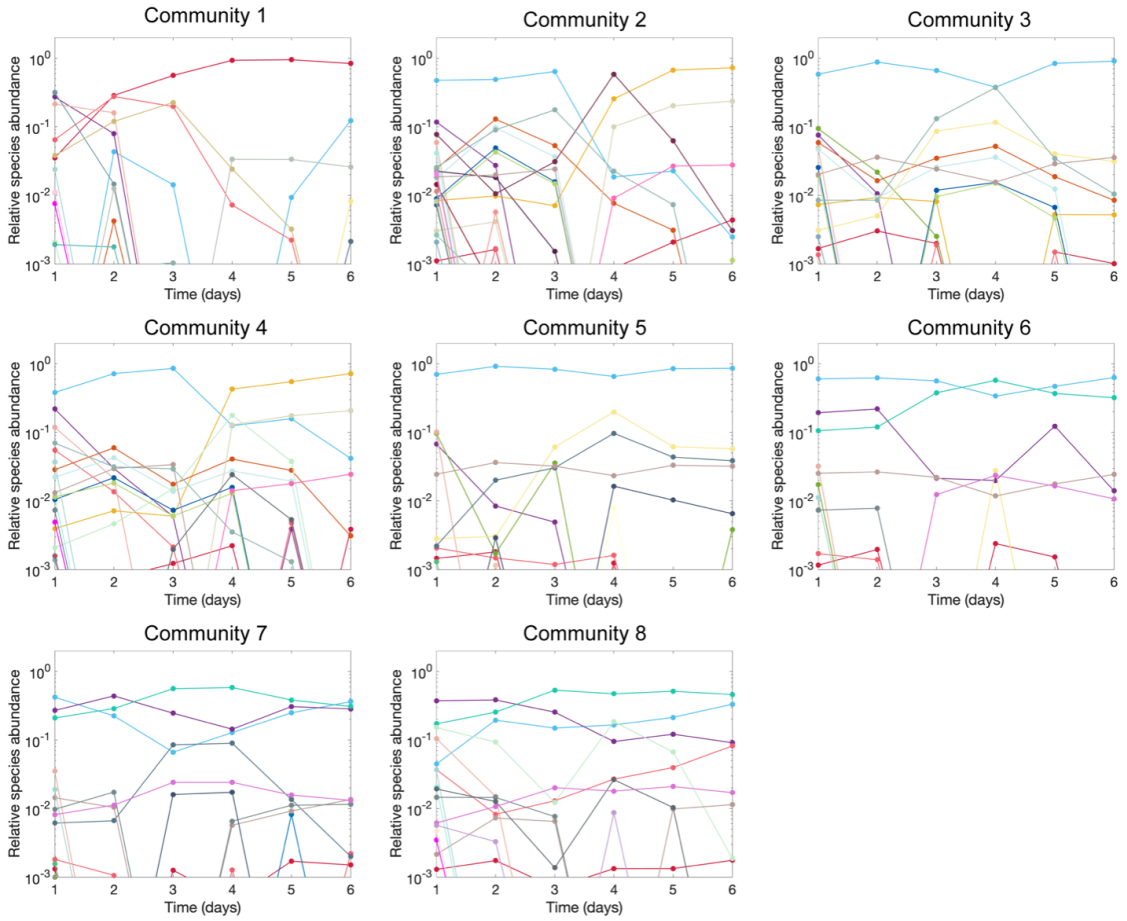

Figure 3-13: Time series for the relative species abundances of the fluctuating communities with species pool size S=20 under strong average interaction strength (high nutrients concentration). Each panel shows the time series for the relative species abundances of one fluctuating community before introducing invaders, where species pool size S=20 under high nutrient.

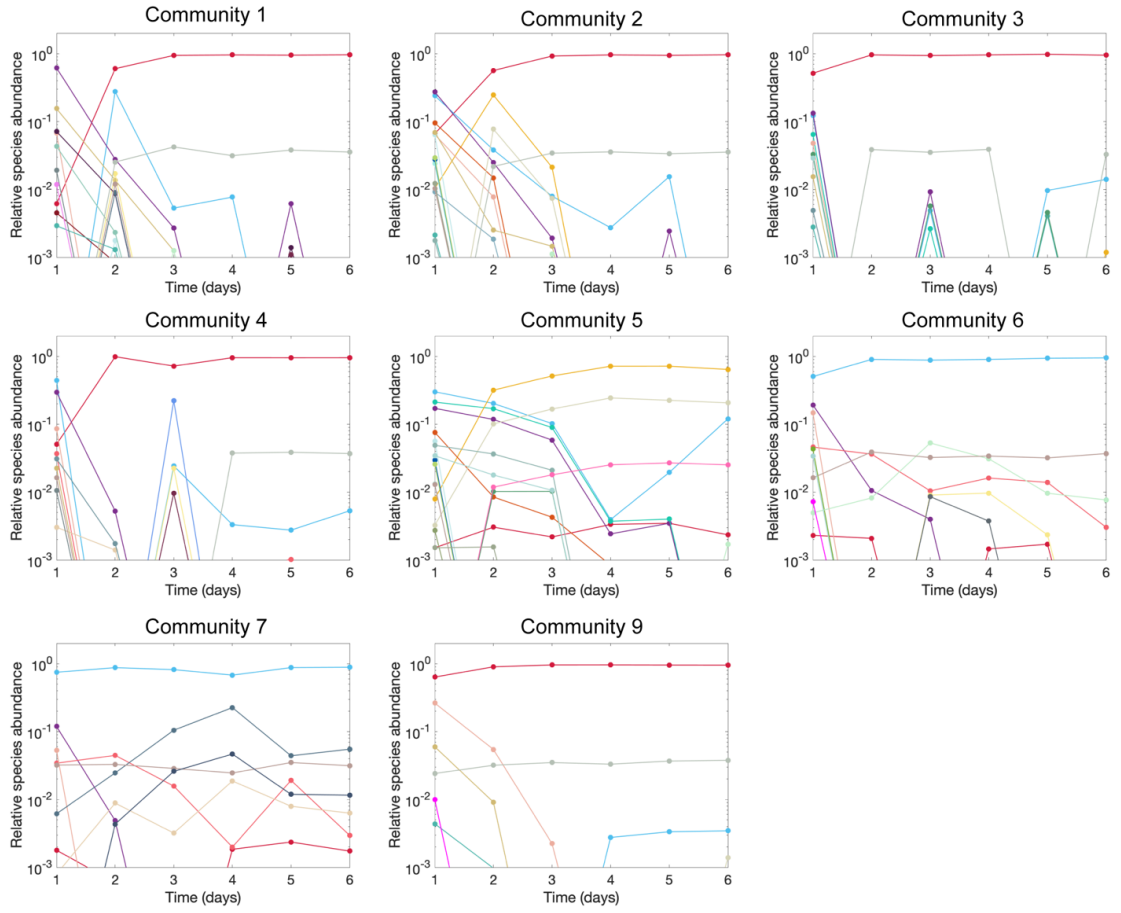

Figure 3-14: Time series for the relative species abundances of the stable communities with species pool size S=20 under strong average interaction strength (high nutrients concentration). Each panel shows the time series for the relative species abundances of one stable community before introducing invaders, where species pool size S=20 under high nutrient.

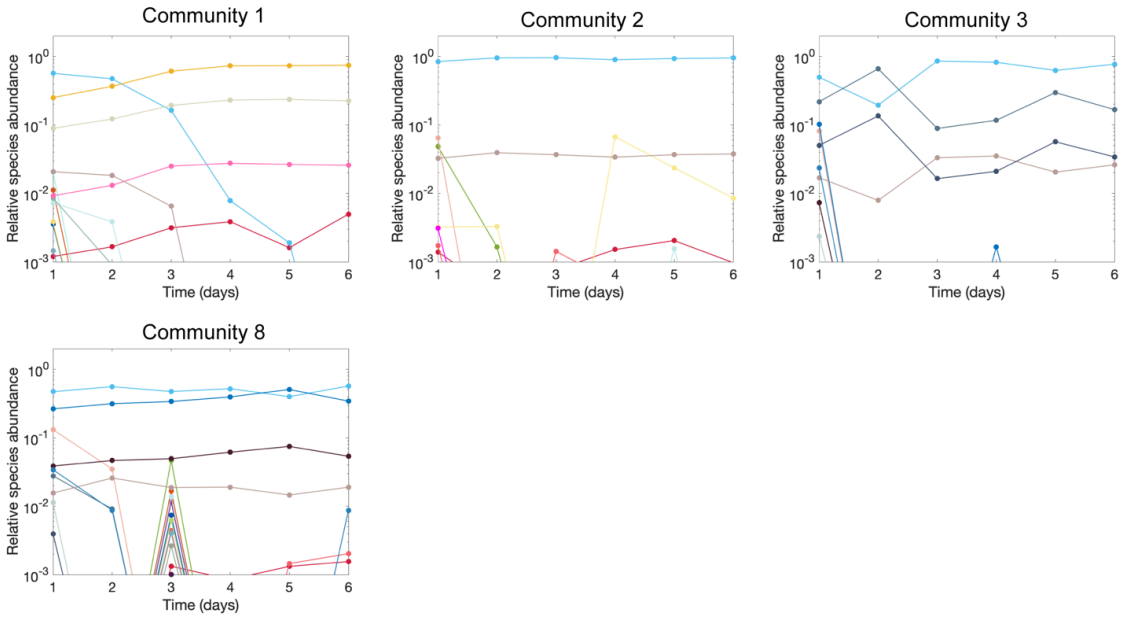

Figure 3-15: Time series for the relative species abundances of the stable communities with species pool size S=12 under strong average interaction strength (high nutrients concentration). Each panel shows the time series for the relative species abundances of one stable community before introducing invaders, where species pool size S=12 under high nutrient.

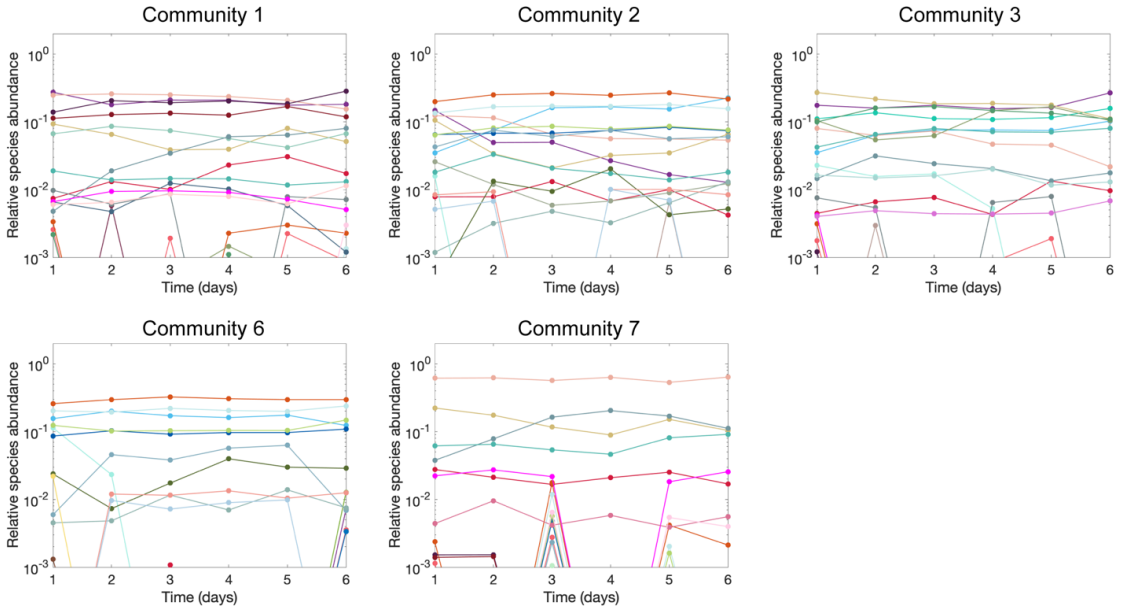

Figure 3-16: Time series for the relative species abundances of the stable communities with species pool size S=20 under weak average interaction strength (low nutrients concentration). Each panel shows the time series for the relative species abundances of one community before introducing invaders, where species pool size S=20 under low nutrient.

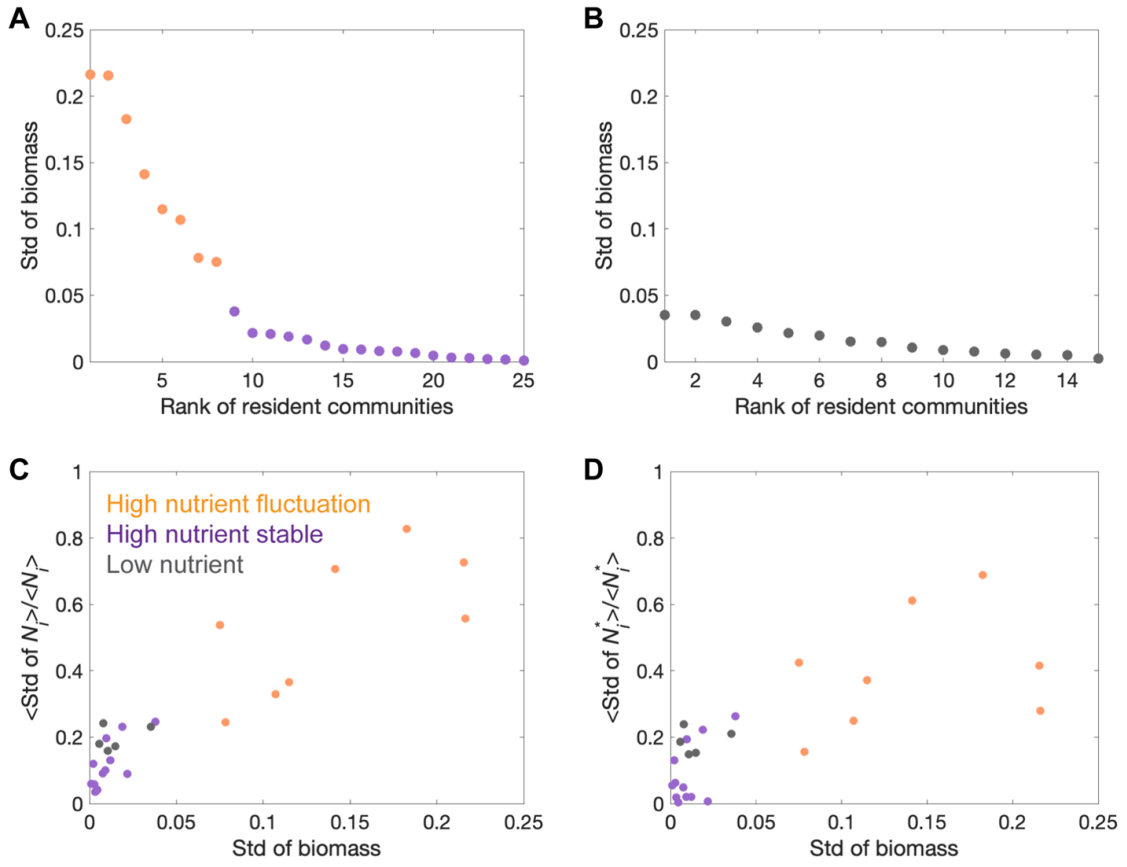

Figure 3-17: Classification of fluctuating and stable resident communities in experiment. (A) The standard deviation of community biomass over day 5, day 6 and day 7 show that the stability threshold of 0.05 can separate the communities into stable ones (purple points) with small biomass deviation and fluctuating ones (orange points) with relatively large biomass deviation under high nutrient. (B) The standard deviation of community biomass under low nutrient are small (all below the stability threshold of 0.05), which were naturally classified into stable communities. (C) The average coefficient of (temporal) variation for absolute species abundances (N_i, computed as the product of total biomass per species relative abundance) exhibit a strong positive correlation with standard deviation of biomass in the experimental communities. The points span into two clusters where fluctuating communities locate on top right region and stable communities locate on bottom left region. (D) The average coefficient of (temporal) variation for relative species abundances (N_i^*, relative species abundance through 16s sequencing) also exhibits a strong positive correlation with standard deviation of biomass in the experimental communities. The results suggest that fluctuation in community biomass cooccurs with fluctuation in relative species abundances.

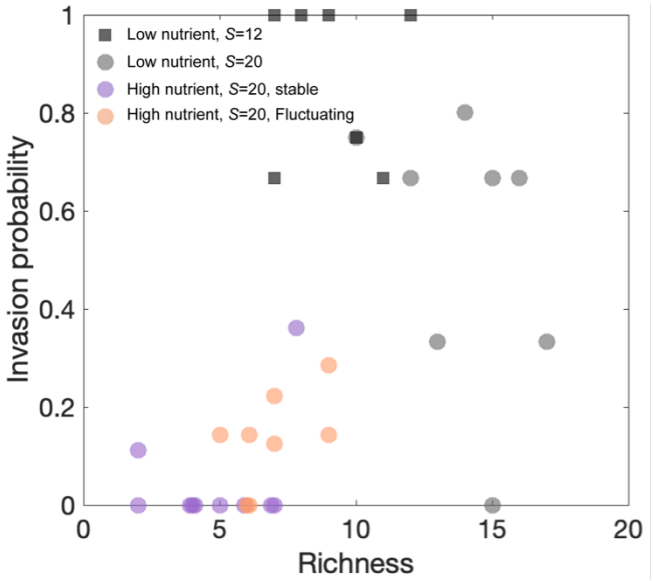

Figure 3-18: Different invasibility-richness relationships in experiment depending upon how the richness is changed. Invasibility positively correlates with richness when varying interaction strength (positive correlation between S=20 communities under low and high nutrient). Invasibility positively correlates with richness when randomly sample S=20 communities under high nutrient, due to fluctuating communities display larger richness and larger invasion probability. Invasibility negatively correlates with richness when increasing species pool size from S=12 to S=20 under low nutrient.

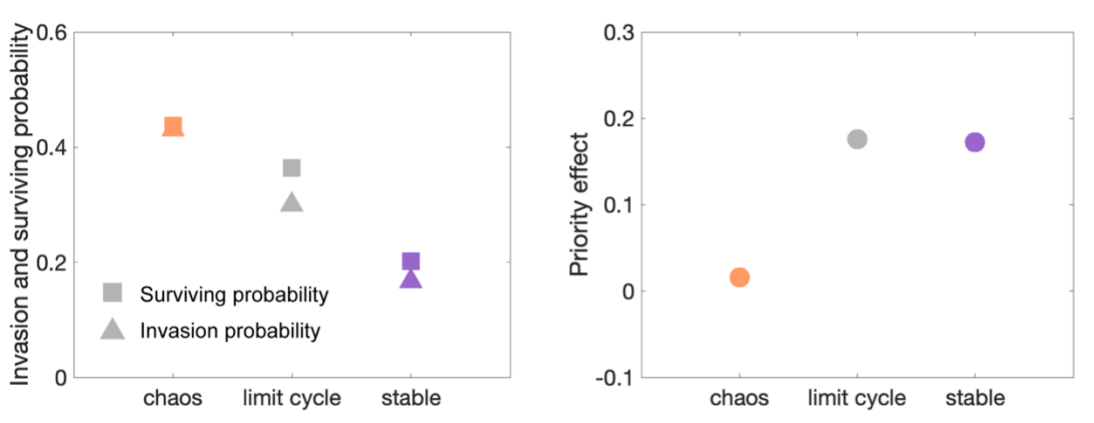

Figure 3-19: Priority effect originates from alternative stable states and limit cycle oscillations rather than chaotic fluctuations in simulations. Lotka-Volterra model simulations show that both surviving probability and invasion probability increase as community dynamics transition from alternative stable states to limit cycle oscillations and to chaos. Communities with chaotic fluctuations in species abundance do not display significant priority effect which can be explained by its ergodicity [24], whereas communities with limit cycle oscillations and alternative stable states both show significant priority effect. The simulation in this figure was performed under S=40 and $<\alpha_{ij}>$=0.65 over 1000 replicates, among which we observed 223 chaotic fluctuating communities, 340 limit cycle oscillations, and 437 alternative stable states. The fluctuating communities were classified into chaos when its Lyapunov exponent is positive, while classified into limit cycle when its Lyapunov exponent is negative.

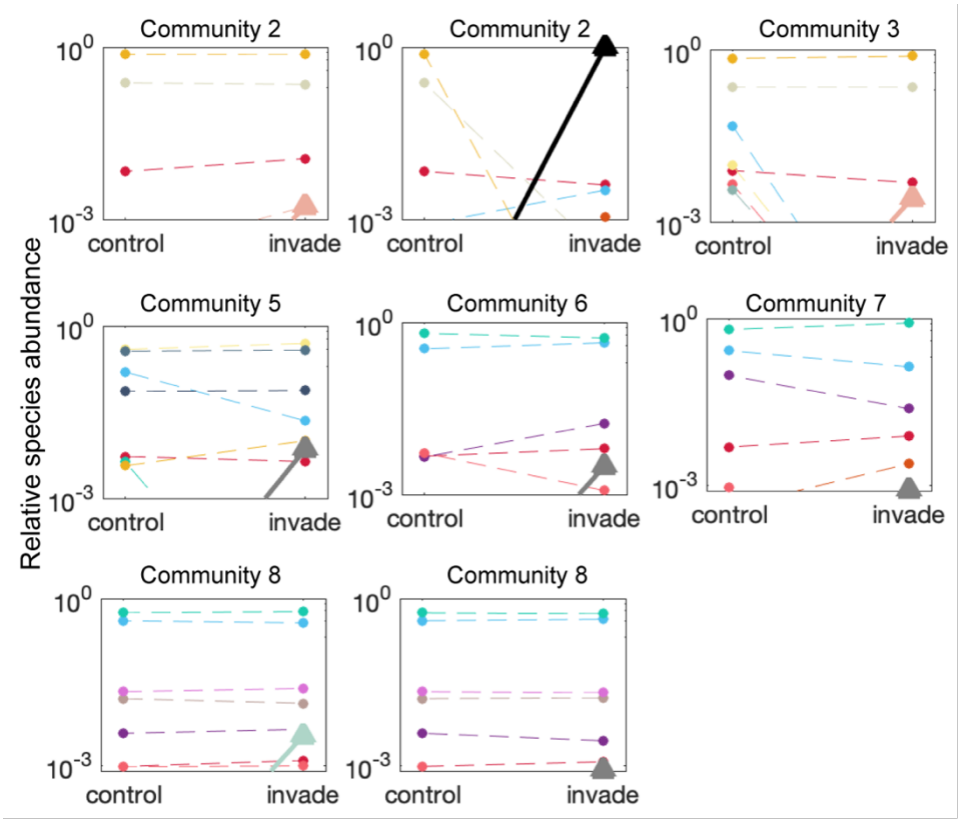

Figure 3-20: Successful invasions lead to change in species composition in fluctuating communities with S=20 under high nutrient, which can be shown by comparing the relative species abundance between invaded communities and control communities without introducing invader. The circles and triangles in the figure represent resident species and invader species, respectively. The successful invasions can cause the extinction of other resident species (circles drop below the extinction threshold under invasion) and the colonization of other resident species (circles go beyond the extinction threshold under invasion).

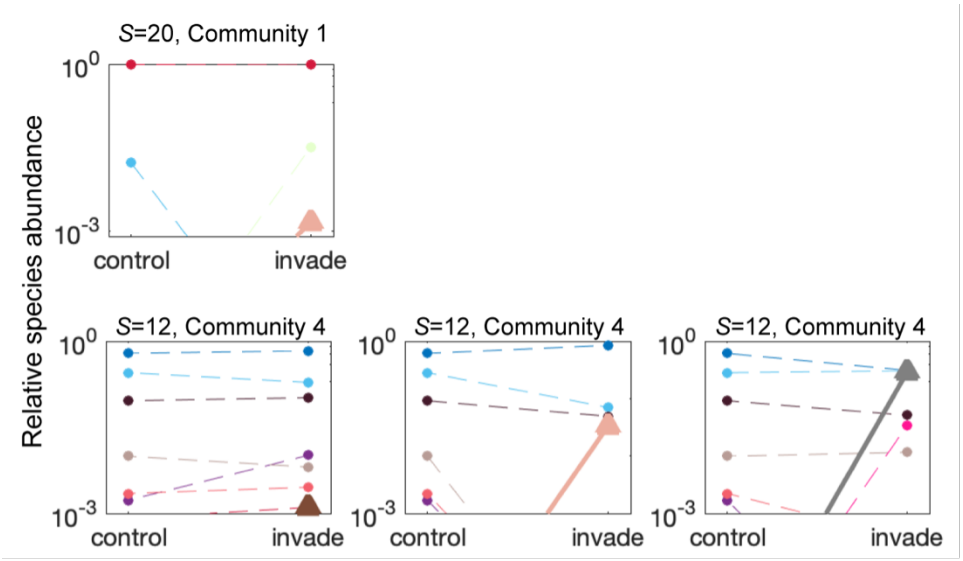

Figure 3-21: Successful invasions lead to change in species composition in stable communities under high nutrient, which can be shown by comparing the relative species abundance between invaded communities and control communities without introducing invader. The circles and triangles in the figure represent resident species and invader species, respectively. The successful invasions can cause the extinction of other resident species (circles drop below the extinction threshold under invasion) and the colonization of other resident species (circles go beyond the extinction threshold under invasion).

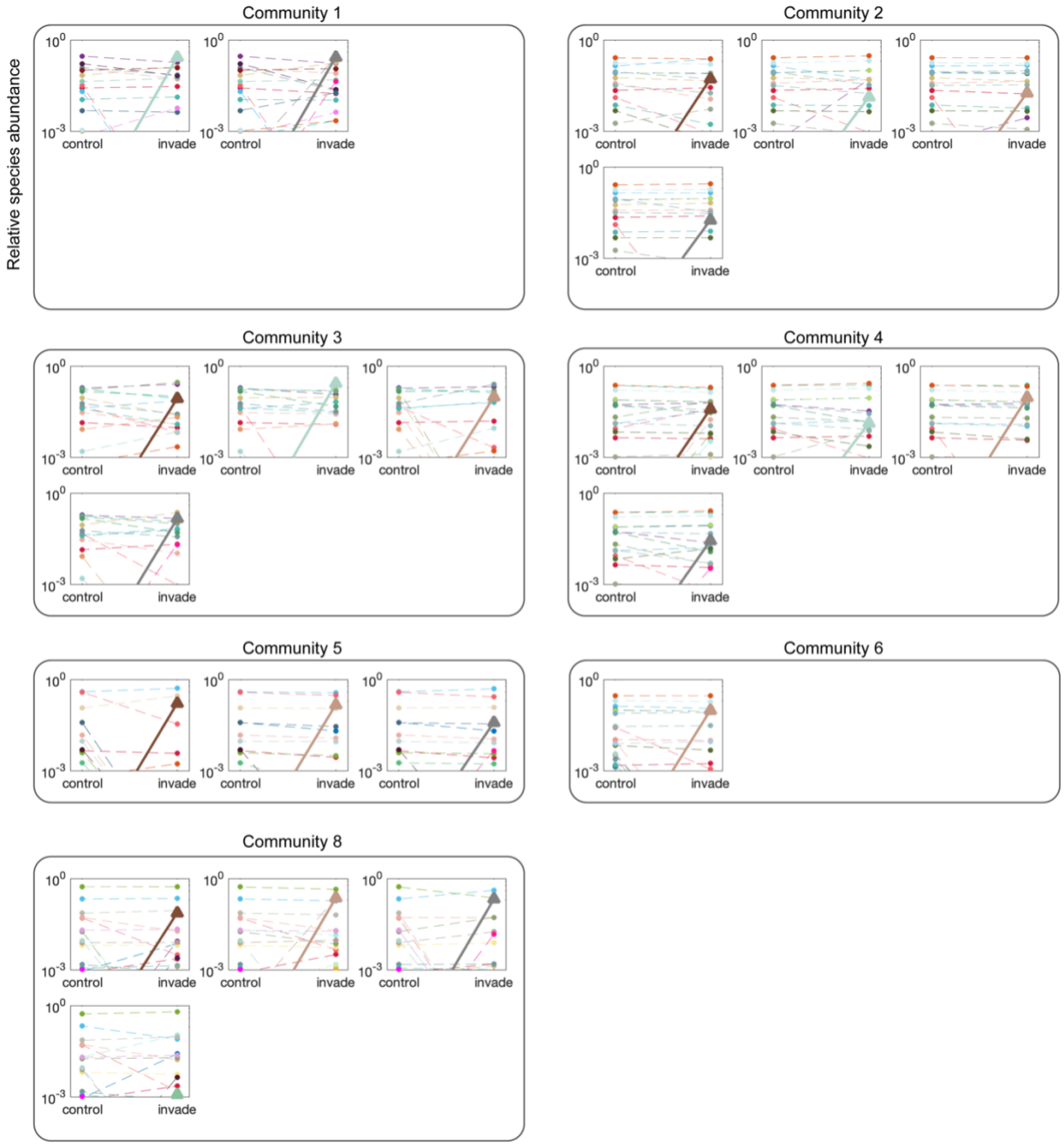

Figure 3-22: Successful invasions lead to change in species composition in communities with S=20 under low nutrient, which can be shown by comparing the relative species abundance between invaded communities and control communities without introducing invader. The circles and triangles in the figure represent resident species and invader species, respectively. The successful invasions can cause the extinction of other resident species (circles drop below the extinction threshold under invasion) and the colonization of other resident species (circles go beyond the extinction threshold under invasion).

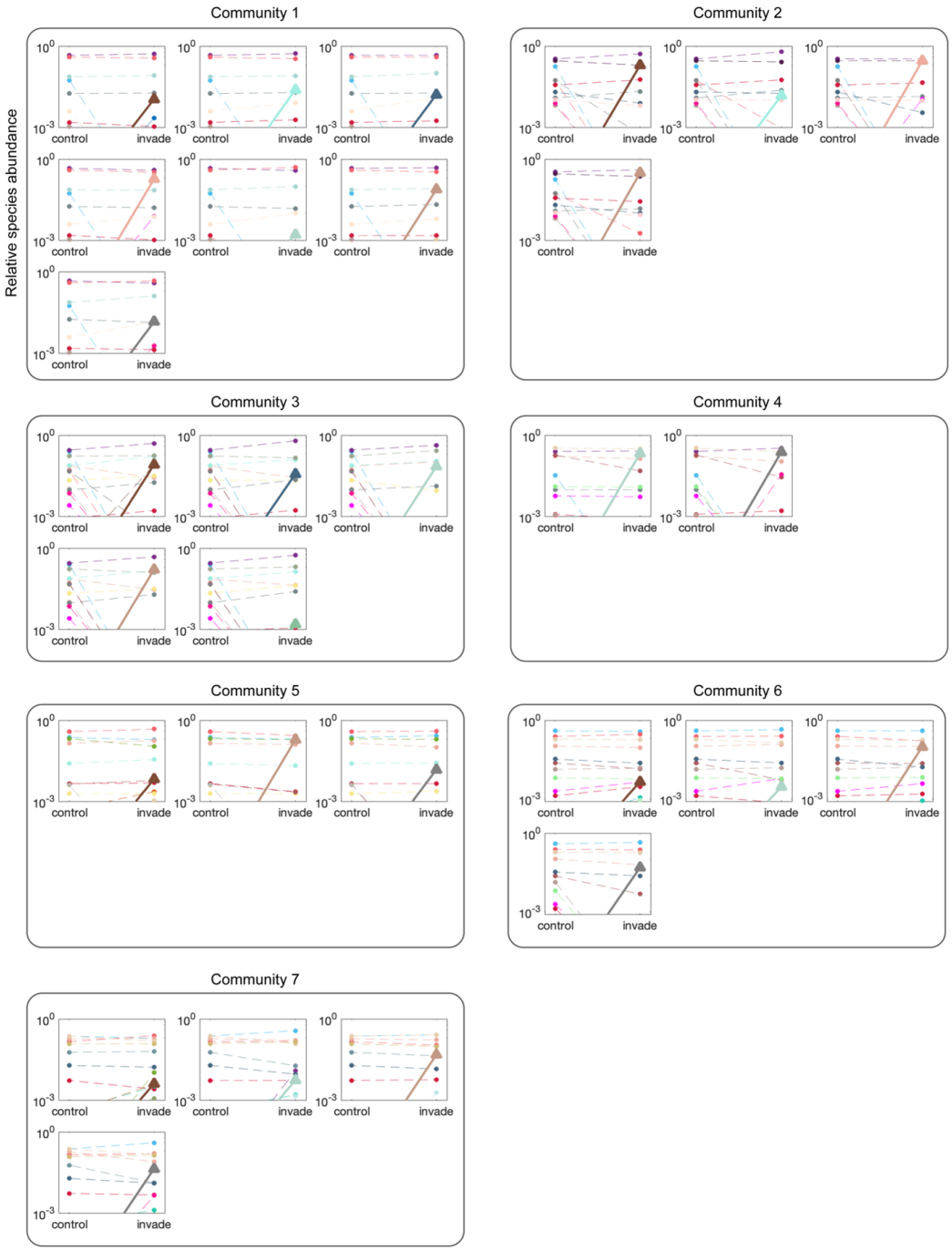

Figure 3-23: Successful invasions lead to change in species composition in communities with S=12 under low nutrient, which can be shown by comparing the relative species abundance between invaded communities and control communities without introducing invader. The circles and triangles in the figure represent resident species and invader species, respectively. The successful invasions can cause the extinction of other resident species (circles drop below the extinction threshold under invasion) and the colonization of other resident species (circles go beyond the extinction threshold under invasion).

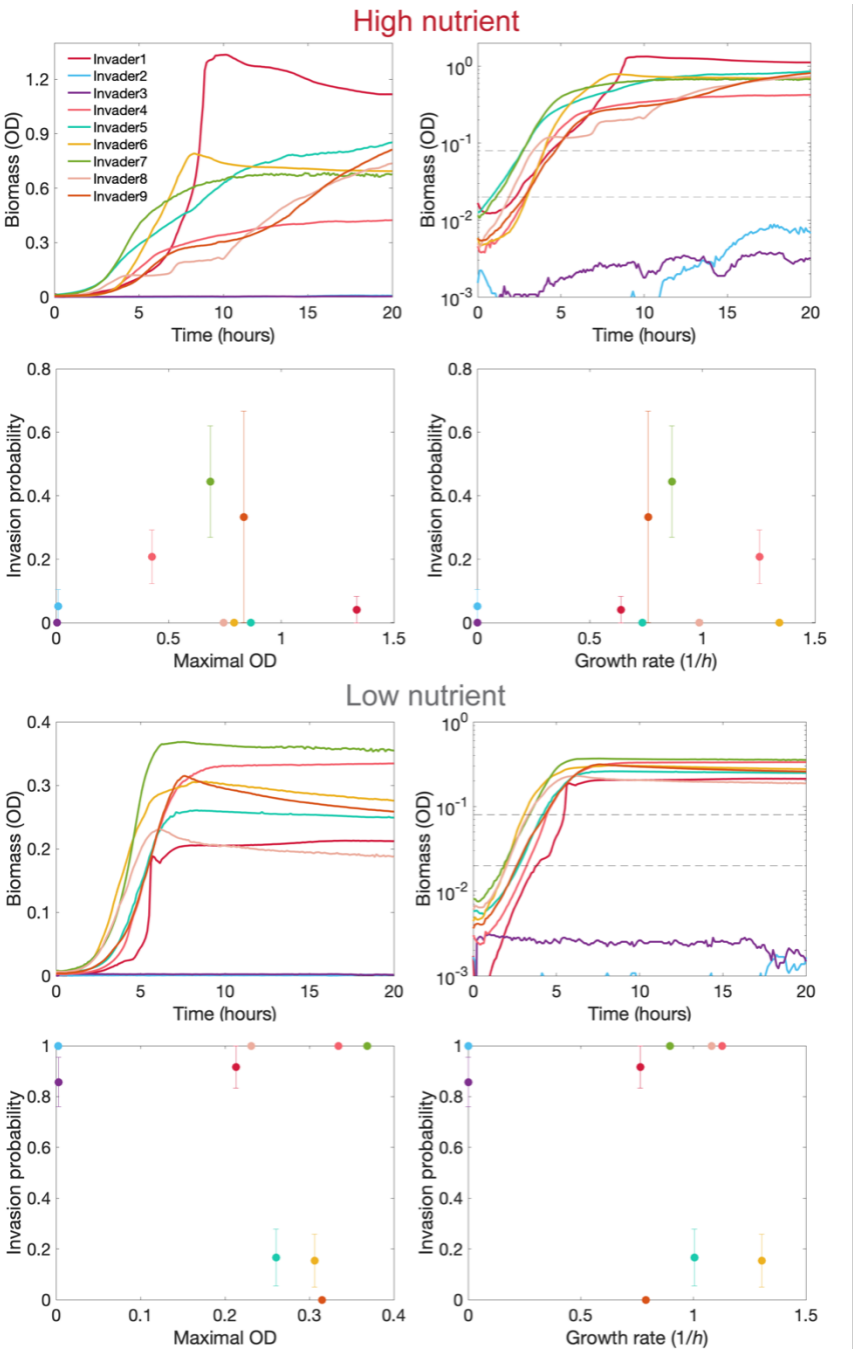

Figure 3-24: There is no correlation between the invasiveness of invaders and their carrying capacities and growth rates. The growth curves of invaders were measured after a dilution of 10^5 folds. The carrying capacity of invaders were quantified by the maximal OD over 24 hours of growth. The growth rates of invaders were quantified by fitting the slopes of growth curves between the two horizontal dashed lines in the figure on logarithmic scale for biomass. There is no statistically significant correlation between invasion probability of invaders with their carrying capacities and growth rates, under both high nutrient and low nutrient. The phylogeny of invader 1 to invader 9 are: Flectobacillus, Pseudomonas, Pedobacter, Pseudomonas, Pantoea, Bacillus, Enterobacterales, Pantoea, Chryseobacterium.

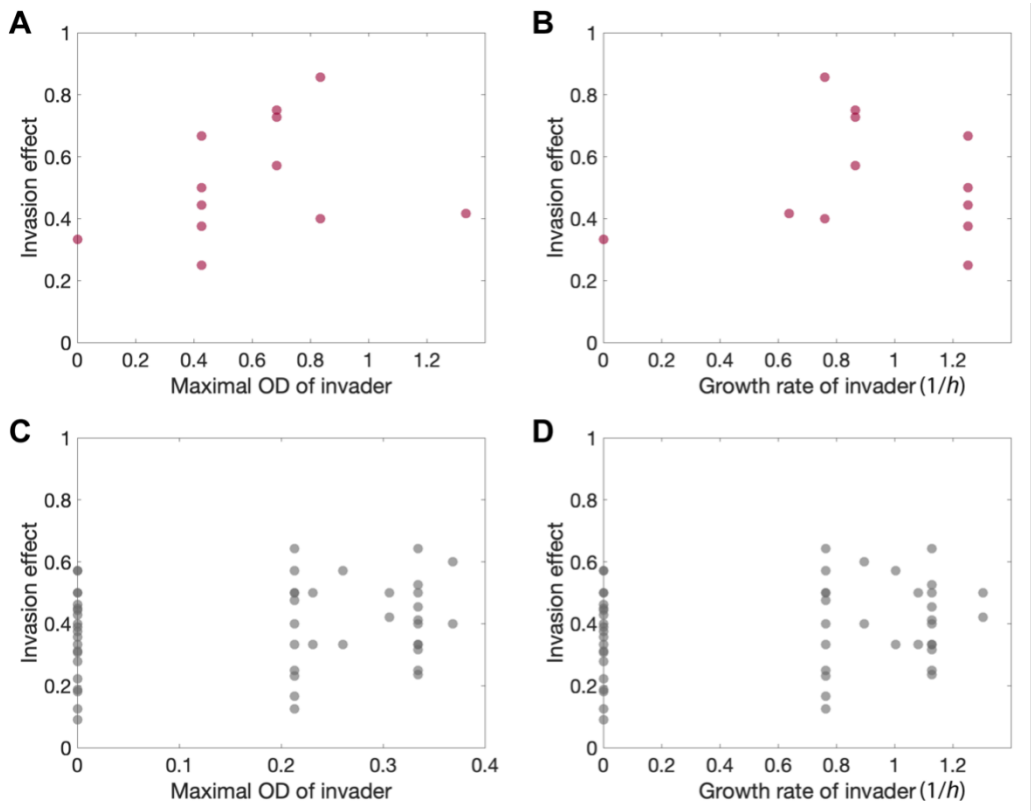

Figure 3-25: There is no statistically significant correlation between invasion effect and invader properties. Under high nutrient, invasion effect does not show statistically significant correlation with carrying capacity (A) and growth rate (B). Under low nutrient, invasion effect does not show statistically significant correlation with carrying capacity (C) and growth rate (D).

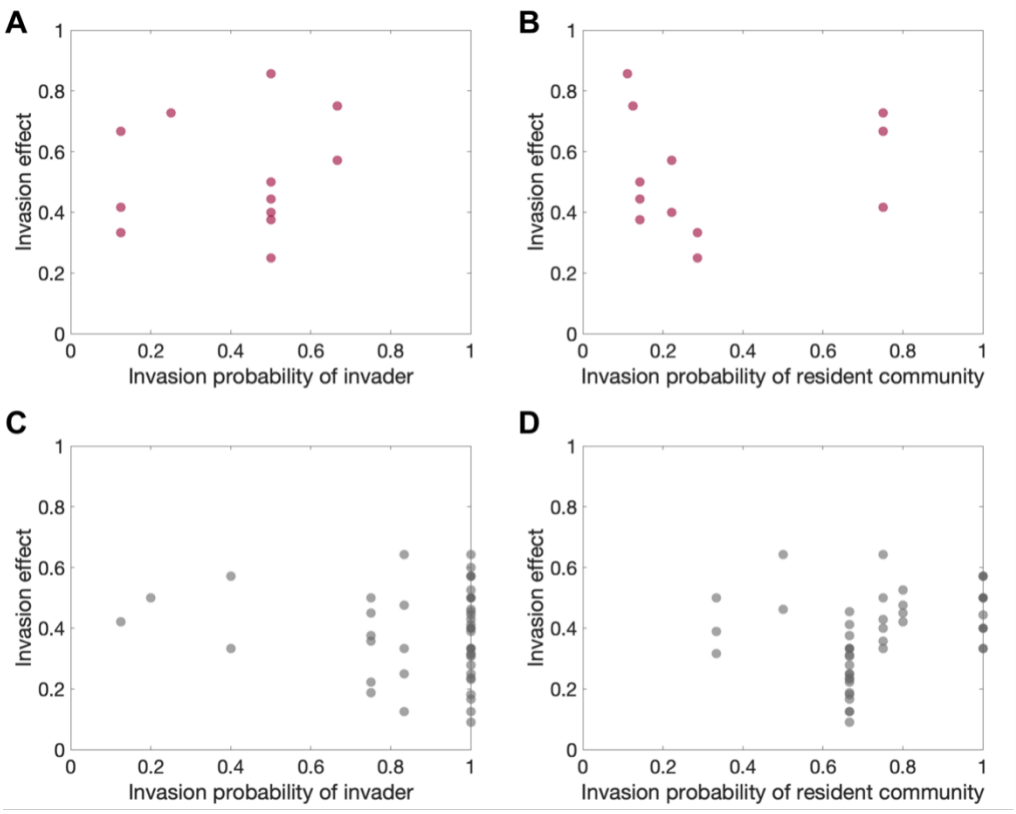

Figure 3-26: There is no statistically significant correlation between invasion effect and invasion probability. Under high nutrient, invasion effect does not show statistically significant correlation with invasion probability of invaders (A) and invasion probability of resident communities (B). Under low nutrient, invasion effect does not show statistically significant correlation with invasion probability of invaders (C) and invasion probability of resident communities (D).

Chapter 4

Conclusion

4.1 Resolving diversity-stability debate and diversity-invasibility debate

The diversity-stability debate has long been a focal point in ecological discussions, examining the intricate relationship between biodiversity and ecosystem stability [87, 60]. Over time, ecologists have presented differing views: some contend that a greater species diversity enhances ecosystem resilience to disturbances [126], because of "portfolio effect" where varied species can offset each other's variability. In contrast, others argue that the intricate web of interactions in diverse systems, potentially leading to competition, might heighten susceptibility to fluctuations and even collapse [124, 87, 60]. As global ecosystems face mounting anthropogenic pressures, deciphering this relationship is becoming ever more critical. This debate is not merely academic—it profoundly influences conservation priorities and strategies. In this thesis, the intricacies of the diversity-stability debate are dissected, highlighting its importance and implications in current ecological research.

Our combined model and experimental results underscore a mutual dependency between persistent fluctuations and high realized diversity. This aligns with two pivotal ideas in theoretical ecology: May's proposition linking complexity to instability and Chesson's perspective that temporal fluctuations can bolster diversity [84, 30].

However, the finding that two broad parameters can independently sculpt the landscape of community diversity and dynamics suggests caution is needed when drawing conclusions about the biodiversity-stability relationship. For a specific interaction strength, there is a negative correlation between stability, species pool size, and realized diversity, implying more species-rich communities may be less stable. Conversely, when species pool sizes are constant, stability and diversity have a positive correlation: weakly interacting communities display both higher stability and diversity, while strongly interacting ones tend to be less stable and diverse. This complex interplay between defining parameters might explain some of the incongruities observed in field studies probing the diversity-stability nexus [87, 60].

The diversity-invasibility debate is a central topic in the realm of ecology, addressing the relationship between native species diversity and an ecosystem's vulnerability to invasions by non-native species [74, 118]. Historically, many ecologists believed that ecosystems with greater biodiversity would naturally fend off invasions, with the theory that such diverse ecosystems would more efficiently utilize available resources, leaving little room for invasive species [62, 28, 112]. Yet, some researchers argue that more diverse habitats might actually present more niches, potentially facilitating invasions [74]. Given the increasing impact of invasive species on global ecosystems and their implications for biodiversity, ecosystem services, and human welfare, this relationship's understanding is crucial. This thesis dives deep into the diversity-invasibility debate, offering insights into this complex and pressing ecological issue.

Contrary to the prevalent notion that diverse communities are inherently more resistant to invasions, there exists an ongoing debate due to conflicting diversity-invasibility relationships documented in various studies [118, 74, 146, 39]. Our findings show that these observed relationships differ significantly based on the method of diversity alteration, whether it's through the number of species, stability, or interaction strength. In our study, we've brought clarity to the debate, illustrating that by normalizing diversity with species pool size to derive a "survival fraction," there emerges a consistent positive relationship between invasibility and this survival

fraction across diverse conditions. Though direct quantification of survival fraction in natural communities is challenging, assessing the proportionality of local to regional richness provides a potential surrogate, suggesting its potential role as a predictor for invasion probability. [105].

The interplay of diversity types in ecology—alpha, beta, and gamma—and the core species number variables, namely richness, survival fraction, and species pool size, offers intriguing insights when applied to natural communities [105]. Delving deeper, richness and species pool size provide a window into alpha (local diversity) and gamma (regional diversity) diversities. In parallel, beta diversity, quantified as the ratio of regional to local diversity, inversely corresponds to the survival fraction. This leads us to an intriguing observation: a universal positive correlation between invasibility and survival fraction inherently signifies a negative correlation with beta diversity. The next frontier in this research would be exploring how these identified community-level attributes might forecast invasion outcomes across various spatiotemporal frameworks, diverse environmental conditions, and among different organism groups.

4.2 Spatial-temporal dynamics in microbial communities

In this thesis, my research predominantly delved into well-mixed microbial communities, revealing a myriad of intricate dynamical behaviors. Moving forward, I am keen to explore the impact of spatial structures on these microbial communities, thereby introducing another layer of complexity to their inherent dynamics. While at smaller scales, natural communities can be effectively modeled using well-mixed ordinary differential equations, larger scales introduce spatial heterogeneity [129]. Here, the specific spatial configuration becomes pivotal in shaping both the diversity and dynamic behaviors of these ecosystems.

Spatial ecology delves into understanding how the spatial distribution and orga-

nization of organisms influence ecological processes and patterns at multiple scales [123]. This interdisciplinary field integrates principles from ecology, geography, and landscape science to unravel the intricate web of interactions that organisms share with their environment. Central to spatial ecology is the concept that the distribution of habitats, resources, and organisms across a landscape can significantly affect ecological dynamics, including species dispersal, population growth, and species interactions [123]. Whether analyzing organisms migration patterns, predicting the spread of invasive species, or understanding the effects of habitat fragmentation, spatial ecology provides invaluable insights that are crucial for biodiversity conservation and ecosystem management in an increasingly fragmented world [90].

One intriguing discrepancy I've observed is that while natural ecosystems boast high biodiversity, laboratory ecosystems often display limited biodiversity [56], in line with theoretical model predictions [14]. This leads me to question: Can migrations within interconnected communities augment biodiversity by fostering long-term fluctuations in population abundances? To investigate this, I plan to experimentally culture natural soil microbes across connected patches, creating a microbial metacommunity. Our prior results underscore that population fluctuations are inherently linked with high-diversity communities [56]. Maintaining these ecosystems in persistent non-equilibrium states necessitates migrations, counteracting the negative feedback loop between diversity and population fluctuations. In essence, migration might act as a safety net, allowing dwindling species in one community to be replenished from another, thereby constantly reshaping local communities and fostering dynamic species interactions at the metacommunity level [96].

Lastly, the astonishing biodiversity observed in nature, coupled with its intricate networks of species interactions, has remained an enigma for decades [85]. Ever since Robert May's seminal paper argued the inherent instability of large complex systems, the role of spatial dynamics in fostering biodiversity has been in the spotlight [72]. While some theories suggest that spatial structures, coupled with dispersal, might stabilize dynamics and thereby maintain high diversity [94], others contend that it could lead to dispersal-driven spatial-temporal chaos, thereby enhancing diversity

[96]. With a focus on natural soil microbes, I intend to bridge the gap between theory and practice, studying microbial interactions across interconnected habitats. My hypothesis is that interspersed migrations between these habitats might bolster biodiversity through the creation of spatial-temporal fluctuations in species counts [96]. Specifically, I posit that moderate dispersal rates could optimize asynchronous fluctuations across these habitats, thereby preserving diversity by intermittently boosting rare species [36]. If validated, our findings would serve as pioneering experimental evidence, demonstrating that species dispersal within a fragmented landscape could amplify global diversity by up to three-fold.

4.3 Multi-stable states and glass-like transitions in microbial communities

In this thesis, I have elucidated the emergence of fluctuations and multistable states in phases governed by strong interactions and a vast species pool [56]. However, several dimensions of these alternative stable states remain to be thoroughly explored. Fundamental questions arise, such as the quantity of alternative stable states contingent on interaction strength and species count, the factors influencing the resilience and attraction basin of these states, the prevalence of coexistence between fluctuating and stable attractors within identical species sets, and the potential for demographic noise to initiate glass-like transitions between varied stable states [63]. Another intriguing matter is distinguishing the nuanced differences between transitions among alternative stable states and deterministic chaotic fluctuations [63].

In the realm of ecology, the concept of alternative stable states refers to the idea that certain ecosystems can exist in multiple, distinct equilibrium conditions that are characterized by markedly different species compositions or structural attributes [16]. Once an ecosystem is pushed by disturbances or gradual environmental changes past specific thresholds, it might shift abruptly from one stable state to another, rather than following a linear response. This phenomenon has been observed in various

systems, ranging from freshwater lakes transitioning between clear and turbid water states, to grasslands transforming into deserts or forests [16]. Understanding alternative stable states is pivotal because these shifts can sometimes be irreversible, or the ecosystem might require significant interventions to return to its original state [110]. This concept underscores the importance of ecosystem resilience and the potential consequences of human and environmental pressures on global habitats [110].

Natural ecosystems, comprising specific species sets, can manifest differing yet stable species compositions over durations [8]. A prevailing debate centers around whether such multi-stability and community turnovers arise due to environmental alterations or inherent community interactions [56, 14]. In our pursuit to bridge theoretical understanding with experimental validation, I will meticulously examine the behavior of experimental microbial communities within controlled environments. My observations will bring to light the emergence of biomass-dependent alternative stable states and the transitions reminiscent of glass-like shifts between these states.

Specifically, initiating communities from diverse species compositions will reveal uninvadable alternative stable states in high-interaction scenarios. In contrast, in low-interaction scenarios, most communities are expected to converge towards a universal attractor [24, 56]. Surprisingly, augmenting the community size, or the total species number, may not substantially influence the average count of alternative states [63]. When probing multiple-stable-state communities, a trend is expected to emerge: states with greater biomass typically exhibit more expansive attractor basins [25].

Furthermore, demographic noise intrinsic to the community, coupled with environmental perturbations, could instigate shifts between alternative states [63, 25]. Such transitions are notably amplified with an uptick in demographic noise. Conclusively, our findings will underscore that potent interspecies interactions can foster multiple stable states in microbial communities skewed towards high biomass. Moreover, various forms of noise can catalyze transitions between these states, underscoring the importance of both internal and external factors in shaping community dynamics [63, 25]. As I look to the future, delving deeper into these intricate dynamics will be pivotal in enhancing our understanding of alternative stable states and glass-like

transitions in microbial communities and its broader implications.

4.4 Emergent behaviors in different multi-cellular living systems

Our exploration into the realm of microbial ecosystems has unearthed intriguing patterns and behaviors. Historically, researchers have used a multitude of models to dissect the inner workings of such ecosystems, each with its set of assumptions and simplifications. A transformative insight from our research is the consistent emergence of dynamical phases irrespective of the specificities of the models in play. Whether we dove into the intricacies of the pH model, dissected the Lotka-Volterra framework, or navigated through the resource-consumer model, we were met with an undeniable commonality: strikingly analogous phase diagrams [56]. Such widespread congruence across diverse models hints at a profound model-free universality. This discovery challenges traditional scientific paradigms, suggesting that beyond the complexity and diversity in these systems lies an underlying tapestry of foundational principles that govern behavior. Recognizing this universality serves as a beacon, guiding us towards understanding the very essence of microbial ecosystems, beyond the limitations of any single model or framework. As we venture deeper into this domain, it becomes increasingly clear that a holistic outlook, unshackled from model-specific constraints, offers the most promise in deciphering broad biological patterns and behaviors that are ubiquitously present across diverse environments and organisms.

Parallel to our microbial explorations, the realm of cancer biology presents itself as a complex mosaic of cellular interactions and dynamics [67, 88]. Just as microbial communities teem with a plethora of species, tumors too are a bustling hub of cellular diversity. From mesenchymal cells and epithelial cells to a myriad of immune cells [138], each contributes to the elaborate dance of life and death within the tumor microenvironment [51]. The dynamics within tumors bear striking resemblances to microbial ecosystems. Each cell type, with its unique role and function, constantly

interacts, competes, and collaborates with others [138], mirroring the dynamics of microbial species within their native habitats [67, 88].

Drawing parallels between microbial and tumor ecologies, an exciting frontier opens up: the application of knowledge from microbial research to decipher the mysteries of cancer biology [67, 88]. Microbial communities, with their resilience to environmental fluctuations, adaptability, and intricate interspecies interactions, serve as a robust model system [135, 136]. Transposing these insights could empower us to unravel the nuances of tumor heterogeneity, metastatic tendencies, and even the puzzle of therapeutic resistances [92]. As diseases like cancer continue to challenge medical science, an interdisciplinary approach that marries microbial ecology with cancer biology could be the key to unlocking revolutionary therapeutic interventions [67, 88]. As we venture ahead, our vision is to seamlessly integrate microbial ecology with the complexities of cancer biology, carving new pathways in our understanding and management of cancer and myriad other multicellular systems.

Appendix A

Tables

Table A.1: Experimentally measured interspecies interaction matrix α_{ij} under low nutrients concentrations. Each of the 15 pairs resulting from combinations of six randomly chosen isolates from different genera (Leuconostoc, Pseudomonas, Yersinia, Pantoea, Klebsiella, Acinetobacter) in the bacterial library were cocultured for 7 days (with daily dilutions). We measured the equilibrium abundance N_i via sample dilution and colony counting at the end of the experiment. The value of α_{ij} was calculated through the expression $\alpha_{ij}=(K_i\text{-}N_i)K_j/(N_jK_i)$, where K_i is the carrying capacity of species (independently measured as the species abundance in monoculture after 7 dilution cycles). The errors indicate the standard deviation of parameter values measured in three replicates.

	Leu	**Pse**	**Yer**	**Pan**	**Kle**	**Aci**
Leu	1	0.25±0.03	0.31±0.01	0.29±0.04	0.24±0.01	0.03±0.02
Pse	0.55±0.05	1	0.10±0.05	0.63±0.04	0.67±0.09	0.33±0.01
Yer	0.30±0.04	0.28±0.05	1	0.60±0.04	0.28±0.06	-0.05±0.04
Pan	0.39±0.01	0.33±0.03	0.33±0.05	1	0.04±0.02	0.17±0.08
Kle	0.44±0.03	0.54±0.05	0.06±0.03	0.05±0.01	1	0.69±0.13
Aci	0.40±0.07	0.60±0.03	-0.29±0.08	0.47±0.05	0.64±0.02	1

Table A.2: Experimentally measured interspecies interaction matrix α_{ij} under medium nutrient concentrations. Each of the 15 pairs resulting from combinations of six randomly chosen isolates from different genera (Leuconostoc, Pseudomonas, Yersinia, Pantoea, Klebsiella, Acinetobacter) in the bacterial library were cocultured for 7 days (with daily dilutions). We measured the equilibrium abundance N_i via sample dilution and colony counting at the end of the experiment. The value of α_{ij} was calculated through the expression $\alpha_{ij}=(K_i\text{-}N_i)K_j/(N_jK_i)$, where K_i is the carrying capacity of species (independently measured as the species abundance in monoculture after 7 dilution cycles). For competitive exclusion (species i always drive species j to extinction), it can be inferred that $\alpha_{ij}<1$ and $\alpha_{ji}>1$. For bi-stability (the high abundant species drives the low abundant one to extinction), it can be inferred that $\alpha_{ij}>1$ and $\alpha_{ji}>1$. The errors indicate the standard deviation of parameter values measured in three replicates.

	Leu	**Pse**	**Yer**	**Pan**	**Kle**	**Aci**
Leu	1	0.69±0.05	<1	>1	0.08±0.03	0.11±0.02
Pse	0.31±0.03	1	0.41±0.06	0.99±0.04	0.26±0.01	0.25±0.04
Yer	>1	0.24±0.07	1	>1	0.20±0.05	0.21±0.03
Pan	<1	0.98±0.08	<1	1	>1	<1
Kle	0.21±0.04	0.36±0.01	0.18±0.05	<1	1	0.40±0.02
Aci	0.05±0.02	0.32±0.01	0.13±0.06	>1	0.87±0.11	1

Table A.3: Experimentally measured interspecies interaction matrix α_{ij} under high nutrient concentrations. Each of the 15 pairs resulting from combinations of six randomly chosen isolates from different genera (Leuconostoc, Pseudomonas, Yersinia, Pantoea, Klebsiella, Acinetobacter) in the bacterial library were cocultured for 7 days (with daily dilutions). We measured the equilibrium abundance N_i via sample dilution and colony counting at the end of the experiment. The value of α_{ij} was calculated through the expression $\alpha_{ij}=(K_i\text{-}N_i)K_j/(N_jK_i)$, where K_i is the carrying capacity of species (independently measured as the species abundance in monoculture after 7 dilution cycles). For competitive exclusion (species i always drive species j to extinction), it can be inferred that $\alpha_{ij}<1$ and $\alpha_{ji}>1$. For bi-stability (the high abundant species drives the low abundant one to extinction), it can be inferred that $\alpha_{ij}>1$ and $\alpha_{ji}>1$. The errors indicate the standard deviation of parameter values measured in three replicates.

	Leu	**Pse**	**Yer**	**Pan**	**Kle**	**Aci**
Leu	1	0.09±0.04	<1	>1	0.49	<1
Pse	0.03±0.02	1	<1	>1	<1	<1
Yer	>1	>1	1	>1	>1	>1
Pan	<1	<1	<1	1	>1	<1
Kle	0.94±0.07	>1	<1	>1	1	>1
Aci	>1	>1	<1	>1	>1	1

Appendix B

Figures

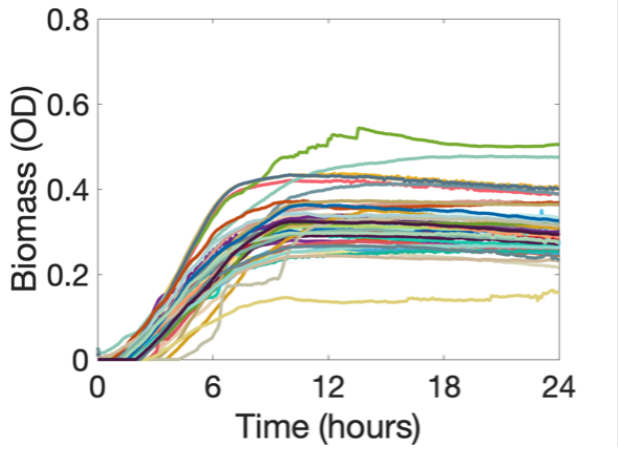

Figure B-1: The time series for the biomass of 48 bacterial isolates show that all species grow to carrying capacity and reach steady state before 24 hours.

Bibliography

[1] Clare I. Abreu, Vilhelm L. Andersen Woltz, Jonathan Friedman, and Jeff Gore. Microbial communities display alternative stable states in a fluctuating environment. *PLOS Computational Biology*, 16(5):e1007934, May 2020.

[2] Martin Ackermann, Bärbel Stecher, Nikki E Freed, Pascal Songhet, Wolf-Dietrich Hardt, and Michael Doebeli. Self-destructive cooperation mediated by phenotypic noise. *Nature*, 454(7207):987–990, 2008.

[3] Francisco Acosta, Richard M Zamor, Fares Z Najar, Bruce A Roe, and K David Hambright. Dynamics of an experimental microbial invasion. *Proceedings of the National Academy of Sciences*, 112(37):11594–11599, 2015.

[4] JC Allen, WM Schaffer, and D Rosko. Chaos and extinction in ecological populations. *Nature*, 364:229–232, 1993.

[5] Stefano Allesina and Si Tang. Stability criteria for complex ecosystems. *Nature*, 483(7388):205–208, 2012.

[6] Ada Altieri, Felix Roy, Chiara Cammarota, and Giulio Biroli. Properties of equilibria and glassy phases of the random lotka-volterra model with demographic noise. *Physical Review Letters*, 126(25):258301, 2021.

[7] Daniel R. Amor, Christoph Ratzke, and Jeff Gore. Transient invaders can induce shifts between alternative stable states of microbial communities. *Science Advances*, 6(8):eaay8676, February 2020.

[8] Daniel R Amor, Christoph Ratzke, and Jeff Gore. Transient invaders can induce shifts between alternative stable states of microbial communities. *Science Advances*, 6(8):eaay8676, 2020.

[9] Philip W Anderson. More is different: Broken symmetry and the nature of the hierarchical structure of science. *Science*, 177(4047):393–396, 1972.

[10] Jean-François Arnoldi, Matthieu Barbier, Ruth Kelly, György Barabás, and Andrew L Jackson. Invasions of ecological communities: Hints of impacts in the invader's growth rate. *Methods in Ecology and Evolution*, 13(1):167–182, 2022.

[11] Colin Averill, Claire Fortunel, Daniel S. Maynard, Johan van den Hoogen, Michael C. Dietze, Jennifer M. Bhatnagar, and Thomas W. Crowther. Alternative stable states of the forest mycobiome are maintained through positive feedbacks. *Nature Ecology & Evolution*, 6(4):375–382, April 2022.

[12] Frederick K Balagaddé, Hao Song, Jun Ozaki, Cynthia H Collins, Matthew Barnet, Frances H Arnold, Stephen R Quake, and Lingchong You. A synthetic escherichia coli predator–prey ecosystem. *Molecular systems biology*, 4(1):187, 2008.

[13] Frederick K Balagaddé, Hao Song, Jun Ozaki, Cynthia H Collins, Matthew Barnet, Frances H Arnold, Stephen R Quake, and Lingchong You. A synthetic Escherichia coli predator–prey ecosystem. *Molecular Systems Biology*, 4(1):187, January 2008.

[14] Matthieu Barbier, Jean-François Arnoldi, Guy Bunin, and Michel Loreau. Generic assembly patterns in complex ecological communities. *Proceedings of the National Academy of Sciences*, 115(9):2156–2161, 2018.

[15] Ugo Bastolla, Miguel A Fortuna, Alberto Pascual-García, Antonio Ferrera, Bartolo Luque, and Jordi Bascompte. The architecture of mutualistic networks minimizes competition and increases biodiversity. *Nature*, 458(7241):1018–1020, 2009.

[16] Beatrix E Beisner, Daniel T Haydon, and Kim Cuddington. Alternative stable states in ecology. *Frontiers in Ecology and the Environment*, 1(7):376–382, 2003.

[17] Elisa Benincà, Bill Ballantine, Stephen P. Ellner, and Jef Huisman. Species fluctuations sustained by a cyclic succession at the edge of chaos. *Proceedings of the National Academy of Sciences*, 112(20):6389–6394, May 2015.

[18] Elisa Benincà, Bill Ballantine, Stephen P Ellner, and Jef Huisman. Species fluctuations sustained by a cyclic succession at the edge of chaos. *Proceedings of the National Academy of Sciences*, 112(20):6389–6394, 2015.

[19] Elisa Benincà, Jef Huisman, Reinhard Heerkloss, Klaus D. Jöhnk, Pedro Branco, Egbert H. Van Nes, Marten Scheffer, and Stephen P. Ellner. Chaos in a long-term experiment with a plankton community. *Nature*, 451(7180):822–825, February 2008.

[20] Elisa Benincà, Jef Huisman, Reinhard Heerkloss, Klaus D Jöhnk, Pedro Branco, Egbert H Van Nes, Marten Scheffer, and Stephen P Ellner. Chaos in a long-term experiment with a plankton community. *Nature*, 451(7180):822–825, 2008.

[21] Pierre Bizeul and Jamal Najim. Positive solutions for large random linear systems. *Proceedings of the American Mathematical Society*, 149(6):2333–2348, 2021.

[22] Tim M Blackburn, Petr Pyšek, Sven Bacher, James T Carlton, Richard P Duncan, Vojtěch Jarošík, John RU Wilson, and David M Richardson. A proposed unified framework for biological invasions. *Trends in ecology & evolution*, 26(7):333–339, 2011.

[23] Bernd Blasius, Lars Rudolf, Guntram Weithoff, Ursula Gaedke, and Gregor F. Fussmann. Long-term cyclic persistence in an experimental predator–prey system. *Nature*, 577(7789):226–230, January 2020.

[24] Guy Bunin. Ecological communities with lotka-volterra dynamics. *Physical Review E*, 95(4):042414, 2017.

[25] Guy Bunin. Directionality and community-level selection. *Oikos*, 130(4):489–500, 2021.

[26] Jeremy Butterfield. Less is different: Emergence and reduction reconciled. *Foundations of physics*, 41:1065–1135, 2011.

[27] Ben J Callahan, Kris Sankaran, Julia A Fukuyama, Paul J McMurdie, and Susan P Holmes. Bioconductor workflow for microbiome data analysis: from raw reads to community analyses. *F1000Research*, 5(1492):1492, 2016.

[28] Ted J Case. Invasion resistance arises in strongly interacting species-rich model competition communities. *Proceedings of the National Academy of Sciences*, 87(24):9610–9614, 1990.

[29] Andrea Cavagna, Alessio Cimarelli, Irene Giardina, Giorgio Parisi, Raffaele Santagati, Fabio Stefanini, and Massimiliano Viale. Scale-free correlations in starling flocks. *Proceedings of the National Academy of Sciences*, 107(26):11865–11870, 2010.

[30] Peter Chesson. Multispecies competition in variable environments. *Theoretical population biology*, 45(3):227–276, 1994.

[31] Hsuan-Chao Chiu, Roie Levy, and Elhanan Borenstein. Emergent biosynthetic capacity in simple microbial communities. *PLOS computational biology*, 10(7):e1003695, 2014.

[32] Robert I Colautti, Anthony Ricciardi, Igor A Grigorovich, and Hugh J MacIsaac. Is invasion success explained by the enemy release hypothesis? *Ecology letters*, 7(8):721–733, 2004.

[33] Pascale Cossart and Philippe J Sansonetti. Bacterial invasion: the paradigms of enteroinvasive pathogens. *Science*, 304(5668):242–248, 2004.

[34] Elizabeth K Costello, Keaton Stagaman, Les Dethlefsen, Brendan JM Bohannan, and David A Relman. The application of ecological theory toward an understanding of the human microbiome. *Science*, 336(6086):1255–1262, 2012.

[35] Itay Dalmedigos and Guy Bunin. Dynamical persistence in high-diversity resource-consumer communities. *PLoS computational biology*, 16(10):e1008189, 2020.

[36] Itay Dalmedigos and Guy Bunin. Dynamical persistence in high-diversity resource-consumer communities. *PLOS Computational Biology*, 16(10):e1008189, October 2020.

[37] Peter De Schryver and Olav Vadstein. Ecological theory as a foundation to control pathogenic invasion in aquaculture. *The ISME journal*, 8(12):2360–2368, 2014.

[38] Reena Debray, Robin A Herbert, Alexander L Jaffe, Alexander Crits-Christoph, Mary E Power, and Britt Koskella. Priority effects in microbiome assembly. *Nature Reviews Microbiology*, 20(2):109–121, 2022.

[39] Camille S Delavaux, Thomas W Crowther, Constantin M Zohner, Niamh M Robmann, Thomas Lauber, Johan van den Hoogen, Sara Kuebbing, Jingjing Liang, Sergio De-Miguel, Gert-Jan Nabuurs, et al. Native diversity buffers against severity of non-native tree invasions. *Nature*, pages 1–9, 2023.

[40] Mike Dodd, Jonathan Silvertown, Kevin McConway, Jacqueline Potts, and Mick Crawley. Community Stability: A 60-Year Record of Trends and Outbreaks in the Occurrence of Species in the Park Grass Experiment. *Journal of Ecology*, 83(2):277–285, 1995.

[41] John M Drake and David M Lodge. Allee effects, propagule pressure and the probability of establishment: risk analysis for biological invasions. *Biological Invasions*, 8:365–375, 2006.

[42] Alexander Eng and Elhanan Borenstein. Microbial community design: methods, applications, and opportunities. *Current opinion in biotechnology*, 58:117–128, 2019.

[43] Jeremiah J Faith, Janaki L Guruge, Mark Charbonneau, Sathish Subramanian, Henning Seedorf, Andrew L Goodman, Jose C Clemente, Rob Knight, Andrew C Heath, Rudolph L Leibel, et al. The long-term stability of the human gut microbiota. *Science*, 341(6141):1237439, 2013.

[44] Jeremiah J. Faith, Janaki L. Guruge, Mark Charbonneau, Sathish Subramanian, Henning Seedorf, Andrew L. Goodman, Jose C. Clemente, Rob Knight, Andrew C. Heath, Rudolph L. Leibel, Michael Rosenbaum, and Jeffrey I. Gordon. The Long-Term Stability of the Human Gut Microbiota. *Science*, 341(6141):1237439, July 2013.

[45] Yael Fried, Nadav M. Shnerb, and David A. Kessler. Alternative steady states in ecological networks. *Physical Review E*, 96(1):012412, July 2017.

[46] Jonathan Friedman, Logan M Higgins, and Jeff Gore. Community structure follows simple assembly rules in microbial microcosms. *Nature ecology & evolution*, 1(5):0109, 2017.

[47] Gregor F. Fussmann, Stephen P. Ellner, Kyle W. Shertzer, and Nelson G. Hairston Jr. Crossing the Hopf Bifurcation in a Live Predator-Prey System. *Science*, 290(5495):1358–1360, November 2000.

[48] Gregor F Fussmann, Stephen P Ellner, Kyle W Shertzer, and Nelson G Hairston Jr. Crossing the hopf bifurcation in a live predator-prey system. *Science*, 290(5495):1358–1360, 2000.

[49] Leonor García-Bayona and Laurie E Comstock. Bacterial antagonism in host-associated microbial communities. *Science*, 361(6408):eaat2456, 2018.

[50] Joshua E Goldford, Nanxi Lu, Djordje Bajić, Sylvie Estrela, Mikhail Tikhonov, Alicia Sanchez-Gorostiaga, Daniel Segrè, Pankaj Mehta, and Alvaro Sanchez. Emergent simplicity in microbial community assembly. *Science*, 361(6401):469–474, 2018.

[51] Stéphanie Gout and Jacques Huot. Role of cancer microenvironment in metastasis: focus on colon cancer. *Cancer microenvironment*, 1:69–83, 2008.

[52] Ankit Gupta, Rasna Gupta, and Ram Lakhan Singh. Microbes and environment. *Principles and applications of environmental biotechnology for a sustainable future*, pages 43–84, 2017.

[53] Alan Hastings, Carole L Hom, Stephen Ellner, Peter Turchin, and H Charles J Godfray. Chaos in ecology: is mother nature a strange attractor? *Annual review of ecology and systematics*, 24(1):1–33, 1993.

[54] Simon Heilbronner, Bernhard Krismer, Heike Brötz-Oesterhelt, and Andreas Peschel. The microbiome-shaping roles of bacteriocins. *Nature Reviews Microbiology*, 19(11):726–739, 2021.

[55] Susan Hromada, Yili Qian, Tyler B Jacobson, Ryan L Clark, Lauren Watson, Nasia Safdar, Daniel Amador-Noguez, and Ophelia S Venturelli. Negative interactions determine clostridioides difficile growth in synthetic human gut communities. *Molecular systems biology*, 17(10):e10355, 2021.

[56] Jiliang Hu, Daniel R Amor, Matthieu Barbier, Guy Bunin, and Jeff Gore. Emergent phases of ecological diversity and dynamics mapped in microcosms. *Science*, 378(6615):85–89, 2022.

[57] Jef Huisman and Franz J Weissing. Biodiversity of plankton by species oscillations and chaos. *Nature*, 402(6760):407–410, 1999.

[58] Robert E Hungate. *The rumen and its microbes*. Elsevier, 2013.

[59] Maziya Ibrahim, Lavanya Raajaraam, and Karthik Raman. Modelling microbial communities: Harnessing consortia for biotechnological applications. *Computational and Structural Biotechnology Journal*, 19:3892–3907, 2021.

[60] Anthony R Ives and Stephen R Carpenter. Stability and diversity of ecosystems. *science*, 317(5834):58–62, 2007.

[61] Antti Karkman, Jenni Lehtimäki, and Lasse Ruokolainen. The ecology of human microbiota: dynamics and diversity in health and disease. *Annals of the New York Academy of Sciences*, 1399(1):78–92, 2017.

[62] Theodore A Kennedy, Shahid Naeem, Katherine M Howe, Johannes MH Knops, David Tilman, and Peter Reich. Biodiversity as a barrier to ecological invasion. *Nature*, 417(6889):636–638, 2002.

[63] David A Kessler and Nadav M Shnerb. Generalized model of island biodiversity. *Physical Review E*, 91(4):042705, 2015.

[64] Kaito Kikuchi, Leticia Galera-Laporta, Colleen Weatherwax, Jamie Y Lam, Eun Chae Moon, Emmanuel A Theodorakis, Jordi Garcia-Ojalvo, and Gürol M Süel. Electrochemical potential enables dormant spores to integrate environmental signals. *Science*, 378(6615):43–49, 2022.

[65] Marta Kinnunen, Arnaud Dechesne, Caitlin Proctor, Frederik Hammes, David Johnson, Marcos Quintela-Baluja, David Graham, Daniele Daffonchio, Stilianos Fodelianakis, Nicole Hahn, et al. A conceptual framework for invasion in microbial communities. *The ISME Journal*, 10(12):2773–2779, 2016.

[66] Allan Konopka. What is microbial community ecology? *The ISME journal*, 3(11):1223–1230, 2009.

[67] Kirill S Korolev, Joao B Xavier, and Jeff Gore. Turning ecology and evolution against cancer. *Nature Reviews Cancer*, 14(5):371–380, 2014.

[68] Justin Kuczynski, Christian L Lauber, William A Walters, Laura Wegener Parfrey, José C Clemente, Dirk Gevers, and Rob Knight. Experimental and analytical tools for studying the human microbiome. *Nature Reviews Genetics*, 13(1):47–58, 2012.

[69] Helen M Kurkjian, M Javad Akbari, and Babak Momeni. The impact of interactions on invasion and colonization resistance in microbial communities. *PLoS Computational Biology*, 17(1):e1008643, 2021.

[70] Miriam Land, Loren Hauser, Se-Ran Jun, Intawat Nookaew, Michael R Leuze, Tae-Hyuk Ahn, Tatiana Karpinets, Ole Lund, Guruprased Kora, Trudy Wassenaar, et al. Insights from 20 years of bacterial genome sequencing. *Functional & integrative genomics*, 15:141–161, 2015.

[71] Tae J Lee, Jeffrey Wong, Sena Bae, Anna Jisu Lee, Allison Lopatkin, Fan Yuan, and Lingchong You. A power-law dependence of bacterial invasion on mammalian host receptors. *PLoS computational biology*, 11(4):e1004203, 2015.

[72] Simon A Levin. The problem of pattern and scale in ecology: the robert h. macarthur award lecture. *Ecology*, 73(6):1943–1967, 1992.

[73] Simon A Levin and Robert T Paine. Disturbance, patch formation, and community structure. *Proceedings of the National Academy of Sciences*, 71(7):2744–2747, 1974.

[74] Jonathan M Levine. Species diversity and biological invasions: relating local process to community pattern. *Science*, 288(5467):852–854, 2000.

[75] Jonathan M Levine and Carla M D'Antonio. Elton revisited: a review of evidence linking diversity and invasibility. *Oikos*, pages 15–26, 1999.

[76] Wei Li and M Henry H Stevens. Fluctuating resource availability increases invasibility in microbial microcosms. *Oikos*, 121(3):435–441, 2012.

[77] Elena Litchman. Invisible invaders: non-pathogenic invasive microbes in aquatic and terrestrial ecosystems. *Ecology letters*, 13(12):1560–1572, 2010.

[78] David M Lodge. Biological invasions: lessons for ecology. *Trends in ecology & evolution*, 8(4):133–137, 1993.

[79] Jaime G Lopez and Ned S Wingreen. Noisy metabolism can promote microbial cross-feeding. *Elife*, 11:e70694, 2022.

[80] Gary W Luck and C Gretchen. Daily, and paul r. ehrlich. 2003."population diversity and ecosystem services.". *Trends in ecology and evolution*, 18(7).

[81] Daniel Machado, Oleksandr M Maistrenko, Sergej Andrejev, Yongkyu Kim, Peer Bork, Kaustubh R Patil, and Kiran R Patil. Polarization of microbial communities between competitive and cooperative metabolism. *Nature ecology & evolution*, 5(2):195–203, 2021.

[82] F Madeira. mi park. *Lee J., Buso N., Gur T., Madhusoodanan N., Basutkar P., Tivey ARN, Potter SC, Finn RD, et al. The EMBL-EBI Search and Sequence Analysis Tools APIs in*, 2019.

[83] Cyrus Alexander Mallon, Jan Dirk Van Elsas, and Joana Falcão Salles. Microbial invasions: the process, patterns, and mechanisms. *Trends in microbiology*, 23(11):719–729, 2015.

[84] Robert M May. What is the chance that a large complex system will be stable. *Nature*, 237(4137):414, 1972.

[85] Robert M May. How many species are there on earth? *Science*, 241(4872):1441–1449, 1988.

[86] Daniel S Maynard, Zachary R Miller, and Stefano Allesina. Predicting coexistence in experimental ecological communities. *Nature ecology & evolution*, 4(1):91–100, 2020.

[87] Kevin Shear McCann. The diversity–stability debate. *Nature*, 405(6783):228–233, 2000.

[88] Lauren MF Merlo, John W Pepper, Brian J Reid, and Carlo C Maley. Cancer as an evolutionary and ecological process. *Nature reviews cancer*, 6(12):924–935, 2006.

[89] Harry Mickalide and Seppe Kuehn. Higher-order interaction between species inhibits bacterial invasion of a phototroph-predator microbial community. *Cell systems*, 9(6):521–533, 2019.

[90] Atte Moilanen and Marko Nieminen. Simple connectivity measures in spatial ecology. *Ecology*, 83(4):1131–1145, 2002.

[91] Akihiko Mougi and Michio Kondoh. Diversity of interaction types and ecological community stability. *Science*, 337(6092):349–351, 2012.

[92] Nisha Nagarsheth, Max S Wicha, and Weiping Zou. Chemokines in the cancer microenvironment and their relevance in cancer immunotherapy. *Nature Reviews Immunology*, 17(9):559–572, 2017.

[93] Manfred Opper and Sigurd Diederich. Phase transition and 1/f noise in a game dynamical model. *Physical review letters*, 69(10):1616, 1992.

[94] Jacob D O'Sullivan, J Christopher D Terry, and Axel G Rossberg. Intrinsic ecological dynamics drive biodiversity turnover in model metacommunities. *Nature Communications*, 12(1):3627, 2021.

[95] Michael T Pearce, Atish Agarwala, and Daniel S Fisher. Stabilization of extensive fine-scale diversity by ecologically driven spatiotemporal chaos. *Proceedings of the National Academy of Sciences*, 117(25):14572–14583, 2020.

[96] Michael T. Pearce, Atish Agarwala, and Daniel S. Fisher. Stabilization of extensive fine-scale diversity by ecologically driven spatiotemporal chaos. *Proceedings of the National Academy of Sciences*, 117(25):14572–14583, June 2020.

[97] Liba Pejchar and Harold A Mooney. Invasive species, ecosystem services and human well-being. *Trends in ecology & evolution*, 24(9):497–504, 2009.

[98] Andy Purvis and Andy Hector. Getting the measure of biodiversity. *Nature*, 405(6783):212–219, 2000.

[99] Petr Pyšek and David M Richardson. Invasive species, environmental change and management, and health. *Annual review of environment and resources*, 35:25–55, 2010.

[100] Jimmy J Qian and Erol Akçay. The balance of interaction types determines the assembly and stability of ecological communities. *Nature ecology & evolution*, 4(3):356–365, 2020.

[101] Christoph Ratzke, Julien Barrere, and Jeff Gore. Strength of species interactions determines biodiversity and stability in microbial communities. *Nature ecology & evolution*, 4(3):376–383, 2020.

[102] Christoph Ratzke, Julien Barrere, and Jeff Gore. Strength of species interactions determines biodiversity and stability in microbial communities. *Nature Ecology & Evolution*, 4(3):376–383, March 2020.

[103] Christoph Ratzke and Jeff Gore. Modifying and reacting to the environmental ph can drive bacterial interactions. *PLoS biology*, 16(3):e2004248, 2018.

[104] David M Richardson and Petr Pyšek. Fifty years of invasion ecology–the legacy of charles elton, 2008.

[105] Robert E Ricklefs. Community diversity: relative roles of local and regional processes. *Science*, 235(4785):167–171, 1987.

[106] Felix Roy, Matthieu Barbier, Giulio Biroli, and Guy Bunin. Complex interactions can create persistent fluctuations in high-diversity ecosystems. *PLoS computational biology*, 16(5):e1007827, 2020.

[107] Felix Roy, Giulio Biroli, Guy Bunin, and Chiara Cammarota. Numerical implementation of dynamical mean field theory for disordered systems: Application to the lotka–volterra model of ecosystems. *Journal of Physics A: Mathematical and Theoretical*, 52(48):484001, 2019.

[108] Maja Rupnik, Mark H Wilcox, and Dale N Gerding. Clostridium difficile infection: new developments in epidemiology and pathogenesis. *Nature Reviews Microbiology*, 7(7):526–536, 2009.

[109] Dov F Sax, John J Stachowicz, James H Brown, John F Bruno, Michael N Dawson, Steven D Gaines, Richard K Grosberg, Alan Hastings, Robert D Holt, Margaret M Mayfield, et al. Ecological and evolutionary insights from species invasions. *Trends in ecology & evolution*, 22(9):465–471, 2007.

[110] Arne Schröder, Lennart Persson, and André M. De Roos. Direct experimental evidence for alternative stable states: A review. *Oikos*, 110(1):3–19, 2005.

[111] Ashley Shade, Hannes Peter, Steven D Allison, Didier L Baho, Mercè Berga, Helmut Bürgmann, David H Huber, Silke Langenheder, Jay T Lennon, Jennifer BH Martiny, et al. Fundamentals of microbial community resistance and resilience. *Frontiers in microbiology*, 3:417, 2012.

[112] Katriona Shea and Peter Chesson. Community ecology theory as a framework for biological invasions. *Trends in Ecology & Evolution*, 17(4):170–176, 2002.

[113] Nanako Shigesada and Kohkichi Kawasaki. *Biological invasions: theory and practice*. Oxford University Press, UK, 1997.

[114] Wenying Shou, Sri Ram, and Jose MG Vilar. Synthetic cooperation in engineered yeast populations. *Proceedings of the National Academy of Sciences*, 104(6):1877–1882, 2007.

[115] Ricard V Solé, David Alonso, and Alan McKane. Self–organized instability in complex ecosystems. *Philosophical Transactions of the Royal Society of London. Series B: Biological Sciences*, 357(1421):667–681, 2002.

[116] PETER SPOONER. Invasion ecology, 2007.

[117] Daniel Sprockett, Tadashi Fukami, and David A Relman. Role of priority effects in the early-life assembly of the gut microbiota. *Nature Reviews Gastroenterology & Hepatology*, 15(4):197–205, 2018.

[118] John J Stachowicz, Robert B Whitlatch, and Richard W Osman. Species diversity and invasion resistance in a marine ecosystem. *Science*, 286(5444):1577–1579, 1999.

[119] Lewi Stone. The feasibility and stability of large complex biological networks: a random matrix approach. *Scientific reports*, 8(1):8246, 2018.

[120] Ying Taur and Eric G Pamer. Harnessing microbiota to kill a pathogen: Fixing the microbiota to treat clostridium difficile infections. *Nature Medicine*, 20(3):246–247, 2014.

[121] Madhav P Thakur, Wim H Van der Putten, Marleen MP Cobben, Mark van Kleunen, and Stefan Geisen. Microbial invasions in terrestrial ecosystems. *Nature Reviews Microbiology*, 17(10):621–631, 2019.

[122] Robert Tibshirani. Regression shrinkage and selection via the lasso. *Journal of the Royal Statistical Society: Series B (Methodological)*, 58(1):267–288, 1996.

[123] David Tilman and Peter Kareiva. *Spatial ecology: the role of space in population dynamics and interspecific interactions*. Princeton University Press, 1997.

[124] David Tilman, Clarence L Lehman, and Charles E Bristow. Diversity-stability relationships: statistical inevitability or ecological consequence? *The American Naturalist*, 151(3):277–282, 1998.

[125] David Tilman, Peter B. Reich, and Johannes M. H. Knops. Biodiversity and ecosystem stability in a decade-long grassland experiment. *Nature*, 441(7093):629–632, June 2006.

[126] David Tilman, Peter B Reich, and Johannes MH Knops. Biodiversity and ecosystem stability in a decade-long grassland experiment. *Nature*, 441(7093):629–632, 2006.

[127] Jonathan David Touboul, Ann Carla Staver, and Simon Asher Levin. On the complex dynamics of savanna landscapes. *Proceedings of the National Academy of Sciences*, 115(7):E1336–E1345, 2018.

[128] Lindsay Ann Turnbull, Jonathan M Levine, Michel Loreau, and Andy Hector. Coexistence, niches and biodiversity effects on ecosystem functioning. *Ecology letters*, 16:116–127, 2013.

[129] Nick Vallespir Lowery and Tristan Ursell. Structured environments fundamentally alter dynamics and stability of ecological communities. *Proceedings of the National Academy of Sciences*, 116(2):379–388, 2019.

[130] Maarten Van de Guchte, Sebastian D. Burz, Julie Cadiou, Jiangbo Wu, Stanislas Mondot, Hervé M. Blottière, and Joël Doré. Alternative stable states in the intestinal ecosystem: Proof of concept in a rat model and a perspective of therapeutic implications. *Microbiome*, 8(1):153, November 2020.

[131] Johan van de Koppel, Peter M. J. Herman, Pauline Thoolen, and Carlo H. R. Heip. Do Alternate Stable States Occur in Natural Ecosystems? Evidence from a Tidal Flat. *Ecology*, 82(12):3449–3461, 2001.

[132] Naomi Iris van den Berg, Daniel Machado, Sophia Santos, Isabel Rocha, Jeremy Chacón, William Harcombe, Sara Mitri, and Kiran R Patil. Ecological modelling approaches for predicting emergent properties in microbial communities. *Nature ecology & evolution*, 6(7):855–865, 2022.

[133] Wim H Van der Putten, John N Klironomos, and David A Wardle. Microbial ecology of biological invasions. *The ISME journal*, 1(1):28–37, 2007.

[134] Jan Dirk Van Elsas, Mario Chiurazzi, Cyrus A Mallon, Dana Elhottovā, Václav Krištfek, and Joana Falcão Salles. Microbial diversity determines the invasion of soil by a bacterial pathogen. *Proceedings of the National Academy of Sciences*, 109(4):1159–1164, 2012.

[135] Nicole M Vega and Jeff Gore. Simple organizing principles in microbial communities. *Current opinion in microbiology*, 45:195–202, 2018.

[136] Ophelia S Venturelli, Alex V Carr, Garth Fisher, Ryan H Hsu, Rebecca Lau, Benjamin P Bowen, Susan Hromada, Trent Northen, and Adam P Arkin. Deciphering microbial interactions in synthetic human gut microbiome communities. *Molecular systems biology*, 14(6):e8157, 2018.

[137] Jean CC Vila, Matt L Jones, Matishalin Patel, Tom Bell, and James Rosindell. Uncovering the rules of microbial community invasions. *Nature ecology & evolution*, 3(8):1162–1171, 2019.

[138] Jane E Visvader. Cells of origin in cancer. *Nature*, 469(7330):314–322, 2011.

[139] Robert R Warner and Peter L Chesson. Coexistence mediated by recruitment fluctuations: a field guide to the storage effect. *The American Naturalist*, 125(6):769–787, 1985.

[140] Stuart A West, Stephen P Diggle, Angus Buckling, Andy Gardner, and Ashleigh S Griffin. The social lives of microbes. *Annu. Rev. Ecol. Evol. Syst.*, 38:53–77, 2007.

[141] Stefanie Widder, Rosalind J Allen, Thomas Pfeiffer, Thomas P Curtis, Carsten Wiuf, William T Sloan, Otto X Cordero, Sam P Brown, Babak Momeni, Wenying Shou, et al. Challenges in microbial ecology: building predictive understanding of community function and dynamics. *The ISME journal*, 10(11):2557–2568, 2016.

[142] Mark Williamson. *Biological invasions*. Springer Science & Business Media, 1996.

[143] Mark H Williamson and Alastair Fitter. The characters of successful invaders. *Biological conservation*, 78(1-2):163–170, 1996.

[144] Xueling Wu, Zhi-Yong Yang, Yuxing Li, Carl-Magnus Hogerkorp, William R Schief, Michael S Seaman, Tongqing Zhou, Stephen D Schmidt, Lan Wu, Ling Xu, et al. Rational design of envelope identifies broadly neutralizing human monoclonal antibodies to hiv-1. *Science*, 329(5993):856–861, 2010.

[145] Yogev Yonatan, Guy Amit, Jonathan Friedman, and Amir Bashan. Complexity–stability trade-off in empirical microbial ecosystems. *Nature Ecology & Evolution*, 6(6):693–700, 2022.

[146] Erika S Zavaleta and Kristin B Hulvey. Realistic species losses disproportionately reduce grassland resistance to biological invaders. *Science*, 306(5699):1175–1177, 2004.